

THE CHARACTERIZATION, OPTIMIZATION, AND
UTILIZATION OF IMMOBILIZED THIOL
GROUPS ON A POLYMERIC SURFACE

By

HEATHER D N FAHLENKAMP

Bachelor of Science
Oklahoma State University
Stillwater, OK
May 1997

Master of Science
University of Utah
Salt Lake City, UT
May 2000

Submitted to the Faculty of the
Graduate College of the
Oklahoma State University
in partial fulfillment of
the requirements for
the Degree of
DOCTOR OF PHILOSOPHY
December 2003

THE CHARACTERIZATION, OPTIMIZATION, AND
UTILIZATION OF IMMOBILIZED THIOL
GROUPS ON A POLYMERIC SURFACE

Thesis Approved:

Randy S. Lewis

Thesis Adviser

Kenneth A. Hays

Dennis L. Finkel

Master S. Hyl

Warren T. Ford

Joseph Sarlyzi

Dean of the Graduate College

ACKNOWLEDGEMENTS

I would first like to acknowledge and express my gratitude to my adviser, Dr. Randy Lewis for all his guidance and support during my experience at Oklahoma State University. I would also like to acknowledge the other members of my committee, Dr. Warren Ford, Dr. Gary Foutch, Dr. Karen High, and Dr. Marty High, not only for their participation in this project, but also for the insight and guidance they provided throughout my research. I would also like to thank Dr. Khaled Gasem for sitting in on my oral defense on behalf of Dr. Marty High.

I would like to thank the past and present members of Dr. Lewis' research group, especially Dr. Xunbao Duan and Ms. Jill Long, and the other graduate students in the department, especially Carlie Nichols and Brian Neely, for their support and encouragement. I also want to acknowledge all of the support staff in the Chemical Engineering Department for all of their assistance over the years.

Finally, I would like to express my sincerest gratitude and appreciation to my family for all of their love and support, especially my husband Jacob Fahlenkamp and my parents John and Helena Gappa. Without their encouragement, this dream of mine would have never been fulfilled. I would also like to dedicate all of my past research endeavors to my late grandmother, Lois Dalke. Her daily struggles of living with diabetes inspired me to enter the field of biomedical engineering in order to improve the quality of life of those living with disease or injury.

TABLE OF CONTENTS

Chapter	Page
1. INTRODUCTION	1
1.1 Objective #1: Surface Characterization of the Modified Polymer.....	5
1.2 Objective #2: Optimization of the Polymer Modification Process.....	6
1.3 Objective #3: Utilization of the Optimized Polymers in an In Vitro System with Platelets	7
2. REVIEW OF LITERATURE	9
2.1 Blood Components.....	9
2.1.1 Plasma.....	11
2.1.2 Erythrocytes (Red Blood Cells)	12
2.1.3 Platelets	14
2.1.4 Leukocytes (White Blood Cells).....	14
2.2 Platelet Activation.....	15
2.2.1 Physical Changes of Platelet Aggregation.....	16
2.2.2 Biochemistry of Platelet Aggregation.....	19
2.3 Platelet Inhibition.....	20
2.3.1 Synthesis of Nitric Oxide.....	21
2.3.2 Actions of Nitric Oxide.....	22
2.4 Nitric Oxide and Thiol Groups	24
2.4.1 Synthesis of S-Nitrosothiols	25
2.4.2 S-Nitrosothiol Reservoirs.....	26
2.4.3 Transnitrosation: Transfer of Nitric Oxide Between S-Nitrosothiols.....	30
2.4.4 S-Nitrosothiol Breakdown in Biological Systems	32
2.5 A Novel Design to Improve the Haemocompatibility of Blood- Contacting Materials by Utilizing Endogenous Nitric Oxide and Naturally-Occurring Mechanisms.....	35
2.5.1 Description of the Novel Design.....	35
2.5.2 The Rationale for the Design	37

2.6 Past Research	38
2.6.1 Design of a Novel Apparatus to Study Nitric Oxide Inhibition of Platelet Attachment to a Surface.....	38
2.6.2 The Design and Characterization of L-Cysteine Attached to a Surface	41
2.6.3 Testing the Ability of the Design to Inhibit Platelet Attachment to the Surface	44
3. SURFACE CHARACTERIZATION OF THE MODIFIED POLYMER	47
3.1 Introduction.....	47
3.2 Materials and Methods.....	50
3.2.1 Reagents.....	50
3.2.2 Immobilization of L-Cysteine onto PET Surface	51
3.2.3 Fluorescence Labeling of L-Cysteine Modified PET Samples.....	51
3.2.4 X-ray Photoelectron Spectroscopy (XPS) Analysis of Modified PET Samples.....	53
3.2.5 Nitrosation of Free and Immobilized L-Cysteine	55
3.2.6 Chemiluminescence Analysis	56
3.3 Results.....	62
3.3.1 Fluorescence Microscopy Analysis of Modified PET Samples	62
3.3.2 XPS Analysis of Modified PET Samples	66
3.3.3 Chemiluminescence Analysis	71
3.4 Discussion	80
4. OPTIMIZATION OF THE POLYMER MODIFICATION PROCESS	85
4.1 Introduction.....	85
4.2 Materials and Methods.....	88
4.2.1 Reagents.....	88
4.2.2 Modification of PET Samples.....	89
4.2.3 Optimization of L-Cysteine onto PET Surface.....	90
4.2.4 Optimization of 2-Iminothiolane onto PET Surface.....	96
4.2.5 Optimization of Cysteine Polypeptide onto PET Surface.....	103
4.3 Results.....	107
4.3.1 Optimization of L-Cysteine onto PET Surface.....	107
4.3.2 Optimization of 2-Iminothiolane onto PET Surface.....	124
4.3.3 Optimization of Cysteine Polypeptide onto PET Surface.....	130
4.4 Discussion.....	134

5. UTILIZATION OF THE OPTIMIZED POLYMERS IN AN <i>IN VITRO</i> SYSTEM WITH PLATELETS	140
5.1 Introduction.....	140
5.2 Materials and Methods.....	145
5.2.1 Reagents.....	145
5.2.2 Preparation of Platelets for Use in Perfusion Studies	146
5.2.3 Preparation of Optimized Polymers and Control Samples	155
5.2.4 Parallel Plate Perfusion Studies	157
5.2.5 Surface Analysis of the Modified Polymer Samples	161
5.3 Results.....	162
5.3.1 Preparation of Optimized Polymers and Control Samples	162
5.3.2 Parallel Plate Perfusion Studies	162
5.4 Discussion.....	177
6. CONCLUSIONS AND FUTURE WORK.....	181
7. REFERENCES	187
IRB APPROVAL FORM	201

LIST OF TABLES

Table	Page
2.1 Physical Properties of Adult Human Blood.....	10
2.2 Enzyme Systems that Break Down GSNO In Vitro	34
3.1 Atom% of Elements on Blank PET Sample and Modified PET Samples.....	67
3.2 Atom% of Elements on a Modified PET Sample and a Blank PET Sample Placed in an Acidic Nitrite Solution for One Hour, Compared to a Modified PET Sample Not Placed in an Acidic Solution.....	70
3.3 Chemiluminescence Analysis of NO_2^- and CySNO in Solution Following Nitrosation	74
3.4 Chemiluminescence Analysis of CySNO in Solution with Sulfanilamide.....	76
4.1 Plackett-Burman Factorial Design for Optimizing the Process of Attaching L- Cysteine to the Surface of PET	92
4.2 Full Factorial Design for Optimizing the Process of Attaching L-Cysteine to the Surface of PET by Varying Glutaraldehyde Concentration and L-Cysteine Reaction Time and Concentration	97
4.3 Full Factorial Design for Optimizing the Process of Attaching 2-Iminothiolane to the Surface of PET	100
4.4 Improved Factorial Design for Optimizing the Process of Attaching 2- Iminothiolane to the Surface of PET	104
4.5 Full Factorial Design for Optimizing the Process of Attaching Cysteine Polypeptide to the Surface of PET	106
4.6 The Effect of the Factors in the Plackett-Burman Factorial Design for Optimizing the Process of Attaching L-Cysteine to the Surface of PET.....	116

4.7	Atom% of Elements on Optimized L-Cysteine Modified PET Samples.....	122
4.8	Atom% of Elements on 2-Iminothiolane Modified PET Samples	128
4.9	Atom% of Elements on Cysteine Polypeptide Modified PET Samples	133

LIST OF FIGURES

Figure	Page
2.1 The four steps of platelet activation due to contact with a surface.....	17
2.2 Platelet aggregation. (A) Scanning electron micrographs of resting and agonist-stimulated platelets. The appearance of many pseudopodia on activation/stimulation that increases the membrane area, thereby enhancing platelet-platelet interactions. (B) Typical platelet aggregometer tracings of ADP-induced aggregation in citrated platelet-rich plasma at 37°C. The optical density of the suspension decreases progressively as aggregation begins and reaches a plateau when aggregation is maximal (Riddell et al., 1997).....	18
2.3 Summary of the chemistry of the redox-interrelated forms of NO of potential biological significance. The primary reactions of NO ⁻ involve oxygen, superoxide, and redox metals (M). NO ⁻ is reactive with metals and with sulfhydryls. Spontaneous dimerization of NO ⁻ results in the formation of N ₂ O. Nitrosation reactions involve electrophilic aromatic substitutions (Ar) and addition to bases (B ⁻), including peroxide (Stamler et al., 1992)	27
2.4 Illustration of the concept for the design that exploits endogenous NO and naturally-occurring mechanisms to increase the haemocompatibility of blood-contacting surfaces.....	36
2.5 Thin-slit flow chamber device used to investigate the inhibition of platelet deposition on a biomaterial surface under flow conditions via the local delivery of gaseous nitric oxide (Ramamurthi and Lewis, 1998).....	40
2.6 Reaction schemes of immobilizing L-cysteine onto the surface of polyethylene terephthalate (PET) and polyurethane (PU) by first adding an amine group by the use of ethylenediamine and 3-aminopropyltriethoxysilane (APTES), respectively and then using glutaraldehyde as a crosslinker	43
3.1 Experimental set-up of using the chemiluminescence analyzer to measure nitrosated L-cysteine that has been broken off the surface of L-cysteine modified PET.....	61

3.2	Fluorescence microscopy analysis of modified PET samples using 5-IAF. Scans are shown at 80x magnification.....	63
3.3	Film surface characteristics of Melinex S polyethylene terephthalate (PET) provided by DuPont Teijin Films™. One fringe displacement ~ 0.273 μm	65
3.4	Signal from the NO chemiluminescence analyzer for nitrite, CySNO, and an equimolar mixture of the two in both reducing solutions, one with free iodine (A) and one with L-cysteine (B). Values shown are mean values ± standard deviation (n=3).....	72
3.5	Signal from the NO chemiluminescence analyzer for CySNO in the reducing solution of copper chloride supplemented with L-cysteine at pH 7.4 and 50°C. Values shown are mean values ± standard deviation (n=3).....	78
4.1	Reaction schemes of immobilizing L-cysteine onto the surface of polyethylene terephthalate (PET) by first adding an amine group by the use of ethylenediamine and then using glutaraldehyde as a crosslinker	91
4.2	Reaction schemes of immobilizing 2-iminothiolane onto the surface of polyethylene terephthalate (PET) by first adding an amine group by the use of ethylenediamine	99
4.3	Fluorescence microscopy analysis of PET samples in various concentrations of ethylenediamine solutions. The gain setting was constant for all scans. Scans are shown at 400x magnification	108
4.4	Fluorescence microscopy analysis of the effects of various concentrations of ethylenediamine on the physical properties of the surface of PET. The gain setting varied for each scan. Scans are shown at 400x magnification.....	110
4.5	L-cysteine surface concentrations on the PET samples from the Plackett-Burman factorial design for optimizing the process of attaching L-cysteine to the surface of PET, as determined by chemiluminescence analysis. Data shown are mean values ± standard deviation (n=3).....	112
4.6	Mean intensity of fluorescence on the PET samples from the Plackett-Burman factorial design for optimizing the process of attaching L-cysteine to the surface of PET, as determined by chemiluminescence analysis. Data shown are mean values ± standard deviation (n=3)	113
4.7	L-cysteine surface concentrations on the PET samples from the 2-level, 3-factor, and 8-run full factorial design for optimizing the process of attaching L-	

cysteine to the surface of PET, as determined by chemiluminescence analysis. Data shown are mean values \pm standard deviation (n=3)	119
4.8 2-Iminothiolane surface concentrations on the PET samples from the initial 3-level, 2-factor, and 9-run full factorial design for optimizing the process of attaching 2-iminothiolane to the surface of PET, as determined by chemiluminescence analysis. Data shown are mean values \pm standard deviation (n=3).....	125
4.9 2-Iminothiolane surface concentrations on the PET samples from the improved 3-level, 2-factor, and 9-run full factorial design for optimizing the process of attaching 2-iminothiolane to the surface of PET, as determined by chemiluminescence analysis. Data shown are mean values \pm standard deviation (n=3).....	126
4.10 Cysteine polypeptide surface concentrations on the PET samples from the improved 3-level, 2-factor, and 9-run full factorial design for optimizing the process of attaching the cysteine polypeptide to the surface of PET, as determined by chemiluminescence analysis. Data shown are mean values \pm standard deviation (n=3)	131
5.1 Parallel plate flow chamber used to test platelet deposition on the optimized polymers. (a) Side view. (b) Top view. Figure from Duan, 2001.	142
5.2 An example of one of the 5 x 5 grids (outlined by the triple lines) on the haemocytometer used to count platelets by phase microscopy. Sample at 400x magnification.	153
5.3 Scans of the fluorescently labeled platelets on the surface of (a) L-cysteine modified PET and (b) glycine modified PET. Both samples were used in the perfusion study with platelets in a Tyrode's buffer solution. Scans are shown at 800x magnification.	164
5.4 Scans of the fluorescently labeled platelets on the surface of (a) L-cysteine modified PET and (b) glycine modified PET. Both samples were used in the perfusion study with platelets in a 7 μ M BSANO solution. Scans are shown at 400x magnification	165
5.5 Scans of the fluorescently labeled platelets on the surface of (a) L-cysteine modified PET and (b) glycine modified PET. Both samples were used in the perfusion study with platelets in a plasma solution. Scans are shown at 400x magnification	166

5.6	Scans of the fluorescently labeled platelets on the surface of (a) L-cysteine modified PET and (b) glycine modified PET. Both samples were used in the perfusion study with platelets in a whole blood solution. Scans are shown at 400x magnification	167
5.7	Scans of the fluorescently labeled platelets on the surface of (a) 2-iminothiolane modified PET and (b) glycine modified PET. Both samples were used in the perfusion study with platelets in a Tyrode's buffer solution. Scans are shown at 400x magnification.....	169
5.8	Scans of the fluorescently labeled platelets on the surface of (a) 2-iminothiolane modified PET and (b) glycine modified PET. Both samples were used in the perfusion study with platelets in a 7 μ M BSANO solution. Scans are shown at 400x magnification.....	170
5.9	Scans of the fluorescently labeled platelets on the surface of (a) 2-iminothiolane modified PET and (b) glycine modified PET. Both samples were used in the perfusion study with platelets in a plasma solution. Scans are shown at 400x magnification.....	171
5.10	Scans of the fluorescently labeled platelets on the surface of (a) 2-iminothiolane modified PET and (b) glycine modified PET. Both samples were used in the perfusion study with platelets in a whole blood solution. Scans are shown at 400x magnification.....	172
5.11	The amount of platelet attachment on the surface of each modified sample as a percent of each control sample (glycine). The amount of platelet attachment was determined by measuring the radioactivity of the radiolabeled platelets attached to each sample. Values shown are mean values \pm standard deviation (n=3)	173

NOMENCLATURE

ACD	Acid -citrate-dextrose
ADP	Adenosine diphosphate
AlbSNO	S-nitrosoalbumin
APTES	3-Aminopropyltriethoxysilane
BCA	Bicinchoninic acid
BSANO	Nitrosated bovine serum albumin
BSGC	Buffered saline glucose citrate
Ca-CAM	Calcium- calmodulin complex
cAMP	Cyclic adenosine 3',5'-monophosphate
CCD	Citrate-citric acid-dextrose
cGMP	Cyclic guanosine 3',5'-monophosphate
cm	Centimeter
CMFDA	5-Chloromethylfluorescein diacetate
Cr-51	Chromium-51
CuCl	Copper chloride
CySNO	S-nitroso-L-cysteine
DAG	Diacylglycerol
DTNB	5,5-Dithiobis (2-nitrosbenzoic acid) (Ellman's reagent)
EDRF	Endothelium-derived relaxing factor
EDTA	Ethylenediaminetetraacetic acid

fmol	Femtomole
g	Gram
GA	Glutaraldehyde
GSNO	S-nitrosoglutathione
Hb	Hemoglobin
HbSNO	S-nitrosohemoglobin
HCl	Hydrochloric acid
HMW	High molecular weight
HNO ₂	Nitrous acid
5-IAF	5-Iodoacetamidofluorescein
id	Inner diameter
In-111	Indium-111
IP ₃	Inositol 1,4,5-triphosphate
LMW	Low molecular weight
M	Molar
min	Minute
ml	Milliliter
mM	Millimolar
mol	Mole
MW	Molecular weight
N ₂ O ₃	Dinitrogen trioxide
NADPH	Nicotinamide adenine dinucleotide phosphate
NH ₂	Primary amine

nM	Nanomolar
nmol	Nanomole
NO	Nitric Oxide
NO _x	Nitrogen oxide donors
NO ⁺	Nitrosonium
NO ⁻	Nitroxyl
NO ₂ ⁻	Nitrite
NOS	NO synthase
O ₂ ⁻	Superoxide
ODQ	1H-[1,2,4]oxadiazolo[4,3-a]quinoxalin-1-one
PBS	Phosphate buffered saline
PET	Poly(ethylene terephthalate)
PET-Cys	L-cysteine-modified PET
PKC	Protein kinase C
PLC	Phospholipase C
pmol	Picomole
PMT	Photomultiplier tube
PPP	Platelet poor plasma
PRP	Platelet rich plasma
PU	Polyurethane
PVC	Poly(vinyl chloride)
ROC	Receptor-operated channels
RSH	Thiol

RSNOs	S-nitrosothiols
RSO	Radiological safety officer
s	Second
SEM	Scanning electron microscopy
SGC	Soluble guanylate cyclase
SH	Sulfhydryl
SNAP	S-nitroso-N-acetylpenicillamine
Trizma [®]	(Tris[hydroxymethyl]aminomethane)
μl	Microliter
μM	Micromolar
XPS	X-ray photoelectron spectroscopy

CHAPTER 1

INTRODUCTION

The purpose of this research was to improve the haemocompatibility of blood-contacting biomaterials by modifying the surface of the material in such a way that it utilizes naturally occurring compounds and mechanisms in the body to maintain biocompatibility. The Merriam-Webster definition of biocompatibility is the compatibility with living tissue or a living system by not being toxic or injurious and not causing immunological rejection. The term haemocompatibility has been used to describe the biocompatibility of materials in direct contact with blood, or haem. The Clemson University Advisory Board for Biomaterials has formally defined a biomaterial to be “a systemically and pharmacologically inert substance designed for implantation within or incorporation with living systems.” Biomaterials play a central role in extracorporeal devices, from blood oxygenators to kidney dialyzers, and are important components of implants, from vascular grafts to heart valve prostheses. The first biomaterials used clinically were not originally designed as such, but were off-the-shelf materials that clinicians used to improvise until something better was developed. Since limited information was available about how a material interacted with living tissue or fluids, usually a material was chosen solely based on its availability and physical properties. Therefore, dialysis tubing was originally made of cellulose acetate, a commodity plastic, vascular grafts were originally made with polymers derived from

textiles, such as Dacron, and the parts used for artificial hearts were based on commercial-grade polyurethanes. There was some success in using these materials as treatments; however, their use also introduced serious complications. In some cases, the dialysis tubing activated platelets and the complement system. Vascular grafts made from Dacron could only be used if their diameter exceeded about 6 mm, otherwise occlusion occurred due to biological reactions at the blood-material interfaces. Blood-material interactions can also lead to clot formation in an artificial heart, leading to the possibility of stroke or other complications.

As the haemocompatibility of blood-contacting materials continues to improve, their clinical use continues to increase. The following statistics, provided by the American Heart Association, indicate the cardiovascular procedures and implants that involve the use of biomaterials (Association, 2003). Unless otherwise stated, the statistics describe procedures performed in the United States in 2000. From 1979 to 2000, the number of cardiac catheterizations increased 341⁶ percent. An estimated 1,318,000 in-patient cardiac catheterizations were performed. It is estimated that 519,000 coronary artery bypass surgery procedures and 686,000 open-heart surgery procedures, both using an extracorporeal blood oxygenator device, were performed. An estimated 1,025,000 angioplasty procedures were performed, with percutaneous transluminal coronary angioplasty procedures accounting for 561,000 of the angioplasty procedures and stenting accounting for the rest. The number of implantable defibrillators, pacemakers, and heart valves included 34,000; 152,000; and 87,000; respectively. These statistics of procedures and implants only show one area in which blood-contacting materials are in use. The statistics would be even higher when considering the entire

field that utilizes blood-contacting materials. As a result, it is evident how important it is to continue to improve and develop more haemocompatible biomaterials.

To improve the haemocompatibility of blood-contacting surfaces, two strategies are available. The first strategy is to design new materials so that their surfaces are completely biocompatible. In general, it is very difficult to develop a material with the required mechanical properties that also has the desired surface biocompatibility. The second strategy is to modify the blood-contacting surface of existing materials in order to improve the haemocompatibility. Surface modification is a more generally applied technique to obtain haemocompatible surfaces than the development of new materials.

There are three general approaches used to modify the surface of a biomaterial in order to make it more haemocompatible. The first is to increase the surface hydrophilicity by grafting hydrophilic chains onto the surface. Most commonly used modifications are long chains of poly(ethylene oxide) grafted onto other polymer surfaces, such as polyurethane (PU) or poly(vinyl chloride) (PVC) (Brinkman et al., 1989; Golander and Kiss, 1988; Nojiri et al., 1990). A problem with this approach is that if the surface must interact with the surroundings, these long chains can create a great steric hindrance that can affect the biological properties of the biomaterial. The second approach is to disguise the surface in such a way that it will not be recognized by blood as a foreign surface, by such methods as endothelialization, albumin passivation, and phospholipid mimicking surfaces (Durrani et al., 1986; Herring et al., 1984; Kottke-Marchant et al., 1989). A problem with this approach is that covering the surface with such factors changes the surface properties and can also affect the biological properties of the biomaterial. The last approach is to provide the surface with a biologically active

compound, which inhibits blood foreign material interactions. This is often done by grafting the biologically active compound into the material, and then the compound is released from the material over time, making the material haemocompatible. Some common biologically active compounds used in such applications include heparin, enzymes, and nitric oxide (NO) (Heyman et al., 1985; Kitamoto et al., 1991; Tullett and Rees, 1999). The major problem with this approach is that the release rates of the biologically active compounds from the biomaterials can be difficult to control and can lead to dangerously high levels released into the body. Also, once the entire compound is released, the material loses its haemocompatibility.

The approach taken by this research was to modify the surface of a biomaterial in such a way that it utilizes naturally occurring components and mechanisms that are readily available and that will not expire. One of the naturally occurring components utilized by this design is endogenous NO bound to serum albumin in human plasma (Stamler et al., 1992a). By attaching L-cysteine to the surface of a biomaterial one of the naturally occurring mechanisms used by this design is the transfer of NO from the serum albumin to the L-cysteine through transnitrosation (Meyer et al., 1994; Scharfstein et al., 1994). The nitrosated L-cysteine is very unstable due to the presence of naturally present metal ions in blood (Beloso and Williams, 1997; Singh et al., 1996); therefore, NO is released from the surface and is available to inhibit platelet attachment. The benefits of this design include:

- The design utilizes naturally occurring components and mechanisms.
- The design is self-replenishing so that it may continue to inhibit platelet attachment to the surface of the biomaterial for long periods of time.

- The design has a localized effect that only prevents platelet attachment at the biomaterial surface.

The objectives for this project include surface characterization of the modified material in order to depict changes to the surface and to accurately measure these changes, optimization of the process to modify the biomaterial in order to maximize its effectiveness, and to utilize the material in a system with platelets in order to measure the effectiveness of the material to prevent platelet attachment. These objectives are outlined in more detail below.

1.1 Objective #1: Surface characterization of the modified polymer

Measuring the amount of L-cysteine that is attached to the solid surface has been difficult with current techniques due to such limitations as, steric hindrance, reactions with other species, and concentrations below detectable limits. Techniques used for surface characterization and measurement in this research included fluorescence microscopy, x-ray photoelectron spectroscopy (XPS), and several chemiluminescence-based assays that were used to measure thiols on surfaces and solutions.

The advantage of fluorescence microscopy is the ability to visualize the surface coverage of a fluorescent probe. Some disadvantages with fluorescence microscopy include lack of specificity of the fluorescence probe and the analysis is more qualitative and does not directly measure surface molar concentrations.

The advantage of XPS is that it is a highly precise and detailed analysis of only the surface of a material. The disadvantage of XPS is that it only shows atomic percentages on a surface, which makes it difficult to determine a molar surface concentration.

The chemiluminescence-based assays were the most successful in measuring surface molar concentrations of L-cysteine. The advantage of this method is that it can accurately measure (within 1% error) molar concentrations of L-cysteine in solution with a detection limit in the pmol range. The one disadvantage to this method is that L-cysteine must first be broken off of the surface and into solution prior to measurement, therefore leaving the sample unable to be reused.

Currently, there are few methods to accurately measure thiols in solution at low concentrations ($\leq 1 \mu\text{M}$) and no available methods to measure molar surface concentrations of thiols attached to a surface. Therefore, this research is significant in furthering the ability to measure thiols both in solution and on surfaces at low concentrations. Some of the surface measurement techniques could also be easily adapted to measure various other small molecules on surfaces.

1.2 Objective #2: Optimization of the polymer modification process

The hypothesis was that the addition of more L-cysteine sites or different L-cysteine-containing moieties on the polymer will increase the NO-release rate per unit area and will increase the inhibition of platelet deposition. The following systems were used in the optimization of the polymer modification process: 1. L-cysteine residues, 2. a L-cysteine containing moiety, 2-Iminothiolane, and 3. a polypeptide containing multiple cysteine residues. Each system was attached to PET by using linker groups. Optimization of each was performed by using full factorial and Plackett-Burman factorial designs that vary the reaction times and molar concentrations of each group involved in

the modification process. The optimal design was determined by measuring the relative amount of the thiol groups on the surface by techniques described in Objective #1.

Few studies have shown the attachment of L-cysteine and 2-iminothiolane to a solid surface, and although there are many examples of polypeptide chains attached to a solid support, little has been studied about a polypeptide containing multiple cysteine residues attached to a surface. Therefore, the optimization and characterization studies using these systems have greatly increased the present state of knowledge about the degree of attachment to a solid surface and the behavior of the attached system.

1.3 Objective #3: Utilization of the optimized polymers in an in vitro system with platelets

The hypothesis was that the optimized polymers will significantly decrease platelet attachment to the polymer surface compared to control samples. As described previously, the modified polymer inhibits platelet attachment by utilizing naturally occurring nitrosothiols in the plasma that can transfer NO to the attached thiol on the modified polymer. There are other plasma components, such as metal ions, that promote the release of NO from nitrosothiols (Beloso and Williams, 1997; Singh et al., 1996). Therefore, the plasma containing the nitrosothiols must be present with the platelets in order for the modified polymer to inhibit platelet attachment. Studies were performed using solutions containing platelets in a buffer solution only, in a solution of nitrosated serum albumin, and in a solution of plasma. Hemoglobin found in red blood cells in whole blood has also been shown to react readily with NO in solution and take part in transnitrosation between circulating nitrosothiols (Winterbourn, 1990). In order to study the effect of whole blood on platelet inhibition, platelets in a solution of whole blood was

also tested. Control samples included both blank PET and PET modified with an unreactive, non thiol-containing residue.

There are many studies that investigate the mechanisms involved when platelets come into contact with foreign surfaces or modified surfaces and the degree of reaction to the surface. However, this system was unique because it investigated how platelets react to thiol containing groups on a surface releasing small fluxes of NO. These studies also gave further insight into the role of nitrosothiols along with the possible role of other blood constituents in the mechanisms involved to inhibit platelet attachment.

CHAPTER 2

REVIEW OF LITERATURE

To fully understand how the modified material increases the haemocompatibility of blood-contacting biomaterials by utilizing naturally occurring mechanisms and components, one must first understand all of the biological processes involved. This chapter will review the important mechanisms and components involved in the interactions of various blood components with biomaterials. In practice, a material must not cause certain events, such as adhesion, platelet aggregation, blood coagulation, or obstruction of blood flow. Also in this chapter will be discussed some of the important components and mechanisms that can prevent the interaction of blood components with biomaterials and how these are utilized in the design of the modified biomaterial. Finally, a brief review of the past research leading up to this project will be discussed at the end of the chapter.

2.1 Blood Components

Blood is the vehicle of transportation that makes possible the cellular interactions and mechanisms that occur within the human body. Blood, which makes up about 6% of body weight, is a suspension of various types of cells in a complex aqueous medium, the plasma (Beutler and Williams, 1995). Table 2.1 summarizes the physical properties of

TABLE 2.1

Physical Properties of Adult Human Blood

Property	Value
Whole Blood	
pH	7.35 – 7.40
Viscosity (37 °C)	3.0 cP (at high shear rates)
Specific Gravity (25/4 °C)	1.056
Venous Hematocrit	
Male	0.47
Female	0.42
Whole Blood Volume	~78 ml/kg body weight
Plasma or Serum	
Colloid Osmotic Pressure	~330 mm H ₂ O
pH	7.3 – 7.5
Viscosity (37 °C)	1.2 cP
Specific Gravity (25/4 °C)	1.0239
Formed Elements	
Erythrocytes (Red Blood Cells)	
pH	7.396
Specific Gravity (25/4 °C)	1.098
Count	
Male	5.4×10^9 /ml whole blood
Female	4.8×10^9 /ml whole blood
Average Life Span	120 days
Production Rate	4.5×10^7 /ml whole blood/day
Hemoglobin Concentration	0.335 g/ml of erythrocyte
Platelets	
Count	$\sim 2.8 \times 10^8$ /ml whole blood
Diameter	$\sim 2 - 5 \mu\text{m}$
Leukocytes	
Count	$\sim 7.4 \times 10^6$ /ml whole blood
Diameter	7 – 20 μm

Data from (Cooney, 1976)

blood. The elements of blood serve multiple functions essential for respiration, metabolism, and the defense of the body against injury.

2.1.1 Plasma

To study plasma and its constituents, venous or arterial blood must be mixed with an anticoagulant to inhibit coagulation, or clot formation. Plasma is separated from the blood cells by centrifugation. If blood is drawn without adding an anticoagulant, then it will clot and the cell-depleted fluid phase of blood, devoid of fibrinogen, is called serum.

The normal adult has an average of 25 to 45 ml of plasma per kg of body weight (Berne and Levy, 1993). Many substances are dissolved in plasma, including electrolytes, proteins, lipids, carbohydrates, amino acids, vitamins, hormones, nitrogenous breakdown products of metabolism, and gaseous oxygen, carbon dioxide, and nitrogen. The concentrations of these constituents are influenced by diet, metabolic demand, and the levels of hormones and vitamins. Normally, the composition of blood is maintained at biologically safe and useful levels by a variety of homeostatic mechanisms. The balance may be upset by impaired function in a multitude of disorders, particularly those involving the lungs, the cardiovascular system, kidneys, liver, and endocrine organs.

There are hundreds of different proteins that are dissolved in plasma. The normal protein concentration in plasma is about 7 g/dl (Berne and Levy, 1993). The bulk of protein belongs to two groups, albumin and the various immunoglobulins. Albumin is a protein that is synthesized by hepatic parenchymal cells. It has a molecular weight of 69,000 and is normally present at an average concentration of 4 g/dl (Fournier, 1999). Because albumin diffuses poorly through intact vascular endothelium, it provides the

critical colloid osmotic or oncotic pressure that regulates the passage of water and diffusible solutes through the capillaries. Albumin is also the carrier for substances that are adsorbed to it. Such substances include normal components of blood, such as bilirubin and fatty acids, and certain exogenous agents, such as drugs. Albumin also supplies some of the anions needed to balance the cations of plasma.

Among the proteins, the antibodies (immunoglobulins) are normally second to albumin in concentration. Antibodies become active after the stimulation of lymphocytes in response to exposure to antigens, which are agents usually foreign to the normal body that evoke formation of specific antibodies. Immunoglobulins are synthesized by plasma cells in the lymphoid organs and are critical as a defense against infection. The gamma globulins constitute the bulk of immunoglobulins in plasma. Other plasma proteins include: (1) the clotting factors needed for blood coagulation; (2) the components of complement, a group of proteins that mediate the biological effects of immune reactions; (3) many enzymes or their precursors; (4) enzyme inhibitors; (5) specific carriers of such constituents as iron, copper, hormones, and vitamins; (6) scavengers of agents inadvertently released into plasma (Berne and Levy, 1993).

2.1.2 Erythrocytes (Red Blood Cells)

The most abundant cells found in blood are the red blood cells or erythrocytes comprising about 95% of the cellular components of blood (Fournier, 1999). The mature erythrocyte is an anuclear cell surrounded by a deformable membrane well adapted to the need to traverse narrow capillaries. The erythrocytes are biconcave disks, each with a diameter of about 8 μm , a thickness of 2 μm at its edge, and a volume of about 94 μm^3 (Beutler and Williams, 1995). In normal adults, the red cells make up approximately

47% of the volume of blood in males and about 42% in females (Berne and Levy, 1993). The percentage of the volume of blood made up by erythrocytes is defined as the hematocrit. The red blood cell count (the concentration of red cells in blood) normally averages about 5.4 million/ μl in adult men and 4.8 million/ μl in women (Berne and Levy, 1993). The average life span of the normal erythrocyte in the circulation is 120 days (Berne and Levy, 1993). The major role of red blood cells is the transport of oxygen by hemoglobin contained within the red blood cells.

The principal protein constituent of the cytoplasm of the mature erythrocyte is hemoglobin. Normal blood has about 15 g/dl of hemoglobin in adult men and about 13.5 g/dl in adult women (Berne and Levy, 1993). Hemoglobin is a complex protein synthesized in the marrow by the nucleated precursors of erythrocytes and has a molecular weight of 68,000 (Berne and Levy, 1993). It is composed of two dissimilar pairs of polypeptide "globin" subunits, two alpha chains and two nonalpha chains; the latter are either β , γ , or δ chains (Beutler and Williams, 1995). Each globin subunit is attached covalently to a prosthetic group consisting of a tetrapyrrole, heme. Heme is synthesized from glycine and succinyl-coenzyme A by a sequence of steps that lead to the formation of a pyrrole, porphobilinogen, and then to a tetrapyrrole ring compound, protoporphyrin IX. A mitochondrial enzyme, ferrochelatase, inserts an atom of ferrous iron into protoporphyrin IX to form heme. Oxygen binds reversibly to the iron incorporated into the heme unit. The combination of oxygen with hemoglobin in pulmonary capillaries and release of oxygen from hemoglobin in the capillaries of other tissues are all part of the respiratory system.

2.1.3 Platelets

The platelets are the next most abundant cell type found in blood, comprising about 4.9% of the cell volume (Beutler and Williams, 1995). Normal human blood contains approximately 1000 billion (10^{12}) platelets, $(150 - 350) \times 10^6 / \text{ml}$ (Berne and Levy, 1993). They circulate as anucleate disks, 2 –5 μm in diameter, and have an expected life span of 10 days within the human circulation (Schrör et al., 1994). Their job is to survey the lining of blood vessels, the endothelium. In acute damage and extravasation, platelets are activated by contact with exposed collagen and aggregate together at the wound site to initiate clotting and stop bleeding (Authi et al., 1993). Their small size and high number reflect their fundamental role in the process of hemostatic repair, to form mechanical plugs during the normal hemostatic response to vascular injury. However, in certain situations, overactive platelets can prematurely adhere to the internal walls of normal arteries and capillaries, perhaps a result of high blood pressure (Jobin, 1970), raised plasma cholesterol (Gupta, 1969), or smoking (Hawkins, 1972). The abnormal behavior has pathological consequences by impeding blood flow and contributing to the constriction of arteries, it promotes a variety of vascular complications, including thrombosis, premature heart disease, myocardial infarcts, and strokes (Harrison, 1997). It is essential that during normal vascular hemostasis, platelet activation is tightly controlled.

2.1.4 Leukocytes (White Blood Cells)

The remaining 0.1% of the cellular components of blood consists of the white blood cells or leukocytes, which form the basis of the cellular components of the immune system (Fournier, 1999). Normal blood contains between 4000 and 10,000 leukocytes/ μl

(Berne and Levy, 1993). Of these cells, about 40% to 75% are neutrophils, 20% to 45% are lymphocytes, 2% to 10% are monocytes, 1% to 6% are eosinophils, and less than 1% are basophils (Berne and Levy, 1993). Further description of these cell types goes beyond the scope of this thesis. This research investigates the increased haemocompatibility of the modified biomaterial and not the immunogenicity of the material, or its reaction with the immune system.

2.2 Platelet Activation

Platelets can become activated due to a variety of reasons, including the following: (1) when platelets are removed from the circulation, (2) when platelets contact an abnormal blood vessel or extravascular tissue, (3) when platelets are exposed to a physiological activator (platelet agonist), or (4) when platelets contact a foreign material (Authi et al., 1993). Four general platelet activation responses resulting from contact with a foreign material have been identified: (Holmsen, 1994)

1. *Adhesion*: Platelets form a carpetlike monolayer on a blood vessel wall at the site of injury and exposed subendothelium, or on the surface of a foreign material.
2. *Shape Change*: Disk-shaped resting cells are rapidly converted to spiculated spheres, resembling lumps of tissue with spikes or points on the surface.
3. *Aggregation*: Platelet surface receptors for fibrinogen (GPIIb-IIa complex) become activated, allowing platelet-platelet interactions to occur.
4. *Granule Secretion*: Due to a series of intracellular signalling events that cause platelet granule membranes to fuse with invaginations in the plasma

membrane, called the open canalicular system, leading to discharge of the granule content into the extracellular space.

Figure 2.1 shows the steps of platelet activation due to contact with a surface. Of all of the steps, aggregation is the most notable, since during this step platelet activation becomes irreversible and leads to problems related to thrombosis and embolism.

2.2.1 Physical Changes of Platelet Aggregation

In response to stimuli, platelets adhere to each other and form aggregates of various sizes. Aggregation is the result of numerous interlinked reactions at the surface of the platelet membrane and in the cytoplasm. Initially, platelets are activated by binding of agonists, including adenosine diphosphate (ADP), serotonin, thrombin, or collagen, to their respective receptors in the platelet surface membrane (Kroll and Schafer, 1989; Siess, 1989). Aggregation then occurs within one minute of activation (Savi and Herbert, 1996). Platelet-platelet interactions develop when the GPIIb-IIIa complex is activated to bind fibrinogen. Each molecule of fibrinogen recognizes two GPIIb-IIIa complexes, which allows molecular bridges to form between two adjacent platelets (Perutelli and Mori, 1992). When the stimulation of platelets is minor, the aggregated platelets dissociate from each other and freely resuspend; this is called, “primary aggregation” and is a reversible process (Kroll and Schafer, 1989). A strong stimulus results in what is called, “secondary aggregation” which is irreversible due to the secretion of platelet granular constituents such as ADP (Meyers et al., 1979). This degranulation and release of ADP promotes further aggregation (autocrine stimulation) and leads to the formation of a plug over the damaged area (Holmsen, 1994). Examples of reversible and irreversible aggregation are shown in Figure 2.2. As shown, the higher

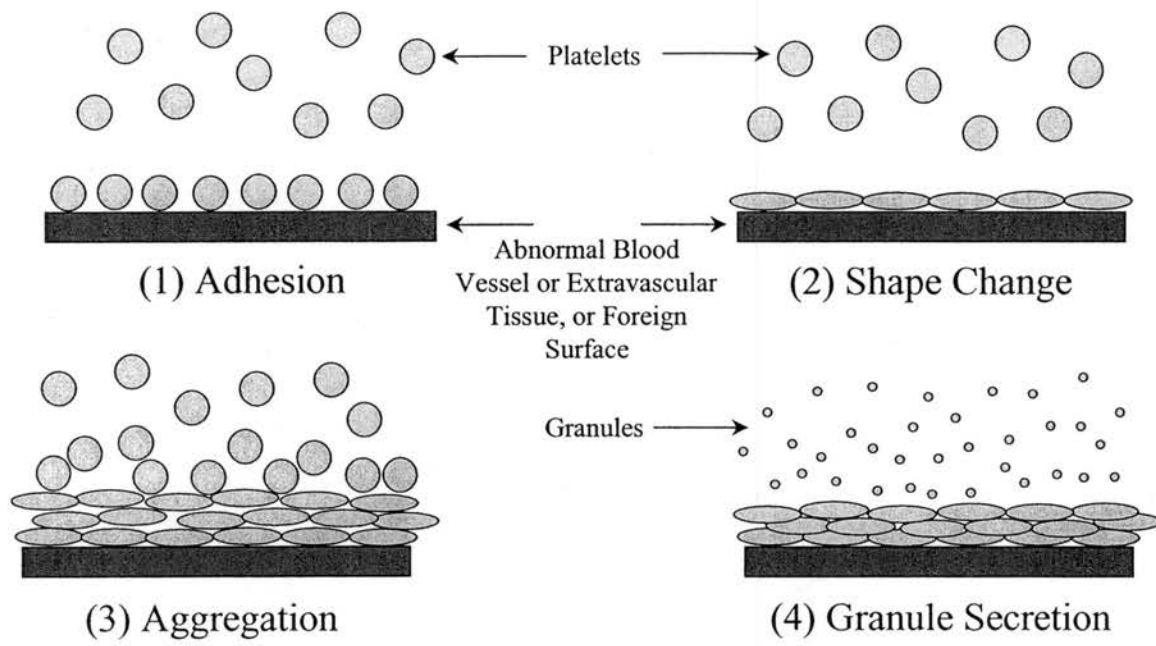


Figure 2.1 The four steps of platelet activation due to contact with a surface.

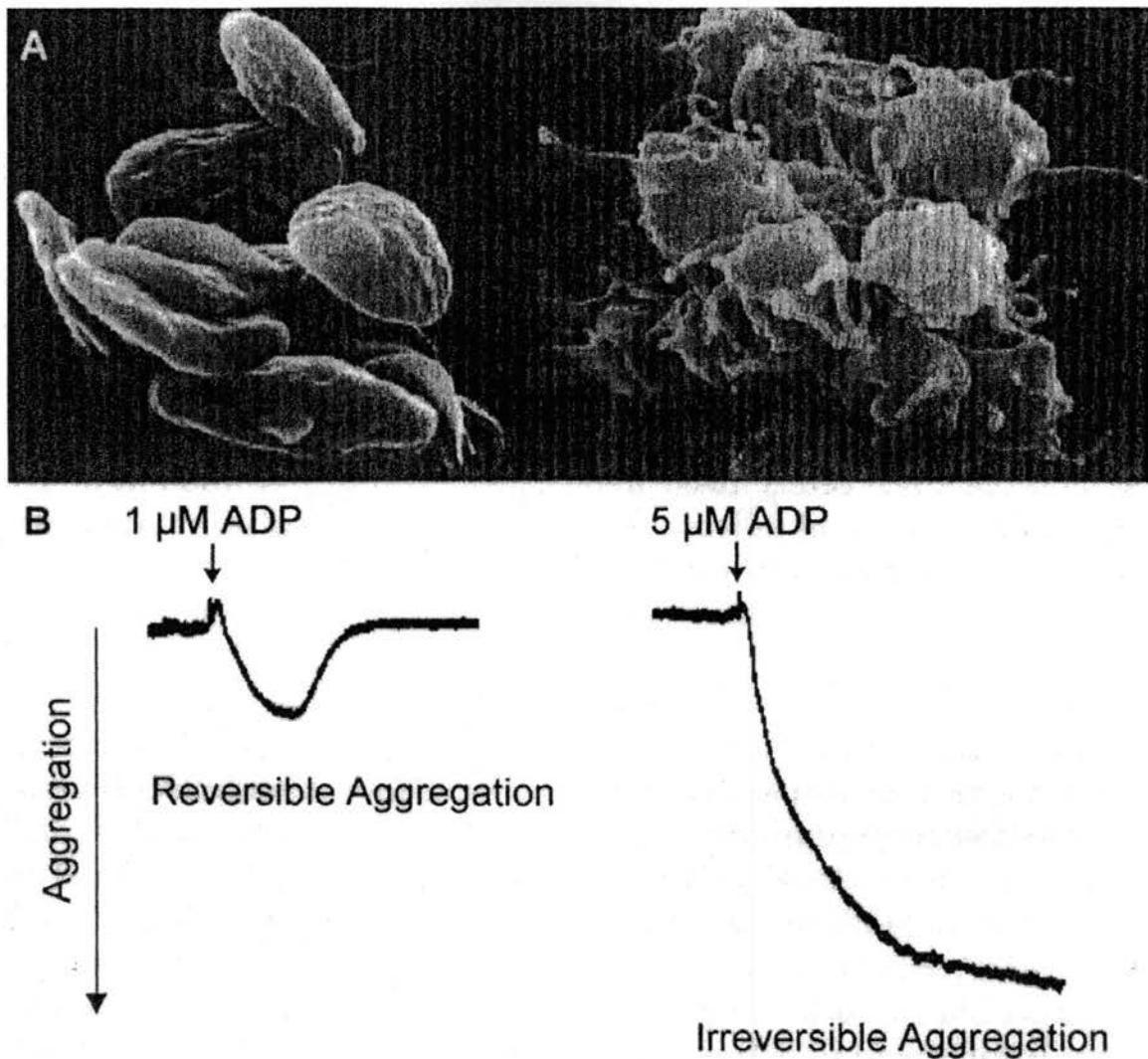


Figure 2.2 Platelet aggregation. (A) Scanning electron micrographs of resting and agonist-stimulated platelets. The appearance of many pseudopodia on activation/stimulation that increases the membrane area, thereby enhancing platelet-platelet interactions. (B) Typical platelet aggregometer tracings of ADP-induced aggregation in citrated platelet-rich plasma at 37°C. The optical density of the suspension decreases progressively as aggregation begins and reaches a plateau when aggregation is maximal (Riddell et al., 1997).

concentration of ADP leads to irreversible aggregation and noticeable shape changes of the platelets.

2.2.2 Biochemistry of Platelet Aggregation

Calcium signaling is central to the process of platelet aggregation and has been reviewed by Sage, et al. (Sage et al., 1993). Most aggregating agents act via the G protein-coupled receptors to activate phospholipase C (PLC), with the released diacylglycerol (DAG) and inositol 1,4,5-triphosphate (IP₃) stimulating protein kinase C (PKC) and mobilizing intracellular Ca²⁺, respectively (Brass, 1991; Puri and Colman, 1997; Savi and Herbert, 1996). Aggregating agents also cause an influx of extracellular Ca²⁺, which is thought to be triggered by the discharge of intracellular Ca²⁺ stores (Haynes, 1993). Intraplatelet Ca²⁺ levels, in both the cytoplasm and releasable store (the dense tubular system) are tightly regulated by a system of pumps, leaks, and receptor-operated channels (ROC), which are modulated by other second messengers. These include cyclic adenosine 3',5'-monophosphate (cAMP), cyclic guanosine 3',5'-monophosphate (cGMP), and DAG, which stimulate their respective protein kinases. Therefore, Ca²⁺ homeostasis at rest and Ca²⁺ mobilization during aggregation are controlled by these protein kinases, which modulate the activities of pumps, ROCs, or other regulatory proteins by phosphorylation (Haynes, 1993). In addition, cytoplasmic Ca²⁺ is self-regulated, mediated by its calmodulin complex (Ca-CAM), which activates numerous regulatory enzymes.

2.3 Platelet Inhibition

The activation of human platelets is inhibited by numerous agents, examples include inhibitors of thrombin (e.g. hirudin) (Glusa, 1991), scavengers of ADP (e.g. apyrase) (Walsh et al., 1977), inhibitors of thromboxane A₂ generation (e.g. aspirin) (Vane, 1994), and physiological and pharmacological agents which raise intraplatelet cyclic nucleotides (Haynes, 1993). Under basal conditions and in response to numerous vasoactive agents, vascular endothelial cells synthesize and secrete two of the most important physiological inhibitors of platelet activation: prostacyclin and the endothelium-derived relaxing factor (EDRF), which increase levels of the intracellular messenger molecules, cAMP and cGMP, respectively, in human platelets (Haynes, 1993; Vane, 1994).

EDRF was first described in 1980 when it was recognized that an endothelium-derived labile humoral substance was responsible for mediating the vascular relaxations induced by acetylcholine (Furchgott and Zawadzki, 1980). Later it was shown that EDRF was also a potent inhibitor of platelet aggregation (Azuma et al., 1986; Radomski et al., 1987a) and that it caused an increase of cGMP in platelets or other target cells (Furchgott and Zawadzki, 1980; Radomski et al., 1987b). However, the biochemical pathways regulating the production and downstream physiological effects of EDRF were only revealed following the discovery that the biological and chemical properties of EDRF were identical to those of nitric oxide (NO) (Ignarro et al., 1987a; Ignarro et al., 1987b; Palmer et al., 1987).

2.3.1 Synthesis of Nitric Oxide

As a free radical gas, NO is a diffusible and reactive molecular messenger with diverse biological actions throughout the body including in the vascular, immune, and nervous systems (Anggard, 1994; Butler and Williams, 1993; Christopherson and Bredt, 1997; Harrison, 1997; Mayer and Hemmens, 1997; Michel and Feron, 1997; Moncada et al., 1991; Nathan, 1997; Sase and Michel, 1997; Schmidt and Walter, 1994). In the brain, NO modulates synaptic plasticity and influences brain development, memory formation, and behavior. In the peripheral nervous system, it resembles a classical neurotransmitter to regulate gut motility, regional blood flow, and neuroendocrine function (Christopherson and Bredt, 1997; Michel and Feron, 1997). NO release is an important means for controlling infection, by the expression of an inducible NO synthase isoform by macrophages in response to immunological or inflammatory stimuli (Nathan, 1997). The continuous generation of NO by the vascular endothelium is crucial for the regulation of blood pressure and blood flow (Michel and Feron, 1997; Sase and Michel, 1997; Schmidt and Walter, 1994). The endothelium-derived NO has a critical role in preventing premature platelet adhesion and aggregation (Moncada et al., 1991).

NO is generated by the five-electron oxidation of the terminal guanidinium nitrogen of the amino acid L-arginine, yielding L-citrulline as the coproduct (Knowles and Moncada, 1994). The mechanism is a complex two-stage stereospecific reaction involving molecular oxygen and reduced nicotinamide adenine dinucleotide phosphate (NADPH) as cosubstrates, with numerous other redox cofactors. This formation of NO from L-arginine is catalyzed by NO synthase (NOS) (Knowles and Moncada, 1994; Mayer and Hemmens, 1997). Earlier studies, based on cellular location, regulation of

activity, and substrate/inhibitor profiles indicated that there were three distinct NOS isoforms:

- NOS-I or nNOS: a calcium and calmodulin (Ca-CAM) -requiring constitutive enzyme present in neurons and skeletal muscle (Christopherson and Bredt, 1997; Mayer and Hemmens, 1997; Schmidt and Walter, 1994).
- NOS-II or iNOS: a calcium-independent isoform isolated from macrophages, vascular smooth muscle cells, and hepatocytes following induction by specific cytokines (Anggard, 1994; Mayer and Hemmens, 1997; Nathan, 1997).
- NOS-III or eNOS: a constitutive form found in vascular endothelial cells and regulated by Ca-CAM (Michel and Feron, 1997; Sase and Michel, 1997).

Due to the numerous roles of NO in cell biology, the distribution of the three isoforms overlaps in many tissues and cell types, the subcellular location of the three isoforms is variable, the same isoform in different cells may evoke different biological effects, and the eNOS and nNOS are also inducible (Michel and Feron, 1997).

2.3.2 Actions of Nitric Oxide

Usually, molecules acting as inter- or intracellular messengers interact with defined receptors on target cells to induce a specific response. However, NO does not comply with this typical signaling process, due to its lipophilic and free radical properties. Instead, it diffuses three-dimensionally away from its point of synthesis to interact with numerous metal- and thiol-containing molecules (Moncada et al., 1991). Although this process may appear random, these properties of NO are crucial to mediate many of its biological effects. However, the best characterized target site for NO is the

iron bound within the heme moiety of soluble guanylate cyclase (SGC) (Buechler et al., 1994).

In contrast to adenylate cyclase, which is exclusively membrane-bound, guanylate cyclase exists in both cytosolic and particulate fractions of cells (Brass, 1991; Buechler et al., 1994). Particulate guanylate cyclase is found in the plasma membrane of many cells and at least five isoforms have been cloned and characterized. The exact physiological roles of particulate guanylate cyclase isoforms remain unresolved, although their primary function may be as receptors for atrial natriuretic peptides (Garbers, 1992). It is the soluble isoform of guanylate cyclase that plays a central role in the NO-cGMP signal transduction pathway (Buechler et al., 1994). SGC is a Mn^{2+} -dependent enzyme found in the cytosolic fraction of most mammalian cells and is very abundant in platelets (Buechler et al., 1994; Chhajlani et al., 1989).

Platelet SGC has been purified to a homogeneity and consists of an 83 kDa α -subunit and a 71 kDa β -subunit (Chhajlani et al., 1989). Although each monomer contains a near-identical catalytic domain, with a high degree of homology to particulate guanylate cyclase, both α - and β -subunits are required for catalytic activity (Buechler et al., 1994). A key characteristic of SGC is the presence of heme as a prosthetic group. Recent studies have shown that both subunits of SGC are required to form a functional heme-binding site within the enzyme (Foerster et al., 1996). NO interacts with SGC through this heme group to induce a conformational change that stimulates the conversion of GTP to cGMP (Anggard, 1994; Radomski and Moncada, 1993).

Cumulative evidence suggests that the major mechanism by which NO inhibits platelet activation is through activation of platelet SGC to increase levels of cGMP

(Radomski and Moncada, 1993). As a result, the inhibitory effects of NO can be reproduced by addition of cGMP analogues, and the antiplatelet action of NO donors can be blocked by treating platelets with 1H-[1,2,4]oxadiazolo[4,3-a]quinoxalin-1-one (ODQ), a specific and potent inhibitor of SGC (Moro et al., 1996; Nguyen et al., 1991; Riddell et al., 1997). However, other mechanisms of NO action that are independent of cGMP production have also been described (Gordge et al., 1998). These include NO-mediated ADP ribosylation, inhibition of glyceraldehyde-3-phosphate dehydrogenase and inhibition of intracellular calcium mobilization (Brune and Lapetina, 1989; Dimmeler and Brune, 1992; Dimmeler et al., 1992; Menshikov et al., 1993). The relative functional importance of such non-SGC-non-cGMP-mediated actions of NO has not yet been determined.

The effects of NO on platelet function differ significantly from those of many other antiplatelet agents. These include the cyclooxygenase inhibitor acetylsalicylic acid (aspirin), which irreversibly inhibits platelet activation by preventing the formation of the proaggregatory thromboxane A₂ (Vane, 1994). By contrast, NO inhibits platelet activation at an earlier stage and its effects are quickly and completely reversible (Buechler et al., 1994; Radomski and Moncada, 1993). Thus, in addition to inhibiting platelet adhesion to the vessel wall, NO also interferes with the initial thrombus formation by inhibiting aggregation and the autocrine stimulation and recruitment of adjacent platelets (Freedman et al., 1997; Radomski and Moncada, 1993).

2.4 Nitric Oxide and Thiol Groups

Ignarro et al. demonstrated that reactions with cellular thiols contributed to the bioactivities of certain pharmacological nitrogen oxide (NO_x) donors in 1981, several

years before making the observation that NO is synthesized endogenously in mammalian cells (Ignarro et al., 1987b; Ignarro et al., 1981). Kowaluk and Fung later showed that S-nitrosothiols (RSNOs) exerted bioactivities independent of breaking down to NO (Kowaluk and Fung, 1990). There was little information about thiol-NO interactions until Stamler et al. perceived RSNOs as nitrosonium (NO^+) and nitroxyl (NO^-) donors with chemical reactivities distinct from those of NO, which were: (1) capable of forming in and modifying proteins, and (2) present in mammalian tissue (Gaston et al., 1993; Stamler et al., 1992a). S-nitrosothiols have also been shown to have similar biological actions as of NO and play an important role in many processes, including platelet inhibition, signal transduction, DNA repair, host defense, blood pressure control, ion channel regulation, and neurotransmission (Brune et al., 1998; Campbell et al., 1996; delaTorre et al., 1998; Gow and Stamler, 1998; Lander et al., 1996; Persichini et al., 1998; Radomski et al., 1992).

2.4.1 Synthesis of S-Nitrosothiols

The reactivity of NO with sulfhydryl (RSH) groups depends on the electron configuration of its 2p- Π antibonding orbital (Stamler et al., 1992c). The presence of one (radical) electron in this orbital does not ordinarily promote reactivity with R-SH groups, although it allows reaction with thiyl radical species. On the other hand, loss of this electron to form NO^+ promotes strong electrophilicity and reactivity towards most biological RSH species (Arnelle and Stamler, 1995; Stamler et al., 1992c). A second electron in the 2p- Π orbital, forming NO^- , may under certain circumstances promote the reactivity with relatively electropositive R-SH species, particularly in the presence of ferrous ion or other transition metals (Arnelle and Stamler, 1995; Stamler et al., 1992c;

Vanin et al., 1997). A summary of the chemistry of the redox-interrelated forms of NO of potential biological significance is illustrated in Figure 2.3.

The third order reactivity of NO with oxygen under physiological conditions (rate constant in aqueous phase $\sim 6.6 \times 10^6 \text{ M}^{-2}\text{s}^{-1}$) predicts relatively slow production of dinitrogen trioxide (N_2O_3) as a nitrosating agent in the form of ($\text{NO}^+ \dots \text{NO}_2^-$) (Wink et al., 1993). This reaction is accelerated 300-fold in the hydrophilic core of biological membranes (Liu et al., 1998). On the other hand, reactions of NO with superoxide are so rapid as to be diffusion limited ($k \sim 7 \times 10^9 \text{ M}^{-1}\text{s}^{-1}$) (Haddad et al., 1994). Both amines and sulfhydryl groups are highly susceptible to reactions with N_2O_3 and ONOO^- (Gow et al., 1997; Liu et al., 1998; Schmidt et al., 1996; Wink et al., 1991). Thiol nitrosation (RSNO) is preferred under physiological conditions, both because of the tendency of amines to be more basic and because, unlike deamination of primary amines after NO^+ -induced diazotization, loss of the RSNO group thiolate does not generally occur rapidly (Stamler et al., 1992c; Wink et al., 1991). Reactivity of these nitrosating species toward carbon groups is less than toward amino groups and sulfhydryl groups. Therefore, S-nitrosation of proteins has been demonstrated to be preferred over N- and C-nitrosation under physiological conditions and that large, stable reservoirs of S-NO, but not N-NO or C-NO, species have been identified in tissues (Gaston et al., 1993; Giovannoni et al., 1997; Jia et al., 1996; Kluge et al., 1997; Simon et al., 1996; Stamler et al., 1992a).

2.4.2 S-Nitrosothiol Reservoirs

Titration of free $-\text{SH}$ groups by radioactive SH-modifying reagents, ultraviolet-visible spectrophotometry, and electrospray ionization-mass spectrometry can be used to monitor the binding of NO to peptides (on precise amino acids) (Catani et al., 1998;

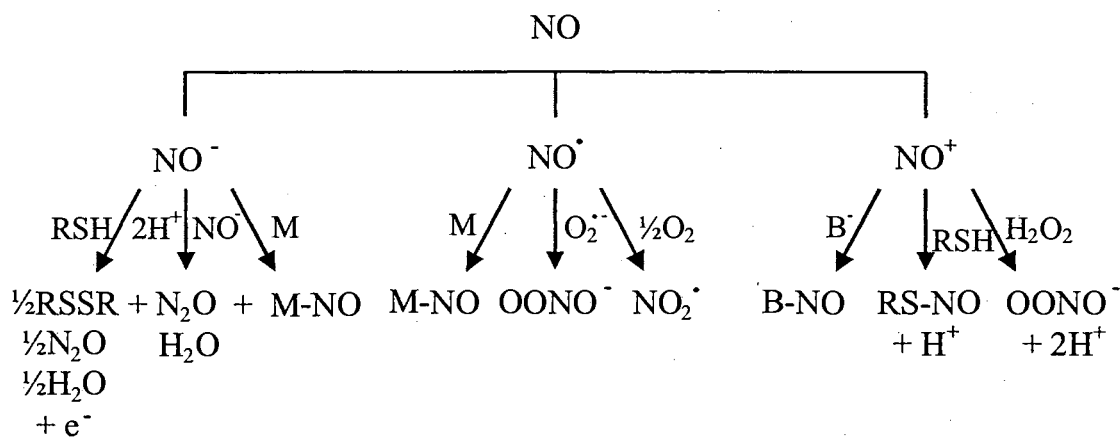


Figure 2.3 Summary of the chemistry of the redox-interrelated forms of NO of potential biological significance. The primary reactions of NO involve oxygen, superoxide, and redox metals (M). NO⁻ is reactive with metals and with sulfhydryls. Spontaneous dimerization of NO⁻ results in the formation of N₂O. Nitrosation reactions involve sulfhydryl (RSH) and addition to bases (B⁻), including peroxide (Stamler et al., 1992).

delaTorre et al., 1998; Mirza et al., 1995). These techniques have demonstrated that cysteine residues are rapidly nitrosated, while reactions with other amino acids occur at much slower rates. Cysteine residues are therefore the main targets of S-nitrosation. It should be noted that the RS-NO bond is labile and therefore difficult to study and quantify (Mirza et al., 1995).

Numerous studies have concentrated on the chemistry and pharmacology of RSNOs, including their synthesis, properties, reactions that lead to NO (NO^+) formation, and reactions where the NO group can be transferred to other thiol groups, but the main issue that remained was the possibility of such chemical reactions (S-nitrosation) occurring *in vivo* and not only at acidic pH (Pryor et al., 1982; Pryor and Lightsey, 1981). This issue had been controversial until new methods were developed to measure the free redox-modulated forms of NO, such as NO^+ , *in vivo*. Gow et al. have recently proposed a mechanism for the formation of RSNOs *in vivo* (under physiological conditions) (Gow et al., 1997). They proposed a mechanism whereby NO reacts directly with reduced thiol to produce a radical intermediate, R-S-N-O-H. This intermediate then reduces an available electron acceptor to produce a RSNO. Under aerobic conditions, O_2 acts as the electron acceptor and is reduced to produce superoxide (O_2^-).

The formation of a RSNO has now been shown to occur *in vivo* for an array of proteins (Butler et al., 1995; Lander, 1997). RSNOs like S-nitrosoalbumin (AlbSNO), S-nitrosoglutathione (GSNO), or S-nitroso-L-cysteine (CySNO) have been detected and quantified *in vivo* and they may be responsible for some of the well-documented physiological processes that have been previously attributed to NO itself (Kluge et al., 1997). The single free cysteine of serum albumin, Cys-34, has been shown to be

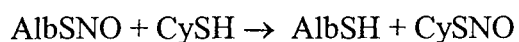
particularly reactive toward NO under physiological conditions, primarily because of its anomalously low pK (Stamler et al., 1992a). Studies have reported a range of RSNO concentrations measured in human plasma. One study shows that human plasma contains $\sim 7 \mu\text{M}$ RSNOs, of which 96% are S-nitrosoproteins, 82% of which is accounted for by AlbSNO (Stamler et al., 1992a). Another study measured the concentration of RSNOs in human plasma to be in the 20 nM range (Marley et al., 2000). By contrast, plasma levels of free nitric oxide are only in the $3 \pm 0.58 \text{ nM}$ range (Stamler et al., 1992a). It has been hypothesized that naturally produced NO circulates in plasma primarily complexed in RSNO species, mainly as AlbSNO. This abundant, relatively long-lived adduct likely serves as a reservoir with which plasma levels of highly reactive, short-lived free NO can be regulated. The chemical half-life of released NO is very short and is inactivated within $\sim 0.2 \text{ s}$ (Kelm and Schrader, 1990). In comparison with NO, RSNOs are often very stable compounds with half-lives up to 40 min, as in the case of AlbSNO (Stamler et al., 1992b).

The high-affinity of NO binding to hemoglobin (Hb) has given further insight into the relationship of heme proteins and of small diffusible signaling molecules. Specifically, NO binds rapidly to the heme iron in Hb ($k_{\text{on}} \sim 10^7 \text{ M}^{-1}\text{s}^{-1}$) and once bound, the NO activity is largely irretrievable ($K_{\text{d}} \sim 10^{-5} \text{ s}^{-1}$) (Stamler et al., 1997). The binding is so strong, that it is unaffected by O_2 or CO. However, these general principles do not consider the allosteric state of Hb or the nature of the allosteric effector, and they mostly are derived from the functional behavior of fully nitrosated Hb, whereas Hb is only partially nitrosated *in vivo*. Stamler et al. who studied blood flow regulation by Hb in the physiological oxygen gradient found that the binding of oxygen to heme irons in Hb

promotes the binding of NO to a particular cysteine residue (Cys β 93), forming S-nitrosohemoglobin (HbSNO) (Stamler et al., 1997). Deoxygenation is accompanied by an allosteric transition in HbSNO [from the R (oxygenated) to the T (deoxygenated) structure] that releases the NO group. HbSNO contracts blood vessels and decreases cerebral perfusion in the R structure and relaxes vessels to improve blood flow in the T structure. Thus, by sensing the physiological oxygen gradient in tissues, Hb exploits conformation-associated changes in the position of Cys β 93 of HbSNO to bring local blood flow into line with oxygen requirements. HbSNO can therefore release NO on deoxygenation in the microcirculation. Pawloski et al. have additionally shown that HbSNO inhibits platelet aggregation and that this mechanism is cGMP independent (Pawloski et al., 1998).

2.4.3 Transnitrosation: Transfer of Nitric Oxide Between S-Nitrosothiols

Plasma albumin reacts with NO to form the bioactive adduct AlbsNO; however, the limited intracellular access of AlbsNO suggests the need for a vascular transfer mechanism of NO from a large plasma AlbsNO pool to affect biological function. NO exchange among thiols has been documented by several investigators under non-physiologic conditions (Bennett et al., 1986; Keaney et al., 1993; Keen et al., 1976; Oae et al., 1978). Scharfstein et al. have reported that the transfer of NO between AlbsNO and low molecular weight (LMW) thiol (transnitrosation), such as L-cysteine, occurs rapidly and completely, *in vitro* under physiologic conditions (Scharfstein et al., 1994). In addition, NO appears to shift transiently from high molecular weight (HMW) to LMW S-nitrosothiol pools *in vivo*, as shown in Equation 2.1 (Scharfstein et al., 1994).



Eq. 2.1

Once transnitrosation has occurred and S-nitrosothiols have been formed, these smaller, less diffusion-limited NO adducts can transport NO more efficiently to the vascular smooth muscle cell or platelet surface. Once at the cell surface, the specific metabolic steps that lead to the activation of intracellular guanylyl cyclase and other target effector sites remain unclear. Possible mechanisms include the direct transport of RSNOs into the cytosol or alternatively, cell surface interactions with membrane bound species bearing thiols or heme-containing prosthetic groups (Mordvintsev et al., 1986). Studies performed by Malinski and Taha support these possible mechanisms by showing that a significant NO gradient exists across the vascular smooth muscle cell and platelet membrane, suggesting that transmembrane NO transport is not a diffusion-limited process (Malinski and Taha, 1992).

Hemoglobin may serve as a catalyst for RSNO formation under conditions of high oxygen affinity, in which S-nitrosation of the single β -chain reduced cysteine (93) is favored (Gow et al., 1997; Jia et al., 1996). The resulting SNO-hemoglobin synthesis in the lung allows for LMW RSNO formation through transnitrosation reactions (Jia et al., 1996). The circulatory system may provide end organs with a steady supply of LMW RSNOs which can diffuse out of the erythrocyte and into tissues (Jia et al., 1996). Furthermore, NOS activation itself may form RSNOs, perhaps through intermediate ONOO⁻ in the presence of thiol (Gow et al., 1997; Schmidt et al., 1996). Additional RSNO synthetic reactions may occur *in vivo*, such as protein nitrosation by nitrous acid (HNO₂) in acidic organelles, but these remain to be shown.

2.4.4 S-Nitrosothiol Breakdown in Biological Systems

RSNOs breakdown to yield the corresponding disulfide and NO shown in Equation 2.2.



Both photochemical and thermal pathways for this reaction have been established and more recently a metal ion-catalyzed route, dominant for decomposition in solution (Field et al., 1977; Pou et al., 1994; Sexton et al., 1994). In the absence of copper ions, RSNOs are stable in solution (Williams, 1996). However, even concentrations of copper ions as low as 10^{-6} M are sufficient to affect decomposition with production of NO. Initially it was believed that the form of copper responsible was the abundant Cu(II), but a more detailed study has shown that it is Cu(I) which is the active catalyst (Askew et al., 1995). Cu(I) is readily formed from Cu(II) through reduction by a thiol, present either as an impurity or formed on hydrolysis of the RSNO. Whether this indicates a biological role for Cu(I) in the release of NO from RSNO stores in the body is still questionable; however, Gordge et al. have observed that the antiplatelet aggregation effect of an RSNO is lessened in the presence of a selective complexing agent for Cu(I) (Gordge et al., 1995). Even when copper ions are complexed to a protein, there is still evidence of metal-catalyzed NO release (Dicks and Williams, 1996). Studies performed by Arnelle and Stamler have shown the stability of RSNOs decrease in the order of AlBSNO > GSNO > S-nitroso-N-acetylpenicillamine (SNAP) > CysNO in the same environment whether it contains metal ion chelators or not (Arnelle and Stamler, 1995). Further, S-

nitrosoproteins are often more stable than the S-nitroso derivatives of amino acids and small peptides (Stamler et al., 1992b).

In many tissues, RSNO concentrations, sites of action, and bioactivities may be regulated more by catabolic processes than by synthesis. Several enzymes have been described to break down LMW RSNOs *in vitro*, as shown in Table 2.2 (Askew et al., 1995; Freedman et al., 1995; Hou et al., 1996; Jensen et al., 1998; Trujillo et al., 1998). The relative distribution of these enzymes in different tissues could dramatically alter RSNO bioactivities. In the lung, for example, γ -glutamyl transpeptidase, which converts GSNO to S-nitrosocysteinyl glycine, may give greater membrane permeability for submucosal/smooth muscle bioactivity (Hogg et al., 1997). Furthermore, glutathione peroxidase theoretically may produce NO with the net effect of inactivating GSNO and eliminating NO_x through NO expiration and/or reaction of NO with heme iron(II) (Freedman et al., 1995; Hou et al., 1996). Additional catabolic enzymes have been proposed to exist in platelets, airway epithelial cells, neutrophils, and *Escherichia coli* (Fang et al., 2000; Gordge et al., 1996; Hausladen et al., 1996). Gordge et al. showed that release of NO from GSNO was catalyzed enzymatically by ultrasonicated platelet suspensions (Gordge et al., 1996).

Inorganic reactions also cause RSNO breakdown. Intermediate Fe(S)NO formulation involving LMW thiol groups may contribute to RSNO catabolism (Vanin et al., 1997). Inorganic reactions with copper are highly relevant to S-nitrosocysteine breakdown *in vitro* (Singh et al., 1996). These may theoretically be less relevant *in vivo*, where free copper(I) concentrations are low. However, Cu(I) chelation results in inhibition of bioactivities, which are thought to be related in GSNO catabolism in

TABLE 2.2

Enzyme Systems that Break Down GSNO In Vitro

Enzyme	Nitrogen Oxide Product
(Thioredoxin) Thioredoxin Reductase (Scharfstein et al., 1994)	Nitric Oxide
Glutathione Peroxidase (Hou et al., 1996)	Nitric Oxide
γ -Glutamyl Transpeptidase (Askew et al., 1995; Hogg et al., 1997)	S-Nitroso-Cysteinyl Glycine
(Xanthine) Xanthine Oxidase (Trujillo et al., 1998)	Peroxynitrite
Glutathione-Dependent Formaldehyde Dehydrogenase (Jensen et al., 1998)	Hydroxylamine

platelets and cardiac myocytes (Gordge et al., 1996; Mayer et al., 1998). The RSNO catabolic effects of other biological transition metals are minimal compared with those of Cu and Fe (McAninly et al., 1993). O_2^- has been shown to cause CySNO and GSNO breakdown with second order (in RSNO) rate constants (Aleryani et al., 1998; Jourdeuil et al., 1998). These reactions are apparently first-order in O_2^- (overall $k \sim 3-6 \times 10^8 \text{ M}^{-2}\text{s}^{-1}$). Therefore, micromolar RSNO concentrations would be degraded only very slowly (pMmin^{-1} range) by these reactions in the presence of nanomolar O_2^- concentrations.

2.5 A Novel Design to Improve the Haemocompatibility of Blood-Contacting Materials by Utilizing Endogenous Nitric Oxide and Naturally-Occurring Mechanisms

2.5.1 Description of the Novel Design

The design exploits endogenous NO and naturally-occurring mechanisms to increase the haemocompatibility of blood-contacting surfaces by mechanisms illustrated in Figure 2.4. First, L-cysteine residues are covalently attached to the surface of a blood-contacting material in such a way that their thiol groups are exposed to the surroundings. When blood flows over the surface of the modified material, the exposed thiol groups are able to extract NO from free nitrosated thiols in the blood, specifically AlBSNO, via transnitrosation. The nitrosated L-cysteine residues on the surface formed following transnitrosation quickly release NO from the surface by catalysis of ascorbate and/or copper, or other reducing thiols. Finally, the NO released into the surrounding area inhibits platelet adhesion, aggregation, and thrombus formation by mechanisms discussed previously. After the decomposition of the CySNOs on the surface of the modified

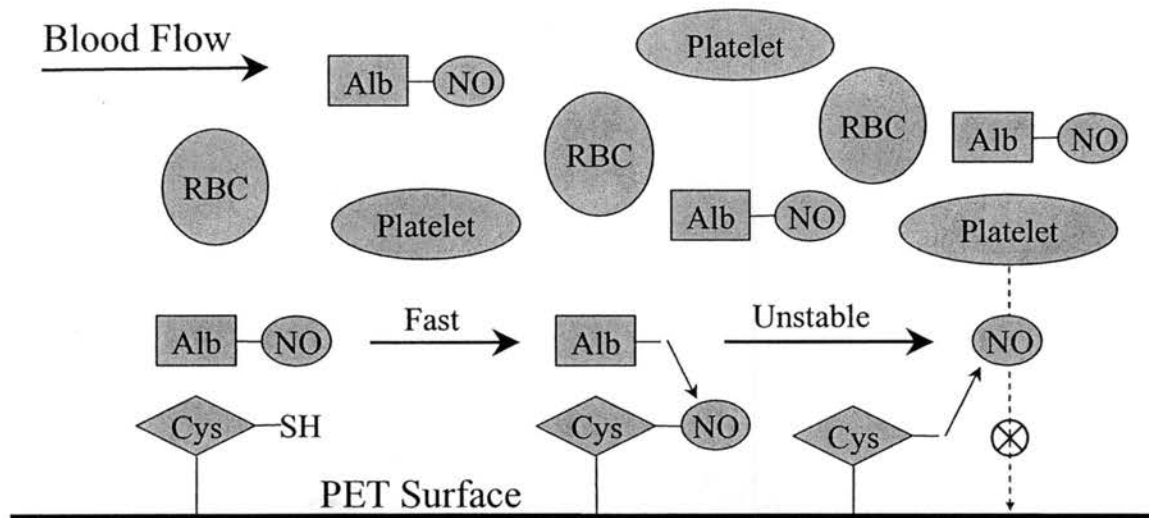


Figure 2.4 Illustration of the concept for the design that exploits endogenous NO and naturally-occurring mechanisms to increase the haemocompatibility of blood-contacting surfaces.

material, the L-cysteine residues are in their reduced form and are available to continue to participate in the transfer and release of NO.

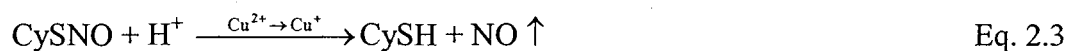
2.5.2 The Rationale for the Design

As discussed in Section 2.3, NO was shown to be a potent inhibitor of platelet activation and aggregation (Azuma et al., 1986; Haynes, 1993; Radomski et al., 1987a) by causing an increase of cGMP in platelets (Furchgott and Zawadzki, 1980; Radomski et al., 1987b). As discussed in Section 2.4.2, there is a large supply of endogenous NO in human blood plasma as NO bound to proteins (S-Nitrosoproteins), mostly as S-nitrosoalbumin (AlbSNO). Stamler et al. have reported that human plasma contains ~ 7 μM RSNOs, of which 96% are S-nitrosoproteins, 82% of which is accounted for by AlbSNO (Stamler et al., 1992a). It has been hypothesized that naturally produced NO circulates in plasma primarily complexed in RSNO species, mainly as AlbSNO. This abundant, relatively long-lived adduct likely serves as a reservoir with which plasma levels of highly reactive, short-lived free NO can be regulated. The chemical half-life of released NO is very short and is inactivated within ~ 0.2 s (Kelm and Schrader, 1990). In comparison with NO, RSNOs are often very stable compounds with half-lives up to 40 min, as in the case of AlbSNO (Stamler et al., 1992b).

A fast and spontaneous transnitrosation reaction (Equation 2.1) exists between AlbSNO and low molecular weight thiols (L-cysteine and glutathione) as shown in Section 2.4.3. Scharfstein et al. have reported that the transfer of NO (called transnitrosation) between AlbSNO and low molecular weight (LMW) thiols, such as L-cysteine, occurs rapidly and completely, *in vitro* under physiologic conditions (Scharfstein et al., 1994). In addition, NO appears to shift transiently from high

molecular weight (HMW) to LMW S-nitrosothiol pools *in vivo*, as shown in Equation 2.1 (Scharfstein et al., 1994). Since L-cysteine is the lowest molecular weight thiol *in vivo*, it is believed that the NO transfer from AlbsNO and CySH is faster than NO transfer to other low molecular weight thiols, such as glutathione. It has also been demonstrated that free L-cysteine, by transnitrosation, can catalyze NO release from AlbsNO (Gordge et al., 1996; Meyer et al., 1994).

NO is quickly released from CySNO due to the instability of CySNO *in vivo*. As discussed in Section 2.4.4, nitrosated high molecular weight thiols such as AlbsNO are much more stable than nitrosated low molecular weight thiols such as CySNO, which is the most unstable RSNO (Arnelle and Stamler, 1995). However, the stability of RSNOs strongly depends on factors such as metal ions, pH, and temperature. As shown in Equation 2.2, nitrosated thiols decompose to yield the corresponding disulfide and the release of NO if no other reducing agents exist, as also discussed in Section 2.4.4. However, the decomposition of CySNO may form NO and reduced L-cysteine if other reducing agents such as thiols and ascorbate are present to reduce Cu^{2+} to Cu^+ , as shown in Equation 2.3 (Hogg, 2000; Stubauer et al., 1999; Williams, 1996).



2.6 Past Research

2.6.1 Design of a Novel Apparatus to Study Nitric Oxide Inhibition of Platelet Attachment to a Surface

The first work in this area for our research group was to establish valid guidelines for the local delivery of NO to reduce platelet deposition on biomaterials. This included

the development of a suitable NO delivery device to study NO inhibition of platelet-biomaterial interactions *in vitro*, and the development of a mathematical model to predict aqueous NO concentration and flux profiles required to inhibit platelet attachment to biomaterials (Ramamurthi and Lewis, 1997; Ramamurthi and Lewis, 1998).

Figure 2.5 shows the thin-slit flow chamber device that was designed to investigate the inhibition of platelet deposition on a biomaterial surface under flow conditions via the local delivery of gaseous NO. A protein-coated polymer was exposed to a flowing platelet suspension, while NO gas permeated through the polymer and into the solution. In one study, the platelets were labeled with a fluorescence dye in order to qualitatively study platelet attachment to the polymer surface. In another study, the platelets were radio labeled with chromium-51 (Cr-51) in order to quantitatively study platelet attachment to the polymer surface. Perfusion rates were based on wall shear rate requirements. Platelet-surface interactions are highly dependent on wall shear rates (Ramamurthi and Lewis, 2000). Physiologically relevant shear rates range between 40 and 5000 s⁻¹ (Turitto, 1982). Shear rates were restricted between 125 and 500 s⁻¹, in order to minimize surface platelet aggregation and thrombus formation, which are substantially enhanced at higher shear rates. The wall shear rate (γ in s⁻¹) was determined from laminar flow analysis in a slit flow chamber, shown in Equation 2.4.

$$\gamma = \frac{3}{2} \frac{Q}{Wb^2} \quad \text{Eq. 2.4}$$

Where Q is the volumetric flow rate (cm³/min), W is the slit width (cm), and b is the half-thickness of the flow slit (cm). Based on the geometry of the flow slit, a flow rate of 1 ml/min corresponds to a shear rate of 250 s⁻¹ and a Reynolds number (based on slit

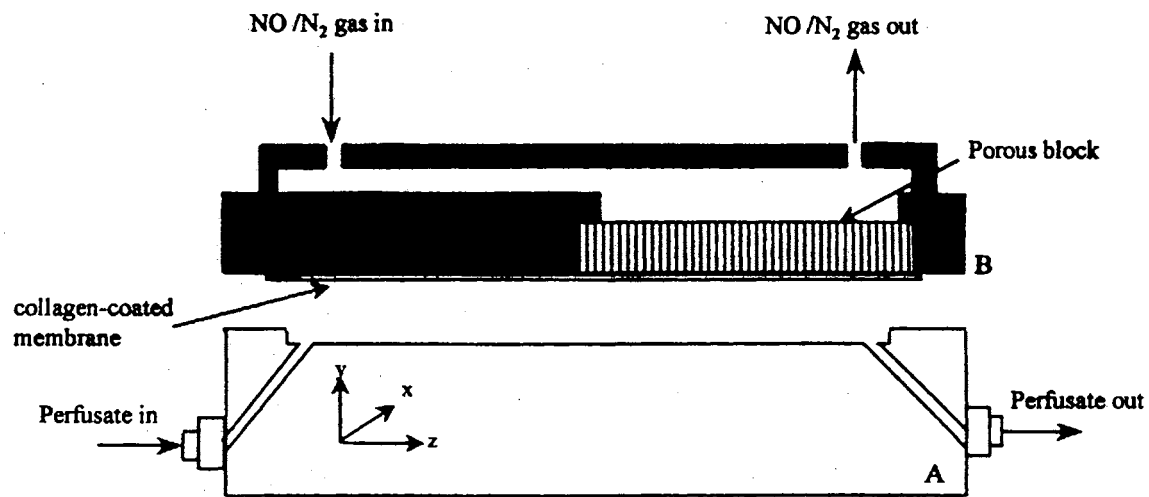


Figure 2.5 Thin-slit flow chamber device used to investigate the inhibition of platelet deposition on a biomaterial surface under flow conditions via the local delivery of gaseous nitric oxide (Ramamurthi and Lewis, 1998).

height) of 2. The NO exposure levels were varied in order to measure the effect of NO inhibition of platelet adhesion to the polymer.

To predict aqueous NO spatial concentrations and fluxes within the flow slit beginning at the porous block, a steady-state dimensionless continuity equation for NO was derived and solved. For a full description of this model, please refer to (Ramamurthi and Lewis, 1997). This study has shown that NO concentrations near the surface on the order of 0.1 nM and surface fluxes on the order of $1 \text{ fmol cm}^{-2} \text{ s}^{-1}$, completely inhibit platelet deposition. Since the concentration of RSNOs in plasma have been shown to be in the micromolar range, there is a sufficient supply of NO that can be transferred to the surface of the L-cysteine-modified polymer by transnitrosation in order to inhibit platelet deposition on the surface. However, the amount of NO released from the surface of the modified material will depend on the concentration of free thiol groups on the surface and the transnitrosation and NO release rates, which were also studied.

2.6.2 The Design and Characterization of L-Cysteine Attached to a Surface

To test the hypothesis that there is sufficient NO in the blood that can be transferred to a modified surface and released in order to prevent platelet attachment to the surface, a preliminary design of L-cysteine attached to a surface was first characterized and then used in studies involving platelets and plasma (Duan, 2001; Duan and Lewis, 2002).

Two popular polymers used in blood-contacting applications, polyurethane (PU) and polyethylene terephthalate (PET), were selected as the substrates to attach L-cysteine. There are two reactive groups on L-cysteine that can be used for immobilization: the primary amine ($-\text{NH}_2$) and the thiol ($-\text{SH}$). A free thiol group is

desired following immobilization of L-cysteine so that NO can be transferred from RSNOs in the blood to the free thiol group and then released into the surroundings to prevent platelet attachment. Therefore, the amino group of L-cysteine was chosen as the reaction group for L-cysteine immobilization. PU and PET have inert surfaces and have to be chemically modified to provide reactive groups for immobilization. This was done by adding an amine group to the surface of the polymer with ethylenediamine for PET and 3-aminopropyltriethoxysilane (APTES) for PU. Glutaraldehyde was chosen as a linker between the amino group of L-cysteine and the aminated polymer surface. The complete reaction scheme used to attach L-cysteine to PET and PU is shown in Figure 2.6:

A chemiluminescence-based assay was developed in order to quantify the amount of L-cysteine on the surface of PET and PU. The first step in this assay is to nitrosate the thiol group on L-cysteine attached to the surface in the presence of equal or excess nitrite under acidic conditions. This step also breaks off the L-cysteine residues due to the acidic conditions. It was believed that the amine bond is the one that actually breaks off, since it is the most susceptible to acidic conditions. Following nitrosation, the nitrosated L-cysteine, now in the solution surrounding the sample, and any remaining nitrite was converted to NO by the use of reducing agents and measured by the use of a NO chemiluminescence analyzer. The reducing solutions are made up of acetic acid with potassium iodide. An excess of free iodine is added in order to convert the nitrosated L-cysteine and the excess nitrite into NO that can be measured. An excess of L-cysteine is added to the reducing solution in order to suppress the conversion of nitrosated L-cysteine to NO and to only measure the amount of excess nitrite converted into NO. The

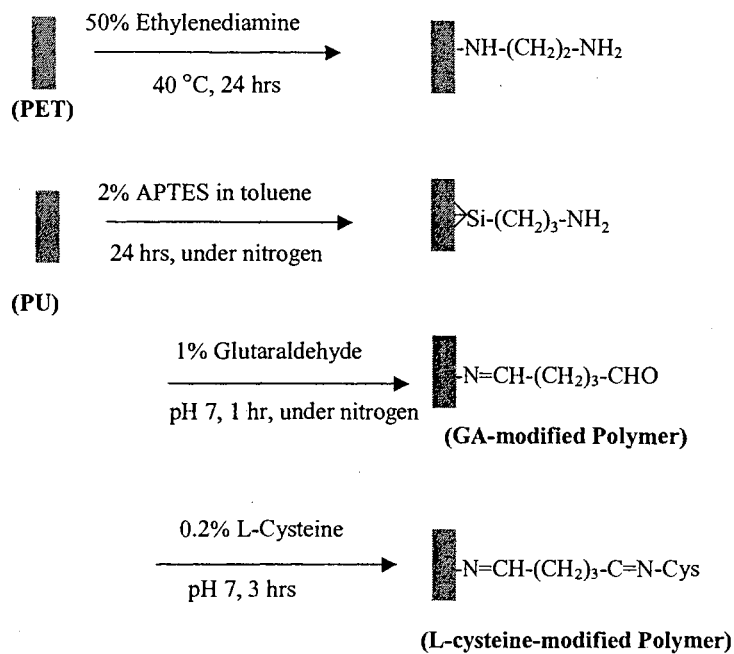


Figure 2.6 Reaction schemes of immobilizing L-cysteine onto the surface of polyethylene terephthalate (PET) and polyurethane (PU) by first adding an amine group by the use of ethylenediamine and 3-aminopropyltriethoxysilane (APTES), respectively and then using glutaraldehyde as a crosslinker.

final concentration of the nitrosated L-cysteine can be determined by calculating the difference between the responses from the two reducing solutions. The detection limit for nitrite using this method was as low as 0.02 nmol per injection. The intra-assay variability was less than 2% and the inter-assay variability was less than 5%. The calculated value of L-cysteine immobilized on the PET surface and polyurethane were consistently $8.1 \pm 1.1 \text{ nmol/cm}^2$ (n=5) and $5.2 \pm 0.9 \text{ nmol/cm}^2$ (n=3), respectively.

2.6.3 Testing the Ability of the Design to Inhibit Platelet Attachment to the Surface

For this study, both stagnant and flow conditions were used to study the haemocompatibility of the modified polymers with platelets. The platelets used in this study were first radio-labeled with isotope Cr-51, so that the amount of platelets could be quantified by measuring the radioactivity of the labeled platelets. Control samples for this study were glycine-modified PET and PU samples under the same experimental conditions. According to the results of the stagnant test the L-cysteine modified PET and PU samples had almost the same number of platelets attached to the samples as the control, when no plasma was present in the platelet suspension. However, when 50% plasma was present in the platelet suspension, the number of platelets attached to the samples was reduced ~ 60% and ~ 50%, respectively, as compared to the control. As indicated by the results from the flow test the number of platelets attached to the surface of the L-cysteine modified PET and PU was about 80% of the number of platelets attached to the surface of the control sample in the absence of plasma. The presence of plasma significantly reduced the number of platelets attached to the L-cysteine modified PET and PU samples to ~ 55% and ~ 25%, respectively, as compared to the control. The results of this study indicate that in order for the L-cysteine modified polymers to inhibit

platelet deposition, they must also be exposed to a source of plasma (containing RSNOs) that likely transfers NO from the plasma to the polymer, in order to inhibit platelet adhesion.

The past studies laid the groundwork for the development of the design. First, the concentration of NO needed to prevent platelets from attaching to a surface was determined. Next, a design to attach L-cysteine to the surface of a polymer was developed and steps were taken to characterize the modified surface. Lastly, the modified material was tested in vitro with platelets in both at both stagnant and flow conditions.

The research described in this thesis continues the work from past studies and attempts to solve any open problems from the past studies. There were some problems when attempting to characterize the surface of the modified material in the past research studies. There were not any methods readily available that could measure L-cysteine attached to a surface at low concentrations ($< 10 \text{ nmols/cm}^2$) and the chemiluminescence method developed by past studies showed some inconsistencies. It was also desired to have alternative methods that could be used to validate the chemiluminescence method. Therefore, Chapter 3 discusses various methods that were used to characterize the surface of the modified polymer.

In past research studies, L-cysteine modified polymer was tested in vitro with platelets in both stagnant and flow conditions in order to measure the amount of platelet attachment to the surface. Although the studies showed a significant reduction in platelet attachment to the modified material, the modified materials were unable to completely inhibit platelet attachment to the surface. It was hypothesized that the addition of more

L-cysteine sites or different L-cysteine-containing moieties on the polymer will increase the NO-release rate per unit area and will increase the inhibition of platelet deposition. Chapter 4 describes the optimization of the polymer modification process that was performed in order to maximize the amount of thiol groups on the surface of the modified polymer. The following groups were used in the modification process: 1. L-cysteine residues, 2. a L-cysteine containing moiety, 2-Iminothiolane, and 3. a polypeptide containing multiple cysteine residues.

In past studies, only the L-cysteine modified polymer was tested in a perfusion chamber with platelet solutions, and the only platelet solutions that were studied were platelets in a buffer solution and platelets in a plasma solution. In Chapter 5, the optimized modified polymers were tested in vitro with platelets under various conditions in order to investigate if the optimized polymers were able to further decrease the amount of platelet attachment to the surface as compared to past studies. These studies investigated not only polymer samples modified with L-cysteine, but also with 2-iminothiolane and a cysteine polypeptide. Also, other platelet solutions were investigated, in addition to the platelets in a buffer solution and platelets in a plasma solution, including platelets in a 7 μ M BSANO solution and platelets in a whole blood solution.

CHAPTER 3

SURFACE CHARACTERIZATION OF L-CYSTEINE MODIFIED POLYMERS

3.1 Introduction

An important step in the development of new biomaterials is the ability to accurately characterize the new material. This is especially important whenever surface modifications are made to the material, since the properties of a surface greatly affect its biocompatibility.

Immobilized L-cysteine on solid substrates (e.g., gel beads) is normally used for affinity chromatography and enzyme immobilization (Tyllianakis et al., 1994). Bui and Thompson reported that L-cysteine was successfully immobilized onto the surface of a biomedical polymer via silane, which was intended to improve the biocompatibility (Bui and Thompson, 1993). After S-nitrosothiols such as nitroso-L-cysteine (CySNO), S-nitroso-glutathione (GSNO), and S-nitroso-bovine serum albumin (BSANO) were shown to have similar biological functions (e.g., vasodilator and inhibitor of platelet aggregation) as free radical nitric oxide, (NO) (Myers et al., 1990; Stamler et al., 1992b) nitrosated L-cysteine immobilized on biomaterials was demonstrated to be able to inhibit platelet adhesion and reduce smooth muscle cell proliferation (Bohl and West, 2000). Furthermore, we reported that L-cysteine attached on polymeric biomaterials, without prior nitrosation, could enhance the haemocompatibility of biomaterials via exploiting endogenous nitric oxide (S-transnitrosation and decomposition of CySNO) (Duan and

Lewis, 2002). This latter method may overcome the disadvantages of NO-releasing polymers, including limited life span and toxicity. Thus, the quantification of immobilized L-cysteine would be necessary for characterizing the attachment of L-cysteine and paving the way for its further applications.

Using available thiol-measuring techniques, it was difficult to characterize the surface of the biomaterial modified with L-cysteine, a common thiol, since many of the techniques were developed for measuring thiols in solution and not thiols attached to a solid surface. Another difficulty was that the low molar concentration of L-cysteine expected on the surface (in the nanomolar range) was below the lowest detectable limits of many of the measurement techniques. This chapter reviews some of the more common surface characterization and thiol measurement methods and describes the problems encountered when using some of the methods to measure immobilized L-cysteine and how some of the methods were adapted to characterize L-cysteine immobilized on a surface.

L-cysteine and other thiol-containing compounds have often been quantified using Ellman's reagent, 5,5-dithiobis (2-nitrosbenzoic acid) (DTNB) (Jocelyn, 1987; Riddles et al., 1979). The disadvantages of this assay include thiol autoxidation, sensitivity to pH, inability to accurately detect concentrations in the nanomolar range, and interference from oxygen, nucleophiles, and nitric oxide donors (Gergel and Cederbaum, 1997; Riddles et al., 1979). Additionally, Tyllianakis et al. found that this method is not suitable for the assay of certain immobilized L-cysteine, which may be contributed to steric hindrance effects of Ellman's reagent (Tyllianakis et al., 1994).

The method reported by Tyllianakis et al. is more accurate to determine immobilized L-cysteine, since it utilizes bicinchoninic acid (BCA) to form a color complex with Cu^+ after Cu^{2+} is reduced by a thiol group. However, color contribution may result from other reducing groups with a redox potential lower than Cu^{2+} (e.g., aldehyde and hydrazido). Another problem with this method is that it is unable to accurately detect concentrations of L-cysteine in the range that is expected on the surface of the modified L-cysteine polymer.

Other methods, such as fluorescence microscopy, (Cook et al., 1996; Swartz, 1996) which utilizes a fluorescent probe specific for thiols that can be visualized on the surface of a modified material, and X-ray photoelectron spectroscopy, (Girardeaux et al., 1996; Kim et al., 2000) which measures the atomic percentages of elements present on a modified surface by measuring the photoelectrons emitted from a surface excited with x-rays, have been more successful methods for detecting immobilized L-cysteine at lower concentrations. However, these qualitative assays cannot determine molar surface concentrations of immobilized L-cysteine.

One focus of this work involves modifying chemiluminescence-based assays developed for aqueous analysis of nitrosothiols for quantitatively determining surface concentrations of immobilized L-cysteine. These assays work via detecting nitrosothiols and/or nitrite changes in surrounding solution following the nitrosation of immobilized L-cysteine with acidified nitrite. These assays are based on the following findings: (i) free and immobilized L-cysteine can be completely nitrosated to form CysNO with acidified nitrite (Byler et al., 1983; Stamler et al., 1992b); (ii) both nitrosothiols and nitrite in the same solution can be measured by using a reducing agent of potassium iodide in glacial

acetic acid that is supplemented with iodine (Samouilov and Zweier, 1998); (iii) adding ammonia sulfamate or sulfanilamide to the reducing solutions abolishes the production of NO from the nitrite in the reducing solution (Marley et al., 2000; Samouilov and Zweier, 1998); (iv) the release of NO from nitrosothiols can be blocked and the NO contribution from nitrite can be measured by using a reducing solution of potassium iodide in glacial acetic acid supplemented with free L-cysteine (Samouilov and Zweier, 1998); and (v) nitrosothiols can be detected by using a neutral pH reducing solution of copper chloride (CuCl) and L-cysteine (Fang et al., 1998). In this work, the immobilized L-cysteine is hydrolyzed by the strong acid during nitrosation and CySNO is detached from the surface. The amount of CySNO that is broken off from the surface is measured by using the methods described above.

3.2 Materials and Methods

3.2.1 Reagents

Glacial acetic acid, potassium iodide, and sodium nitrite were purchased from Fisher Scientific (Fairlawn, NJ). Phosphate buffered saline (PBS, pH 7.4) was obtained from Life Technologies (Gaithersburg, MD). Polyethylene terephthalate (PET) (thickness = 0.2 mm) was supplied by DuPont (Hopewell, VA). 5-Iodoacetamidofluorescein (5-IAF) was purchased from Molecular Probes (Eugene, OR). Ammonia sulfamate, copper chloride, ethylenediamine, glutaraldehyde (GA), glycine, iodine, L-cysteine, sulfanilamide, and all the other reagents were purchased from Sigma Chemical Co. (St. Louis, MO). All water used was of HPLC-grade quality and was deoxygenated by bubbling nitrogen in the water prior to use.

3.2.2 Immobilization of L-Cysteine onto PET Surface

Primary amine groups were first attached onto the PET film surface as previously described (Desai and Hubbell, 1991). As described in the previous chapter, Figure 2.5 depicts the immobilization process that was initially used prior to optimization of the process, which is described later in Chapter 4. Briefly, PET sheets (1 cm × 3 cm) washed by acetone were incubated in 50% aqueous ethylenediamine for 24 hours at 40 °C to incorporate a primary amine at the PET ester linkage. The aminated PET films were then washed with water and cured for at least 24 hours at ambient temperature. The PET films were then incubated with 1% glutaraldehyde in 10 mM PBS with nitrogen bubbling through the solution for one hour to attach glutaraldehyde to the primary amine. Following glutaraldehyde addition, the PET films were rinsed and then immersed in a 0.2% L-cysteine solution and gently shaken overnight to immobilize the L-cysteine to the PET. Prior to each assay, the PET films immobilized with L-cysteine were rinsed thoroughly to remove any absorbed L-cysteine. All steps of the modification process were performed in a glove box under a dry nitrogen atmosphere to avoid oxidizing the thiol groups and oxygen was removed from all solutions by bubbling nitrogen through each solution. Also, all L-cysteine solutions and L-cysteine modified polymer samples were kept covered to prevent damaging light from oxidizing the thiol groups.

3.2.3 Fluorescence Labeling of L-Cysteine Modified PET Samples

Fluorescent labeling is widely used in histochemistry, cell sorting, molecular structure and function studies, and many other experimental techniques for attaching highly sensitive visual and spectrophotometric markers to substances for identification and observation. When fluorescent molecules are irradiated with energy (light) of an

appropriate wavelength, a portion of this energy is absorbed and electrons are excited to a higher energy state. As these electrons return to their ground (unexcited) state, they do so in a series of steps or cascades. The energy associated with these electronic transitions is released and may be emitted as visible light. These releases take place in less than 10^{-4} seconds.

The most desirable characteristics in a fluorescent dye are strong light absorption, excitation stability, the nature of the wavelength shift, and high fluorescence efficiency. One of the most common fluorescent probes for the detection of thiols, such as L-cysteine, is 5-Iodoacetamidofluorescein (5-IAF). Reactions with iodoacetamides are generally carried out in the physiological pH range and usually are rapid at room temperature or below. The iodoacetamide derivative of fluorescein is also the most intensely fluorescent low molecular weight reagent available for detecting thiols.

Possible problems associated with fluorescent staining are fading, autofluorescence, and nonspecific fluorescence. Exposure of the sample to blue light for only three minutes can cause a 50% loss of the intensity. Therefore, steps are taken during the experiments to prevent exposure of the samples to light, such as turning off all artificial lights, preventing natural light from entering the room, covering all samples with aluminum foil during the experiments, and storing all samples in a black film box. Some polymers may naturally autofluoresce without exposure to any fluorescent dyes. Therefore, a blank sample of PET should be checked for any autofluorescence prior to analyzing the L-cysteine modified PET samples. Nonspecific fluorescence may occur when the fluorescent probe reacts with other chemical species on the sample other than the targeted thiol groups. To check for nonspecific fluorescence, the fluorescent probe

should be tested with each of the linker groups attached to the surface of the PET sample, the ethylenediamine and the glutaraldehyde.

A 2 mM 5-IAF stock solution was prepared in a 50 mM phosphate buffer solution (pH 7). The 5-IAF solution was kept completely covered at all times to keep out damaging light that could cause fading. Each of the following PET samples, 1 cm x 1 cm, were incubated with 4 ml of the stock solution for at least 1 hour: 1) blank PET, 2) ethylenediamine attached to PET, 3) ethylenediamine and glutaraldehyde attached to PET, 4) ethylenediamine, glutaraldehyde, and L-cysteine attached to PET, and 5) ethylenediamine, glutaraldehyde, and glycine attached to PET. All of the samples were continuously shaken during the incubation time to ensure complete reaction of the fluorescent probe with the L-cysteine on the sample. The samples were rinsed with water and kept in the dark until further analysis. The surface of each sample was examined by using an argon laser-scanning microscope (Leica TCS SP2, Exton, PA) in confocal mode with a 10.0 x 8.0 oil immersion objective lens. The filter set was set at 488 nm excitation and 515 nm emission.

3.2.4 X-ray Photoelectron Spectroscopy (XPS) Analysis of L-Cysteine Modified PET Samples

XPS provides a non-destructive trace elemental analysis of the outer few atomic layers on a variety of materials and can provide chemical bonding and/or oxidation state information. Photoelectron spectroscopy is based upon a single photon in / electron out process. In XPS, the photon is absorbed by an atom in a molecule or solid, leading to ionization and the emission of a core (inner shell) electron. The kinetic energy distribution of the emitted photoelectrons can be measured using an electron energy

analyzer in order to construct a photoelectron spectrum. For each and every element, there is a characteristic binding energy associated with each core atomic orbital, i.e. each element gives rise to a characteristic set of peaks in the photoelectron spectrum at kinetic energies determined by the photon energy and respective binding energies. The presence of peaks at particular energies therefore indicates the presence of a specific element in the sample under study. Furthermore, the intensity of the peaks is related to the concentration of the element within the sample region. Energy analysis of the photoelectrons emitted from the surface excited with x-rays can be used to characterize a variety of inorganic and organic materials including semiconductors, thin films, electropolished stainless steel, and insulating samples like ceramics, glasses, catalysts, paper, plastics, and biomedical devices. Typical data may include a low resolution survey scan for elemental composition and a high resolution energy scan for chemical bonding information. Detection limits are typically 0.01 – 1 atom% at a depth resolution of 10 – 100 Å.

XPS analysis of samples was performed at the Chemical Engineering and Material Science Department at the University of Oklahoma (Norman, OK) and at the Chemistry Department at Lehigh University (Bethlehem, PA). Each of the following PET samples, 1 cm x 1 cm, was prepared for XPS analysis: 1) blank PET, 2) ethylenediamine and glutaraldehyde attached to PET, and 3) ethylenediamine, glutaraldehyde, and L-cysteine attached to PET.

XPS was also used to ensure that L-cysteine is completely removed from the surface of PET after nitrosation with acidic nitrite. A modified PET sample, 1 cm x 1 cm, was initially placed in 4 ml of a 0.5 M HCl solution containing 40 µM of excess

nitrite. The solution was gently shaken for the same time period used for nitrosation, one hour. The PET sample was removed from the acidic nitrite solution and rinsed prior to analysis. Two control samples were used for comparison in the analysis. One was a blank PET sample subjected to the same experimental conditions described above, and the other was a modified PET sample that was not subjected to the experimental conditions.

3.2.5 Nitrosation of Free and Immobilized L-Cysteine

The chemiluminescence method used for quantifying L-cysteine attached to the polymer surface required nitrosation of L-cysteine (CySNO) on the surface and subsequent removal of CySNO from the polymer. The nitrosation reaction is equimolar between L-cysteine and nitrite (NO_2^-), according to Equation 3.1.



Free L-cysteine and L-cysteine-modified PET (PET-Cys) were nitrosated via an acidified NO_2^- solution, which is a typical method for nitrosating thiols (Byler et al., 1983; Stamler et al., 1992b). During nitrosation, the solutions were gently shaken for one hour. All nitrosation procedures were carried out in capped, amber-colored tubes to prevent NO from escaping from the system and to keep light from entering the system and oxidizing the thiol groups.

For nitrosation of immobilized L-cysteine, PET-Cys was freshly prepared and cut into small pieces (1 cm x 3 cm). Each piece was added to a 4 ml 0.5 M HCl solution initially containing 40 μM NO_2^- . A higher concentration of NO_2^- was used in the nitrosation of PET-Cys in order to ensure that there would be an excess of NO_2^- for

complete nitrosation. For nitrosating free L-cysteine, various ratios of nitrite to L-cysteine were added to a 0.5 M HCl solution. Equimolar concentrations of NO_2^- and L-cysteine, as well as NO_2^- concentrations less than L-cysteine concentrations were used in some cases to consume all of the NO_2^- .

3.2.6 Chemiluminescence Analysis of L-Cysteine Modified PET Samples

Chemiluminescence analysis of samples involved the formation of NO from CySNO and/or NO_2^- and the subsequent reaction of NO with ozone. The reaction between NO and ozone leads to the formation of an excited form of NO_2 (NO_2^*) with subsequent release of electromagnetic radiation of characteristic frequency, as shown in the reaction steps below:



Emission from electronically excited nitrogen dioxide is in the red and near-infrared region of the spectrum and is detected by a thermoelectrically cooled, red-sensitive photomultiplier tube (PMT). NO from the sample and ozone produced in the electrical discharge of the detector are mixed in the chemiluminescence reaction cell. A red cut-off filter between the reaction cell and the PMT selectively transmits the light emitted by the NO/O_3 reaction to be detected by a recorder.

Following nitrosation, a Sievers 270B chemiluminescence NO analyzer (Sievers Corporation, Boulder, CO) was used to measure the amount of nitrosated thiols and/or NO_2^- in each sample, by measuring the equivalent amount of NO released upon exposure to a reducing solution. Several methods utilizing one or more of the research methods

described previously were used in order to determine the most accurate procedure to measure the CySNO detached from the surface of modified PET.

Method 1

This method uses two reducing solutions to measure the amount of L-cysteine on the modified PET surface. Reducing solution A is composed of 0.2 M potassium iodide in glacial acetic acid saturated with iodine. This reducing solution instantaneously converts NO_2^- and nitrosothiols (such as CySNO) to NO; whereupon, the NO is rapidly purged from solution and detected. Thus, the NO purged represents the combined NO_2^- and nitrosothiols concentration. Reducing solution B is composed of 0.2 M potassium iodide in glacial acetic acid supplemented with 25 mM free L-cysteine. Additional L-cysteine has been shown to minimize NO release from GSNO, (Samouilov and Zweier, 1998) such that similar effects were expected for CySNO. The excess L-cysteine in the reducing solution is believed to suppress the release of NO from CySNO, without affecting the excess NO_2^- in solution from being converted to NO. Thus, the NO rapidly purged from this reducing solution represents only the NO_2^- concentration. The reaction between excess NO_2^- and the reducing solution to produce NO is believed to occur at a much faster rate than the nitrosation reaction between excess NO_2^- and L-cysteine. Thus, the NO rapidly purged from this reducing solution represents the NO_2^- concentration. The nitrosothiol concentration was obtained by finding the difference between the concentration of the CySNO plus excess NO_2^- determined by using reducing solution A and the concentration of excess NO_2^- determined by using reducing solution B.

This method was validated by using standard solutions of free L-cysteine. For one test, a 10 μM nitrite solution, a 10 μM CySNO solution, and a solution containing

both 5 μM CySNO and 5 μM nitrite were each measured by using both reducing solutions. The 10 μM CySNO solution was made by adding an equimolar amount of L-cysteine and nitrite to a 0.5 M HCl solution and assuming complete nitrosation. The 5 μM CySNO and 5 μM nitrite solution was made by adding twice the molar concentration of nitrite to L-cysteine to a 0.5 M HCl solution and assuming complete nitrosation with an equimolar amount of excess nitrite remaining in the solution. For another test, 2.5, 5, and 10 μM L-cysteine solutions were nitrosated using 5 μM NO_2^- solutions and then measured.

To measure the amount of L-cysteine on the surface of modified PET samples, samples were obtained during nitrosation of the L-cysteine modified polymer. An acidic NO_2^- solution composed of 40 μM NO_2^- in 0.5M HCl was used to nitrosate the L-cysteine residues on the polymer. The acidic solution breaks the aldehyde bond between glutaraldehyde and L-cysteine (see Results section), thus the nitrosated cysteine breaks off during nitrosation and can be detected. The concentration of CySNO in the solution was then measured by using both reducing solutions A and B.

Method 2

This method measures the amount of L-cysteine on the surface of modified PET by using ammonium sulfamate or sulfanilamide, which are nitrite scavengers. Both ammonium sulfamate and sulfanilamide have been shown to react with nitrite in solution; however, sulfanilamide has been shown to be more effective (Marley et al., 2000). Solutions of 0.5% ammonium sulfamate or sulfanilamide were added to 5, 10, and 100 μM nitrite standard solutions in a 1:5 volume ratio. Any NO release from the standard

solutions was measured by injecting samples into reducing solution A. Thus, since NO_2^- was scavenged, the measurement is representative of only nitrosothiols.

To validate the ability of this method to measure CySNO in solution, sulfanilamide was also used with free L-cysteine in solution nitrosated using either a 1:1 or a 1:2 molar ratio of L-cysteine to nitrite. After the L-cysteine solutions were allowed to nitrosate for 1 hour while shaking gently, a 1:5 volume ratio of 0.5 wt% sulfanilamide to sample was added to react with any excess nitrite. The concentration of CySNO in the solution was measured by using reducing solution A. Since both ammonium sulfamate and sulfanilamide were both shown to do equally well in scavenging excess nitrite in solution, only sulfanilamide was selected to be used to measure CySNO. L-cysteine concentrations of 1 μM and 10 μM were used because this is the range of the solution concentrations expected after CySNO is removed from the modified PET samples.

To measure the amount of L-cysteine on the surface of modified PET samples, samples were obtained by the nitrosation of the L-cysteine modified polymer, as described previously. A 0.5 wt% sulfanilamide solution was added to the sample (1:5 volume ratio of sulfanilamide to sample) containing nitrite and the nitrosated L-cysteine that had been broken off of the PET surface. The concentration of CySNO in the solution was measured by using reducing solution A.

Method 3

This method measures the amount of L-cysteine on the surface of modified PET by measuring the concentration of CySNO directly by using a reducing solution at 50°C containing 100 μM saturated CuCl in a phosphate buffer (pH 7.4) with 1 mM free L-cysteine. The neutral buffer does not promote the release of NO from any excess NO_2^- in

the solution. Thus, the NO released into solution, then purged and detected, is indicative of only the nitrosothiol (i.e. CySNO).

To validate this method, free L-cysteine in solution was nitrosated using either a 1:1 or a 1:2 molar ratio of L-cysteine to NO_2^- . The following L-cysteine concentrations were measured: 1, 5, 10, and 20 μM . To measure the amount of L-cysteine on the surface of modified PET samples, samples were obtained by the nitrosation of the L-cysteine modified polymer, as described previously. The concentration of CySNO in the solution surrounding the sample after nitrosation was measured directly by using the CuCl reducing solution.

For all three methods, the concentrations were determined by using a calibration curve determined by measuring the NO release via the reducing solutions from standard solutions of either NO_2^- and/or nitrosated glutathione.

The experimental set-up for chemiluminescence detection included a purging vial containing the reducing solution connected to the NO chemiluminescence detector and is shown in Figure 3.1. After the appropriate reducing solution was added to the purging vial (D \times H: 20mm \times 70mm), the solution was purged by nitrogen via a fritted disk (Pore Diameter: 25-50 μm) at the bottom of the vial. When using the reducing solution described in Method 3, a purging vial with a water jacket was used in order to keep the reducing solution at a constant temperature of 50 $^\circ\text{C}$. All other reducing solutions were used in the purging vial shown in the figure at room temperature. Aqueous samples from the experiments were obtained using a gas-tight syringe (Hamilton Company, Reno, NV) and then injected into 10 ml of the reducing solution. The NO released from the sample was carried with the nitrogen purge to the detector, where it reacted with ozone to

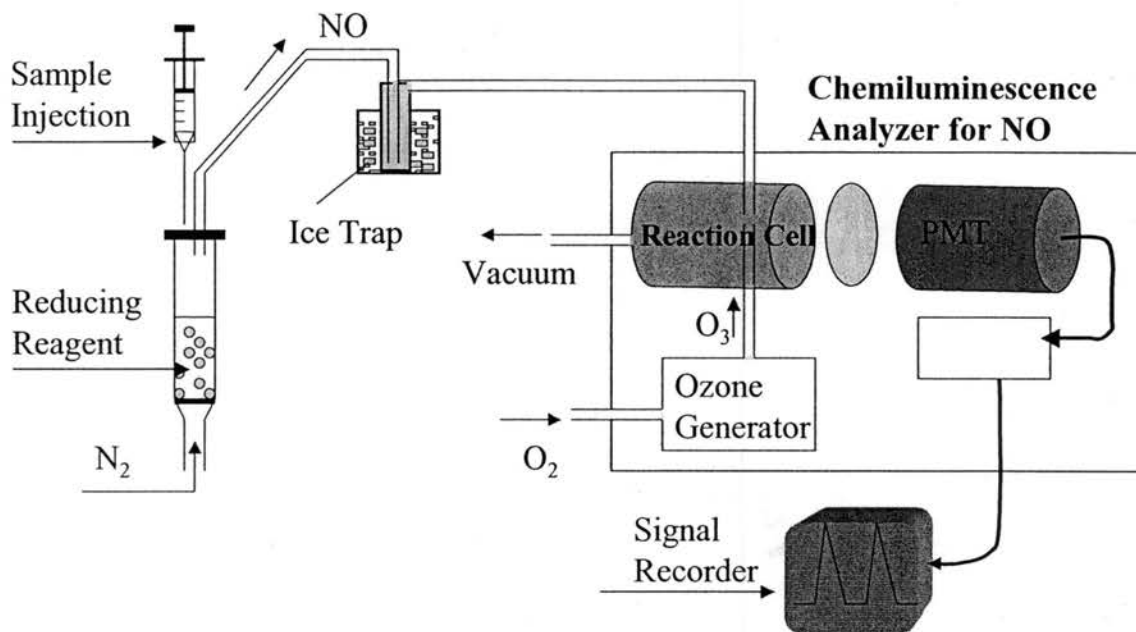


Figure 3.1 Experimental set-up of using the chemiluminescence analyzer to measure nitrosated L-cysteine that has been broken off the surface of L-cysteine modified PET.

give a signal. The volume of each sample varied between 20 and 200 μl depending on the detection limits. The output signal from the detector was sent to an integrator that calculated the area under each sample peak. The areas were compared to the standards for quantification.

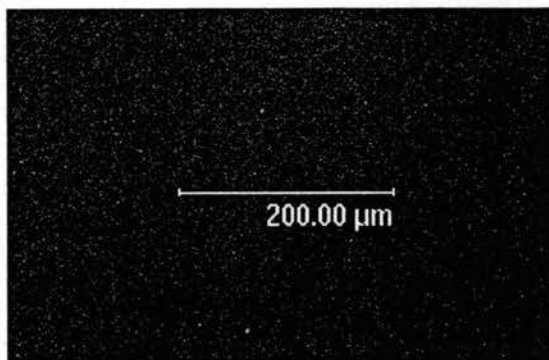
3.3 Results

3.3.1 Fluorescence Microscopy Analysis of L-Cysteine Modified PET Samples

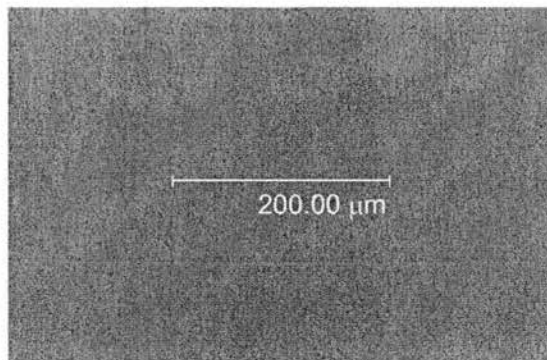
Figure 3.2 shows the scans taken of the surface of the following samples that were labeled with the fluorescent probe 5-IAF: 1) blank PET, 2) ethylenediamine attached to PET, 3) ethylenediamine and glutaraldehyde attached to PET, 4) ethylenediamine, glutaraldehyde, and L-cysteine attached to PET, and 5) ethylenediamine, glutaraldehyde, and glycine attached to PET. A lighter scan is indicative of the more fluorescence on the sample. Thus, the scans that are darker shades (black) show very little to no fluorescence on the samples.

The first scan shows the surface of a blank sample of PET. The scan shows some minor scattered fluorescence on the sample; the sample is essentially non-fluorescent. There were no thiol groups on the blank surface to react with the fluorescent probe; therefore, it is believed that the minor scattered fluorescence is due to autofluorescence from the PET sample.

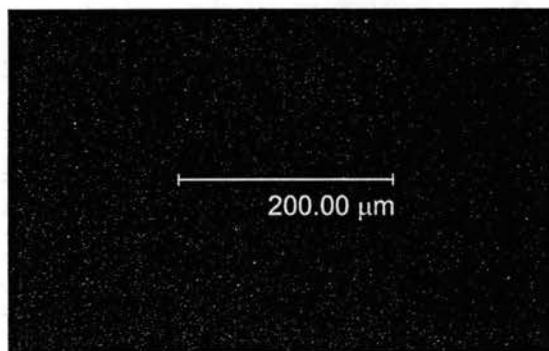
The second scan shows the sample with ethylenediamine attached to the surface. The scan is very bright and highly fluorescent. 5-IAF can also react with primary amines in the absence of thiol groups. The bright fluorescence shows a high concentration of ethylenediamine completely covering the surface of PET.



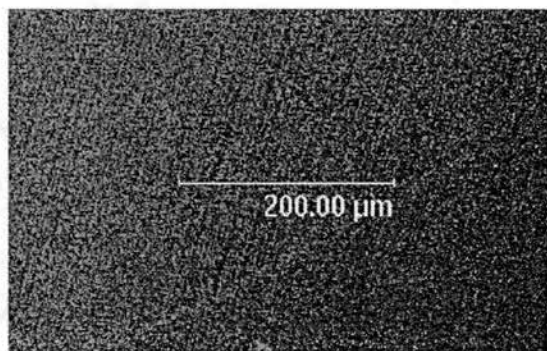
Scan 1. Blank PET



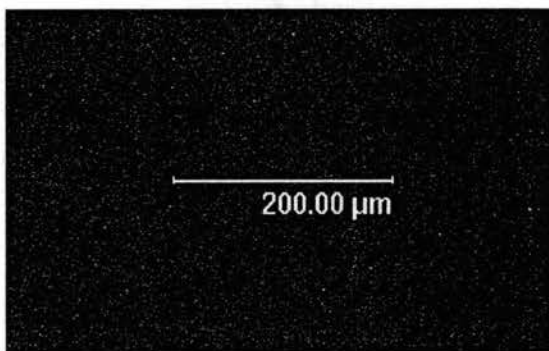
Scan 2. PET + Ethylenediamine



Scan 3. PET + Ethylenediamine +
Glutaraldehyde



Scan 4. PET + Ethylenediamine +
Glutaraldehyde + L-cysteine



Scan 5. PET + Ethylenediamine +
Glutaraldehyde + Glycine

Figure 3.2 Fluorescence microscopy analysis of modified PET samples using 5-IAF.
Scans are shown at 80x magnification.

The third scan shows the sample with ethylenediamine attached to the surface of PET and then glutaraldehyde attached to the terminal amine group of ethylenediamine. Similar to the first scan of blank PET, there is only minor scattered fluorescence on the sample. Since the fluorescent probe does not react with aldehyde groups that are present on the surface after the addition of glutaraldehyde, fluorescence was not expected. It is also important to point out that there appears to be complete coverage of glutaraldehyde on the surface, because any exposed amine groups would react with the fluorescent probe and result in bright fluorescence on the surface.

The fourth scan shows the sample of PET with both linker groups (ethylenediamine and glutaraldehyde) and L-cysteine attached to the surface of PET. This scan shows bright fluorescence on the surface; however, the fluorescence is not as bright and as widespread on the surface as seen in the second scan with just ethylenediamine on the surface. It is believed that this is due to one or a combination of the following reasons: i) 5-IAF is more reactive with amine groups than with thiol groups and/or ii) there is not complete coverage of L-cysteine on the surface, due to possible crosslinking of the glutaraldehyde groups. Also seen in this scan is a series of striations on the surface of the sample. These striations were first noticed in an image sent by DuPont of the surface analysis from a scanning electron microscope, shown in Figure 3.3. It is believed that these striations are a result of fabrication of the PET films and that the crosslinkers and the L-cysteine react with the surface of PET along these striations.

The fifth scan shows the sample of PET with both linker groups and glycine attached to the surface of PET. This sample was used as a control group to test the selectivity of the fluorescent probe. Glycine does not contain any thiol or primary amine

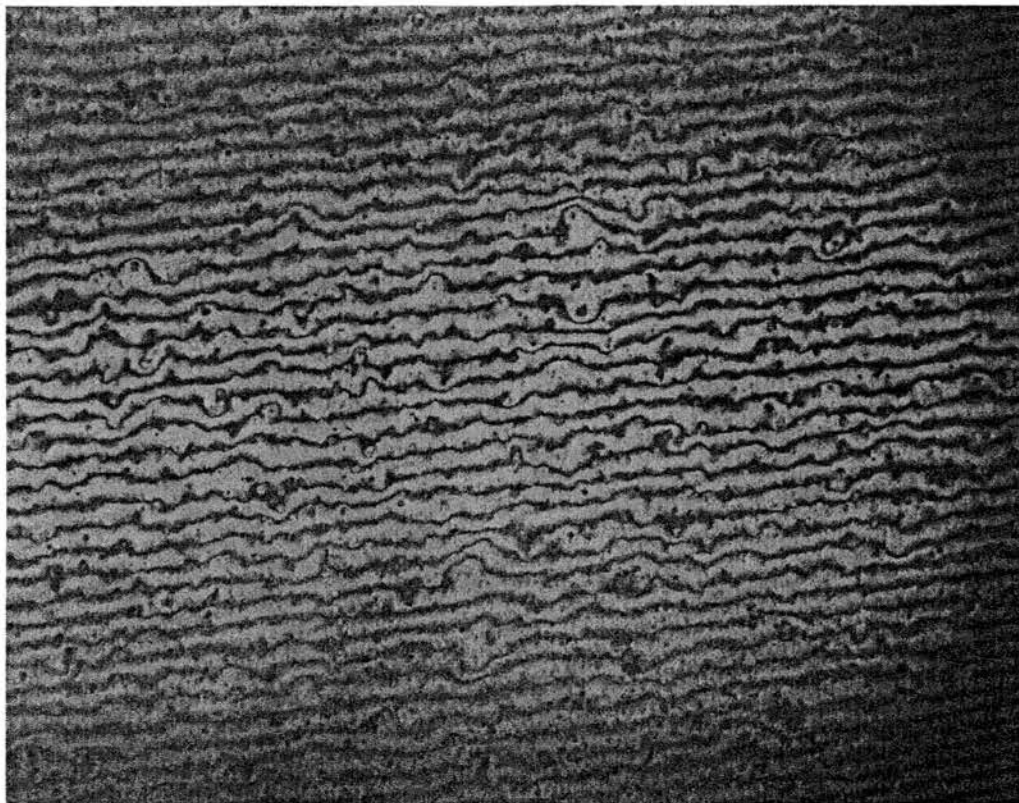


Figure 3.3 Film surface characteristics of Melinex S polyethylene terephthalate (PET) provided by DuPont Teijin Films™. One fringe displacement $\sim 0.273 \mu\text{m}$.

groups that would react with the fluorescent probe. As shown in the scan, only minor scattered fluorescence is shown on the surface of the sample due to autofluorescence.

3.3.2 XPS analysis of L-Cysteine Modified PET Samples

Table 3.1 shows the results of XPS analysis of L-cysteine-modified PET surfaces. The rows labeled “measured” in the table shows the atomic percent of each element measured by XPS. The rows labeled “theoretical” in the table shows the atomic percent of each element determined by assuming there is complete coverage of each group attached to the PET surface and exactly a one-to-one binding between the PET surface, each linker group, and L-cysteine. For example, the monomer that makes up PET contains 10 carbon atoms and 4 oxygen atoms; therefore, assuming that XPS measures one monomer on the surface of PET and that there is no surface contamination, there would be 71.43 atom% of carbon and 28.57 atom% of oxygen on the surface. Assuming next that one ethylenediamine molecule binds to one PET monomer on the surface and that one glutaraldehyde molecule binds to one ethylenediamine molecule, there would be 15 carbon atoms, 4 oxygen atoms, and 2 nitrogen atoms, resulting in 71.43 atom% of carbon, 19.05 atom% of oxygen and 9.52 atom% of nitrogen on the surface. The same reasoning would apply to the addition of L-cysteine to the surface of PET via ethylenediamine and glutaraldehyde. When interpreting the data from XPS analysis, it is important to remember that the analysis is only of the surface of the sample and not the bulk and that measured values may not match theoretical values due to changes occurring at the surface for numerous reasons, including oxidation, contamination, etching, measurement of partial monomers, etc.

TABLE 3.1

Atom% of Elements on Blank PET Sample and Modified PET Samples
(Comparison of Theoretical with Measured by XPS)

Sample Description	Blank PET	PET + ED + GA	PET + ED + GA + Cys
C's (Measured)	74.01 ± 0.32	72.21 ± 0.52	74.21 ± 1.17
C's (Theoretical)	71.43	71.43	66.67
O's (Measured)	25.99 ± 0.31	23.25 ± 0.08	20.57 ± 0.99
O's (Theoretical)	28.57	19.05	18.52
N's (Measured)	0	4.54 ± 0.44	4.70 ± 0.36
N's (Theoretical)	0	9.52	11.11
S's (Measured)	0	0	0.52 ± 0.18
S's (Theoretical)	0	0	3.70

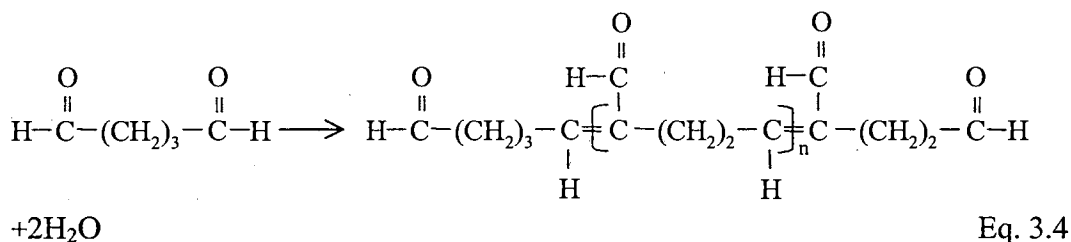
Abbreviations. PET = Polyethylene Terephthalate, ED = Ethylenediamine, GA = Glutaraldehyde, Cys = L-Cysteine, C = Carbon, O = Oxygen, N = Nitrogen, S = Sulfur

Note. Values shown are mean values ± standard deviation (n=2).

For the blank PET sample, the measured atomic percent of carbon is more than the theoretical value and the measured atomic percent of oxygen is less. This could possibly be due to contamination at the PET surface or the XPS sampling includes partial monomers, in addition to entire monomers, such that the theoretical reasoning involving complete monomers is different than that actually measured.

When interpreting the data for the PET sample with ethylenediamine and glutaraldehyde attached, the amount of nitrogen is a good indicator of the amount of ethylenediamine attached to the surface since ethylenediamine is the only component that contains nitrogen. The measured value is approximately one half of the theoretical value, approximately 4.5 atom%, suggesting incomplete coverage of ethylenediamine on the PET surface. Also for this sample, the measured oxygen content is more than the theoretical value, which could also be due to less than a one-to-one binding of ethylenediamine to the PET surface. For example, if there was a 3:1:1 ratio of PET:ethylenediamine:glutaraldehyde, then this would result in theoretical atom% of 71.43, 24.49, and 4.08 for carbon, oxygen, and nitrogen on the surface, respectively, which matches the measured values closer than assuming a 1:1:1 ratio of PET:ethylenediamine:glutaraldehyde. In addition to incomplete coverage of ethylenediamine on the PET surface, there could also be some crosslinking of the glutaraldehyde residues that would also result in lower atom% of nitrogen and a higher atom% of oxygen on the surface. Studies have shown the polymerization of glutaraldehyde can occur quickly in aqueous solutions under alkaline pH conditions to yield an unsaturated product shown next in Equation 3.4 (Monsan et al., 1975; Richards

and Knowles, 1968). However, glutaraldehyde polymeric moieties can also exist in aqueous solutions as low as pH 5 (Richards and Knowles, 1968).



When interpreting the data for the PET sample with both linker groups and L-cysteine attached, the amount of sulfur is a good indicator of the amount of L-cysteine attached to the surface, since L-cysteine is the only group that contains sulfur. The measured amount of sulfur is less than the theoretical value by approximately 86%, suggesting incomplete coverage of L-cysteine on the surface of the modified polymer. It is probable that this was due to the incomplete coverage of ethylenediamine on the surface and/or glutaraldehyde crosslinking on the surface that resulted in fewer sites available for L-cysteine attachment. The interpretation of the XPS results at this point of the analysis becomes very difficult due to the many possible combinations of the groups on the surface. However, the incomplete coverage of L-cysteine on the surface could also be due to other problems such as steric hindrance of the linker groups or L-cysteine, reactivity problems, or equilibrium issues.

XPS was also used to ensure that L-cysteine was completely removed from the surface of a L-cysteine modified PET sample after one hour of nitrosation in an acidic nitrite solution. XPS showed that there was no detectable sulfur on the surface after one hour in the acidic nitrite solution (Table 3.2). When comparing the L-cysteine modified sample to the sample of a blank PET submitted to the same experimental conditions,

TABLE 3.2

Atom% of Elements on a Modified PET Sample and a Blank PET Sample Placed in an Acidic Nitrite Solution for One Hour, Compared to a Modified PET Sample Not Placed in an Acidic Solution

Sample Description	Modified PET in Acidic Nitrite Solution	Blank PET in Acidic Nitrite Solution	Modified PET not in Acidic Nitrite Solution
C's	71.84	73.79	73.38
O's	23.31	26.21	21.26
N's	4.85	0	4.96
S's	0	0	0.40

Abbreviations. PET = Polyethylene Terephthalate, C = Carbon, O = Oxygen, N = Nitrogen, S = Sulfur

there were still levels of nitrogen detected on the surface that indicates ethylenediamine was still present on the surface. Therefore, an imine bond ($\text{RHC}=\text{NHR}'$) was broken, since ethylenediamine was still detected on the surface but L-cysteine was not. However, it is difficult to determine from the results if it was the imine bond between ethylenediamine and glutaraldehyde or the imine bond between glutaraldehyde and L-cysteine. It is believed that the terminal imine bond between glutaraldehyde and L-cysteine was broken since it is not as stable as the imine bond between ethylenediamine and glutaraldehyde, especially if glutaraldehyde crosslinking is present.

3.3.3 Chemiluminescence Analysis of L-Cysteine Modified PET Samples

Method 1

The first test used to validate this method involved measuring the response from a $10\ \mu\text{M}\ \text{NO}_2^-$ solution, a $10\ \mu\text{M}\ \text{CysNO}$ solution, and a solution of $5\ \mu\text{M}\ \text{NO}_2^-$ and $5\ \mu\text{M}\ \text{CysNO}$ in both reducing solutions. Figure 3.4 shows the responses from the solutions in both reducing solutions. For the responses in reducing solution A, the signal from all three standard solutions should be the same, since this reducing solution converts NO_2^- and CysNO to NO to be measured. As shown, there is no significant difference between the responses from all three standard solutions in reducing solution A. For reducing solution B, the signal from the $10\ \mu\text{M}\ \text{NO}_2^-$ solution should be the same as that from the reducing solution A, since this reducing solution also converts NO_2^- to NO to be measured. However, the signal from reducing solution B is suppressed slightly. The suppression of the NO signal from nitrite shows that some of the nitrite may be reacting with the L-cysteine in the reducing solution. For reducing solution B, the signal from the $10\ \mu\text{M}\ \text{CysNO}$ solution should be completely suppressed, since this reducing solution

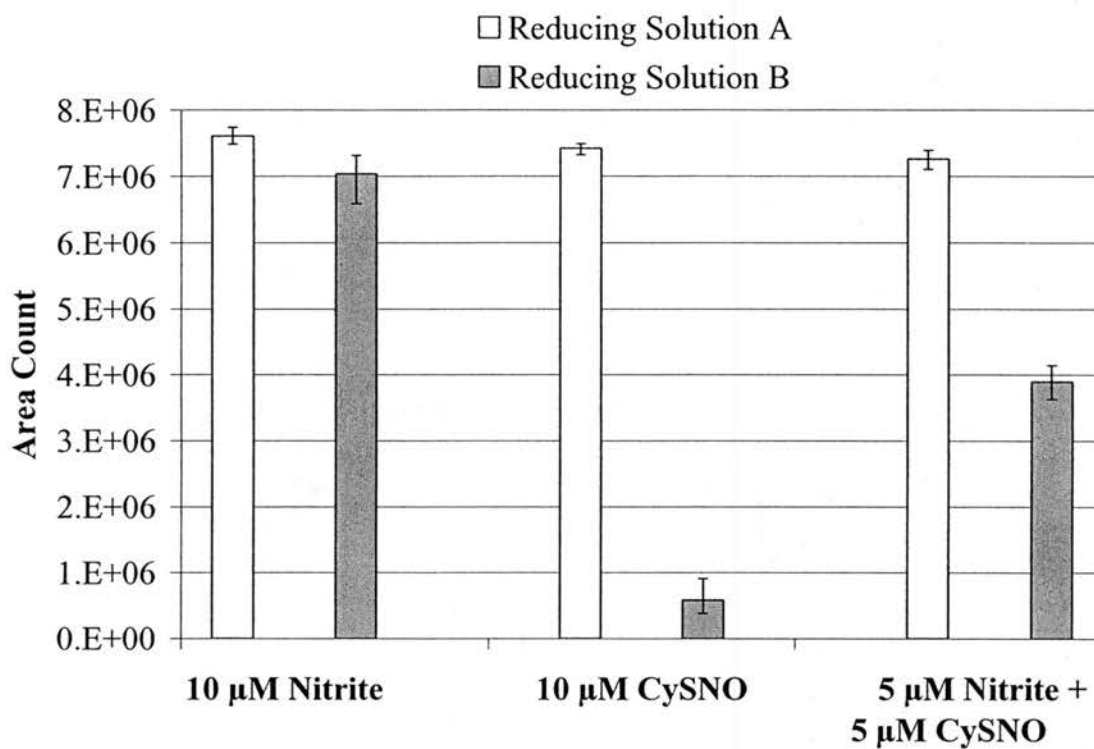


Figure 3.4 Signal from the NO chemiluminescence analyzer for nitrite, CySNO, and an equimolar mixture of the two in both reducing solutions, one with free iodine (A) and one with L-cysteine (B). Values shown are mean values \pm standard deviation (n=3).

suppresses the release of NO from CySNO. However, a small signal was detected. It appears that reducing solution B is only able to suppress the signal from a CySNO solution by approximately 90%. For the solution of 5 μM nitrite and 5 μM CySNO the response from reducing solution B should be only 50% of the response from reducing solution A, due to suppression of the CySNO in reducing solution B. As shown, the signal is only suppressed by 46%. The slight discrepancy may be due to reducing solution B not being able to completely suppress the signal from CySNO as shown for the 10 μM CySNO solution.

As an additional test to validate this method, 2.5, 5 and 10 μM L-cysteine solutions were nitrosated using 5 μM nitrite solutions. The samples were measured and the results are reported in Table 3.3. For reducing solution A, the measured concentrations for all of the solutions should be 5 μM since this was the starting concentration of nitrite added to each solution and reducing solution A converts both NO_2^- and CySNO to NO to be measured. As shown, the mean values range from 4.72 to 5.50 μM . For reducing solution B, the measured concentration for each solution should be equal to the amount of excess nitrite, assuming that all of the L-cysteine was nitrosated, since the NO contribution from CySNO is suppressed in reducing solution B. An excess nitrite concentration of 2.5 μM is expected for the first solution listed in the table and 2.28 μM was measured in this reducing solution. Some of the excess nitrite may have reacted with the L-cysteine in the reducing solution before it could be converted to NO and measured. For the second and third test solutions, there should not be any excess nitrite due to it all reacting with the L-cysteine in the solution; however, a concentration of 0.35 μM and 0.79 μM was measured, respectively. There may have

TABLE 3.3

Chemiluminescence Analysis of NO_2^- and CySNO in Solution Following Nitrosation
(CySNO is calculated by the difference from the responses in two reducing solutions)

[L-Cysteine] in Solution (μM)	$[\text{NO}_2^-]$ in Solution (μM)	Measured $[\text{NO}_2^-]$ and [CySNO] in Reducing Solution A (μM)	Measured $[\text{NO}_2^-]$ in Reducing Solution B (μM)	Calculated [CySNO] (A-B) (μM)	Percent Error in Measurement
2.50	5.00	4.72 ± 0.02	2.28 ± 0.01	2.44 ± 0.03	-2.40 ± 1.20
5.00	5.00	5.39 ± 0.15	0.35 ± 0.03	5.04 ± 0.18	0.80 ± 3.60
10.00	5.00	5.50 ± 0.07	0.79 ± 0.03	4.71 ± 0.10	-5.80 ± 2.00

Note. Values shown are mean values \pm standard deviation (n=3).

been some release of NO from the CySNO in this solution that caused the measured concentration to be higher than expected. As described earlier, not the entire signal from CySNO is suppressed in this reducing solution and the release of NO from CySNO contributes to the measured concentration in this reducing solution. The measured CySNO is the difference between the two reducing solution values. The percent error between the measured and expected CySNO for this method ranged from 0.8% to 5.8% and the standard deviation between samples were shown to be low (Table 3.3).

When using this method to measure the amount of L-cysteine on the surface of a modified sample of PET, the average measured surface concentration was 5.8 ± 1.7 nmols/cm² (n=3). This measured concentration was calculated by assuming that reducing solution B suppresses approximately 90% of the signal from CySNO.

Method 2

The results from the experiment using ammonium sulfamate and sulfanilamide to react with NO₂⁻ in solution in order to suppress the NO signal from NO₂⁻ in the reducing solution showed that both scavengers completely suppressed any detectable signal from all of the nitrite solutions tested (5, 10, and 100 μM: n=3). These results show that ammonium sulfamate or sulfanilamide are both good candidates to suppress the NO signal from excess nitrite in solution such that the contribution of CySNO in solution is only detected.

Sulfanilamide was used in solutions of free L-cysteine nitrosated using either a 1:2 or 2:1 molar ratio of L-cysteine:nitrite in a 0.5M HCl solution. Table 3.4 shows the results for measuring the CySNO in solution. For the lower concentration of CySNO in solution, the percent error in the measurement ranged from 14% for the 1:2 ratio of L-

TABLE 3.4

Chemiluminescence Analysis of CySNO in Solution with Sulfanilamide
(Using the reducing solution of potassium iodide in acetic acid saturated with iodine)

[L-Cysteine] in Solution (μM)	[NO₂] in Solution (μM)	Measured [CySNO] in Reducing Solution A (μM)	Percent Error in Measurement
1.00	1.00	0.71 \pm 0.05	-29.00 \pm 5.00
1.00	2.00	0.86 \pm 0.03	-14.00 \pm 3.00
10.00	10.00	8.43 \pm 0.31	-15.70 \pm 3.10
10.00	20.00	8.64 \pm 0.22	-13.60 \pm 2.20

Note. Values shown are mean values \pm standard deviation (n=3).

cysteine to nitrite to 29% for the 1:1 ratio of L-cysteine to nitrite (n=3). For the higher concentration of CySNO in solution, the percent error in the measurement ranged from 13.6% for the 1:2 ratio of L-cysteine to nitrite to 15.7% for the 1:1 ratio of L-cysteine to nitrite (n=3). Due to the high percent error for this method, it appears that sulfanilamide may affect the measurement of CySNO when using the reducing solution. CySNO is not very stable in solution; therefore, some NO may be released from CySNO and converted back to nitrite that can then be scavenged by sulfanilamide. This would result in a measurement lower than expected, which is seen in the results. This method has been successful when used to measure BSANO in solution, which is larger and more stable than CySNO in solution (unpublished results).

When using this method to measure the amount of L-cysteine on the surface of a modified sample of PET, the average measured surface concentration was 4.1 ± 2.1 nmols/cm² (n=3). This compares to 5.8 nmols/cm² measured by method 1. The measured concentration from this method may be lower than the actual concentration due to the instability of CySNO in the solution containing sulfanilamide, as shown in the analysis of nitrosated free L-cysteine in solution.

Method 3

To validate this method, solutions of free L-cysteine of the following concentrations: 1, 5, 10, and 20 μ M were nitrosated using either a 1:1 or a 2:1 molar ratio of nitrite:L-cysteine. The CySNO concentration in each solution was measured directly by using the reducing solution containing copper chloride with L-cysteine. The results are shown in Figure 3.5. The response from each of the CySNO solutions was proportional to its concentration. The signal for the 5 μ M CySNO solution was

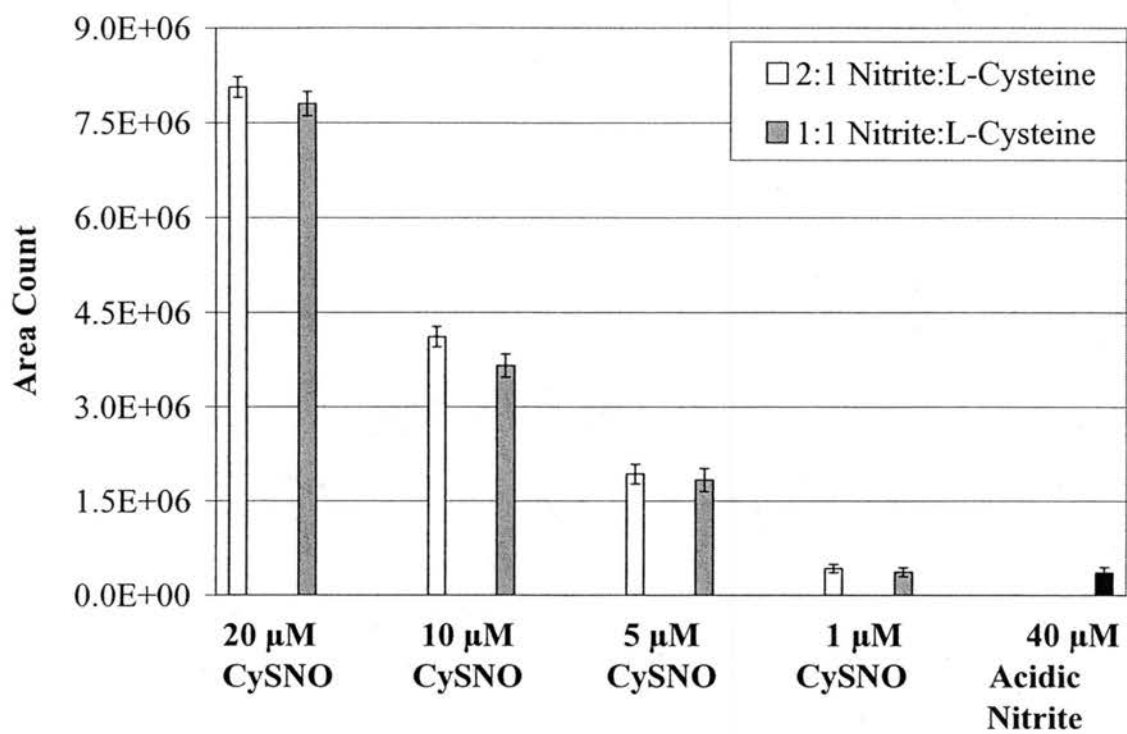


Figure 3.5 Signal from the NO chemiluminescence analyzer for CysNO in the reducing solution of copper chloride supplemented with L-cysteine at pH 7.4 and 50°C. Values shown are mean values ± standard deviation (n=3).

approximately 5 times that of the signal from the 1 μM CySNO solution. The signal from the 10 μM and 20 μM CySNO solutions was approximately 2 and 4 times that of the signal from the 5 μM CySNO solution. The proportional responses were seen for both the 2:1 and 1:1 nitrite to L-cysteine solutions. The response from the 2:1 solution was slightly higher at each concentration compared to the 1:1 solution. This may be due to the reducing solution not being able to completely suppress all of the excess acidic nitrite in the 2:1 solutions. As seen in the figure, there was a low signal detected for a 40 μM acidic nitrite solution, approximately equal to the signal from the 1 μM CySNO solution.

When using this method to measure the amount of L-cysteine on the surface of a modified sample of PET, the average measured surface concentration was 6.5 ± 1.3 nmols/cm² (n=3). This compares to 5.8 nmols/cm² measured by method 1 and 4.1 nmols/cm² measured by method 2. The measured concentration from this method may be higher than the actual concentration if the signal from the excess acidic nitrite in the solution is not completely suppressed by the reducing solution.

For all of the chemiluminescence methods, the detection limit for NO_2^- was as low as 5 pmol per injection, which corresponds to 0.1 μM if a 50 μl sample was injected. Each time samples were analyzed at a significant time following the previous calibration, a corresponding calibration curve was established in order to minimize any inter-assay error.

3.4 Discussion

Several methods were presented that can be used for the surface characterization of a modified PET surface, including the detection of L-cysteine attached to the surface. Currently, there are limited methods available to characterize such a surface, as described in this chapter, and even those methods discussed still have limitations to overcome before the surface can be completely characterized.

Using fluorescence microscopy to characterize a modified surface has many advantages, including visualization of the surface and being able to probe specific areas and/or molecules on a the surface. Unfortunately, there are also problems with using fluorescence microscopy to characterize a modified surface, including fading, autofluorescence, and selectivity. Fading of the fluorescent dye can be avoided by taking steps in the preparation and use of the dye to avoid all possible light sources that can cause the fluorescence intensity to fade. Autofluorescence was not a problem for this study. As shown in the scans of the blank PET samples, there was only a slight amount of autofluorescence, and small amounts can be removed by adjusting the gain setting of the laser of the microscope. There are many fluorescent probes available for detecting thiols; however, as shown in the scans of the PET samples with the ethylenediamine only attached, the fluorescence probe also reacted with the amine group and was not specific for thiols only. This was not a problem for this study, because it was shown that the glutaraldehyde attached to the ethylenediamine did not react with the fluorescent probe and blocked any reaction between ethylenediamine and the probe. Still, the problem of selectivity must be considered when using other fluorescent probes with other modified samples in order to ensure that only the target molecule is being probed. Probably the

greatest limitation of this method is that under the current procedure it is difficult to quantify the amount of fluorescence on the surface of a modified sample and relate it to the molar concentration of L-cysteine on the surface. Recently, some studies have shown that it may be possible to quantify the surface density of a fluorescent label with the optical microscope (Hanley and Harris, 2001; Model and Healy, 2000); however, a good standard sample with a known L-cysteine surface concentration is needed to relate it to the surface density of the fluorescent label. We will continue to explore the possibility to quantify the amount of fluorescence on the modified PET sample and to relate it to the concentration of L-cysteine on the surface.

The elemental analysis of a surface by XPS is a good tool for surface characterization. The measured atom% of elements on the surface could be compared to the theoretical atom% of elements on the surface in order to indicate if there is one-to-one binding. Also, certain elements in some of the groups attached to the surface of PET could be used as markers to indicate the amount of surface coverage. After the addition of ethylenediamine and glutaraldehyde to the surface of PET, nitrogen was used as a marker to indicate the amount of ethylenediamine attached to the surface, since ethylenediamine is the only component that contains nitrogen. After L-cysteine was attached to the surface of PET, sulfur was used as a marker to indicate the amount of L-cysteine attached to the surface, since L-cysteine is the only component to contain sulfur. It is difficult to determine the proportion of each group on the modified surface (i.e. one-to-one binding) due to incomplete coverage and/or crosslinking of some groups that affect the atom% measurements on the surface. As with fluorescence microscopy, the problem with this type of analysis is that it does not give surface concentrations of

molecules on the surface, instead it gives surface percentages of atoms on the surface. However, if a reliable standard sample with known surface concentrations could be developed, then the surface percentages given by XPS analysis could be transformed to surface concentrations. In the future, if a sample could be accurately measured by means of another method, XPS may be favorable to use for the analysis of the unknown samples due to its high sensitivity and accuracy. Due to the high cost of XPS, it may not be readily available to every laboratory and another less costly measurement method with slightly lower accuracy may be more favorable.

Several chemiluminescence-based methods were also presented, which can be used for the detection of immobilized L-cysteine on a PET surface. The chemiluminescence-based methods used to measure L-cysteine utilized a variety of reducing solutions to measure either CySNO and/or excess nitrite in solution. Three methods using different types of reducing solutions were described in this chapter. The accuracy in the measurement of L-cysteine varied depending on the reducing solution used in the various methods. When validating each method by using known standard solutions of L-cysteine, some methods did better than others, however all the methods had problems. Even though the first method had low percent errors in the measurement of the standard solutions, there are some problems to consider. The reducing solution of potassium iodide in glacial acetic acid containing L-cysteine did not seem to be stable and was not able to completely suppress the release of NO from CySNO. Also, since two measurements must be made in order to determine the concentration of CySNO, there is the possibility of introducing twice the amount of experimental error into the measurement. The major problem with the second method that used nitrite scavengers,

ammonium sulfamate and sulfanilamide, was that the scavengers also interfered with the measurement of CySNO. The main problem with the third method was the instability of the reducing solution. The pH of the reducing solution must be maintained near 7 in order to suppress any signal from the excess nitrite in the solution. Due to this instability, only a few samples of the highly acidic solutions could be analyzed at a time before the pH of the reducing solution would decrease. If the samples were neutralized prior to analysis in the reducing solution, the release rates in the reducing solution were too slow to quantify. All three of the measurement methods did result in a measured surface concentration of L-cysteine in the same order of magnitude and only varied by less than 1.8 nmol/cm² standard deviations. Therefore, it is believed that the actual surface concentration of L-cysteine on the surface of a modified PET sample is within the range of 4.1 to 6.5 nmols/cm². The chemiluminescence-based methods must continue to be improved by using various types of reducing solutions, nitrite scavengers, experimental settings, (temperature, pH, etc.) and/or more sensitive analyzers, etc. in order to improve the accuracy of the method.

The chemiluminescence assay is the only method we have found to be able to quantitatively measure the concentration of L-cysteine attached to the surface of a modified PET sample. However, this method could be easily adapted to measure any thiol group immobilized on any type of solid surface, provided that the thiol group could be removed from the surface into the surrounding solution for measurement. This method was also shown to have low detection limits: 5 pmol NO₂⁻ or CySNO can easily be measured at the lower detection limit. This method also has excellent selectivity for thiols. Unlike the fluorescent probe that also reacted with amines or XPS that does not

detect L-cysteine, but rather the sulfur atom in L-cysteine, the chemiluminescence method only measures the thiols that can be nitrosated with NO_2^- .

The major disadvantage to the chemiluminescence method is that the L-cysteine is broken off of the PET sample during the nitrosation process, rendering the sample unusable for additional studies. Therefore, samples can only be characterized after use. Since it would be advantageous to be able to modify a sample, characterize it, and then use it, we are continuing to investigate other methods that could be developed to characterize surfaces modified with L-cysteine, without damaging the modified surface.

The methods described in this chapter to characterize the surface of the L-cysteine modified polymer were used in the optimization process of the polymer modification process (Chapter 4). The methods were used to characterize not only L-cysteine modified polymers, but two other modified polymers containing L-cysteine moieties, 2-iminothiolane and a cysteine polypeptide chain. The characterization methods were used with the optimization methods to determine the modification process that resulted in the most thiol groups on the surface of the modified sample.

CHAPTER 4

OPTIMIZATION OF THE POLYMER MODIFICATION PROCESS

4.1 Introduction

One hypothesis was that the addition of more L-cysteine sites or different L-cysteine-containing moieties on the polymer will increase the NO-release rate per unit area and lead to a greater inhibition of platelet deposition on the modified polymer. Therefore, the polymer modification process was optimized in order to increase the number of L-cysteine sites or different L-cysteine-containing moieties on the polymer. The following moieties were used in the optimization of the polymer modification process: 1) L-cysteine, 2) a L-cysteine containing moiety, 2-Iminothiolane, and 3) a polypeptide containing multiple cysteine residues. Each moiety was attached to PET by using linker groups. Optimization of each moiety was performed by using factorial designs that varied the reaction times and molar concentrations of each group involved in the modification process. The optimal design was determined by measuring the relative amount of the thiol groups on the surface by techniques described in Chapter 3.

In a classical type of scientific experiment, it is customary to hold most of the variable factors constant and to allow only one or two to vary in each experiment. A series of experiments in which only one factor is varied at a time would be both lengthy and costly, and might still be unsatisfactory because of systematic changes in the general background conditions. An alternative approach is to try to investigate variations in

several factors simultaneously. This is the idea of a factorial experiment in which the set of experiments is made large enough to include all possible combinations of levels of the different factors. There are many important advantages in using this type of experimentation as compared with the standard classical method (Bailey, 1995):

- One can obtain a broad picture of the effect of each factor in the different conditions furnished by variations in the other factors.
- The use of a wide range of factor combinations provides a more reliable basis for making practical recommendations that will be valid in variable circumstances.
- If all the factors happen to act independently of each other, one can obtain as much information about each from a single experiment as one would if the whole experiment were devoted to only one factor.
- If the factors are not independent of one another, one can automatically collect a great deal of information about the nature of the interaction.

There are potential problems with trying to include too many factors in one experiment. Although, theoretically, the inclusion of a large number leads to greater efficiency, there is often considerable difficulty in handling and interpreting very complex results (Bailey, 1995).

A design in which there are several factors (n factors), each at two levels, is called a 2^n factorial design. Levels may be two quantitative levels, such as two concentrations, or two qualitative alternatives. In some cases, one level is simply the absence of the factor and the other its presence. So, for the case of optimizing the process of attaching L-cysteine to the surface of the polymer, a 2^n factorial design including six factors

(concentration and reaction time for each of the three reaction steps) would result in 2^6 or 64 experiments. It is also possible to have designs with more than two levels for several factors, as long as all of the factors have the same number of levels. Higher-level designs may give more information, but they are more complicated due to the difficulty in handling and interpreting very complex results.

Using a complete factorial design with two levels to optimize the process of attaching L-cysteine to the surface of PET would result in many experiments that would be very time-consuming and costly to perform. Therefore, a fractional factorial design that consisted of only a fraction of the total number of runs was used. When the fraction of runs is selected appropriately, the effects of factors and even some interactions can be estimated with fewer runs (Frank and Todeschini, 1994). The assumption is that the effect of the majority of interactions is negligible (Frank and Todeschini, 1994).

A commonly used fractional factorial design is the Plackett-Burman design. The term “Plackett and Burman design” has its origin in a paper written by R. L. Plackett and J. P. Burman in 1946 (Plackett and Burman, 1946). It is generally used to indicate certain two-level fractional factorial designs which allow efficient estimation of the main effects of all factors being explored, assuming that all interactions between factors can be ignored. The model is of the form:

$$Y = A_0 + A_1X_1 + A_2X_2 + A_3X_3 + A_4X_4 + \dots + A_nX_n \quad \text{Eq. 4.1}$$

where Y is the response, A_0 is a constant and A_1 to A_n are the coefficients of the response values. The design analyzes the input data and presents rank ordering of the variable with magnitude of effect, and designates signs to the effects to indicate whether an

increase in a factor is positive or not. The effect of each variable is determined by the following expression:

$$(\text{Effect})_i = \frac{\Sigma R(+)-\Sigma R(-)}{n/2} \quad \text{Eq. 4.2}$$

where R(+) is a (+) or high level response, R(-) is a (-) or low level response, and n is the total number of factors. The main effects are interpreted to mean that the net effect of increasing the factor level, averaged over all other factor levels, from low to high is to increase or decrease the response, depending on the magnitude and direction of the main effect value of the factor. The magnitude of the main effect can be related to its significance in the optimization study. The greater the magnitude, the more influence it has on the optimization process. The sign of the main effect is related to the direction the level should be increased or decreased to influence the optimization process.

4.2 Materials and Methods

4.2.1 Reagents

Glacial acetic acid, potassium iodide, and sodium nitrite were purchased from Fisher Scientific (Fairlawn, NJ). Phosphate buffered saline (PBS, pH 7.4) was obtained from Life Technologies (Gaithersburg, MD). Polyethylene terephthalate (PET) (thickness = 0.2 mm) was supplied by DuPont (Hopewell, VA). Oregon Green® 488 carboxylic acid, succinimidyl ester *5-isomer* and 5-Iodoacetamidofluorescein (5-IAF) was purchased from Molecular Probes (Eugene, OR). Potassium Phosphate, monobasic was purchased from EM Science (Gibbstown, NJ). The L-cysteine polypeptide (Cys-

Gly-Cys-Gly-Cys) was purchased from the Molecular Biology Resource Facility (Norman, OK). Ethylenediamine, glutaraldehyde (GA), glycine, 2-iminothiolane hydrochloride, iodine, L-cysteine, Trizma® base (tris[hydroxymethyl]aminomethane), and all the other reagents were purchased from Sigma Chemical Co. (St. Louis, MO). All water used was of HPLC-grade quality and was deoxygenated by bubbling nitrogen in the water prior to use.

4.2.2 Modification of PET Samples

Other than the factors shown in the factorial designs, all other reaction conditions were similar to those used previously in the modification process (see Section 3.2.2) and were held constant for all samples. These constants include the following:

- All steps were performed in a glove box under a N₂ atmosphere.
- Oxygen was removed from all solutions by bubbling N₂ through the solutions.
- All steps involving thiol groups were kept covered to prevent damaging light from the sample.
- Each run in the Plackett-Burman factorial design or in the complete factorial designs was performed in triplicate in order to measure standard deviations.
- PET samples were soaked in 100% acetone for 24 hours prior to the modification procedures in order to remove any impurities from the surface of the sample. The samples were then allowed to dry completely for 24 hours.
- During the reaction step with ethylenediamine, samples were placed in a reciprocating water bath set at a temperature of 40°C and 130 cycles.

- During the reaction step with glutaraldehyde, samples were placed on a hand motion shaker to be well shaken at room temperature, while N₂ was bubbled through each solution containing a sample.
- During the reaction steps with the thiol groups, samples were placed on a hand motion shaker to be well shaken at room temperature.
- All samples were thoroughly rinsed with deoxygenated water after each reaction step.
- All chemiluminescence and fluorescence analyses were performed within 24 hours after completion of the sample modification process. The time of XPS analysis varied depending on the turnaround time of the XPS facility. The extended period of time for XPS did not affect the analysis because, unlike the other two measurement methods that can only measure thiols in their reduced form, XPS can detect thiols on the surface in either their reduced or oxidized form, by measuring sulfur, which is only found in the thiol group on the surface.

4.2.3 Optimization of L-Cysteine onto PET Surface

The reaction scheme used to attach L-cysteine to the surface of PET included the reactions shown in Figure 4.1 along with the constants described in the previous section (Section 4.2.2). For the optimization of the process of attaching L-cysteine onto the surface of PET, Table 4.1 shows a 2-level, 6-factor, and 12-run Plackett-Burman factorial design that was generated by using the Excel design macro DOE KISS 97. This statistical program prepares Plackett-Burman factorial designs at different combinations of levels and factors by using the model shown in Equation 4.1. The six factors in the

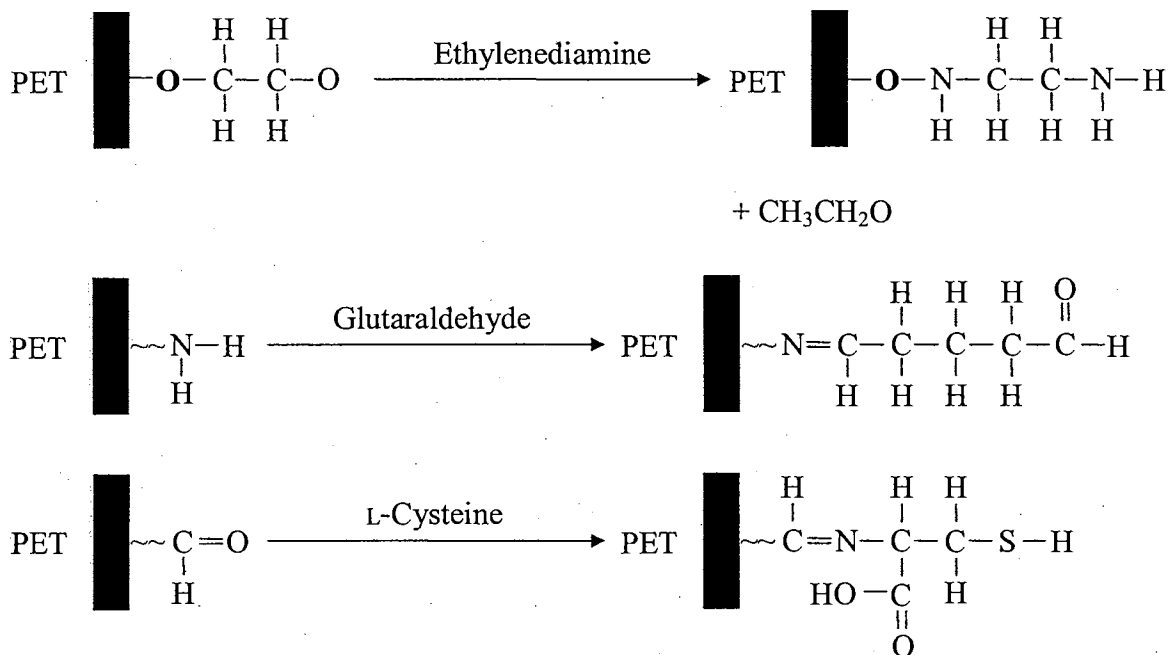


Figure 4.1 Reaction schemes of immobilizing L-cysteine onto the surface of polyethylene terephthalate (PET) by first adding an amine group by the use of ethylenediamine and then using glutaraldehyde as a crosslinker.

TABLE 4.1

Plackett-Burman Factorial Design for Optimizing the Process of Attaching L-Cysteine to the Surface of PET

Run Number	Factors					
	A	B	C	D	E	F
1	1	-1	1	-1	-1	-1
2	1	1	-1	1	-1	-1
3	-1	1	1	-1	1	-1
4	1	-1	1	1	-1	1
5	1	1	-1	1	1	-1
6	1	1	1	-1	1	1
7	-1	1	1	1	-1	1
8	-1	-1	1	1	1	-1
9	-1	-1	-1	1	1	1
10	1	-1	-1	-1	1	1
11	-1	1	-1	-1	-1	1
12	-1	-1	-1	-1	-1	-1

Parameter		Levels	
Code	Factor	-1 (Low)	+1 (High)
A	Ethylenediamine Reaction Time	8 hrs	3 days
B	Ethylenediamine Concentration	30 vol%	70 vol%
C	Glutaraldehyde Reaction Time	15 min	4 hrs
D	Glutaraldehyde Concentration	0.2 vol%	5 vol%
E	L-Cysteine Reaction Time	1 hr	4 days
F	L-Cysteine Concentration	0.0002 wt%	2 wt%

design make up each of the reaction steps to attach L-cysteine to PET, including: 1) ethylenediamine reaction time, 2) ethylenediamine concentration, 3) glutaraldehyde reaction time, 4) glutaraldehyde concentration, 5) L-cysteine reaction time, and 6) L-cysteine concentration. The high (+) and low (-) levels of each factor were determined by setting the levels for the attachment of L-cysteine to PET used in the previous reaction scheme shown in Figure 2.6 as median values. Extreme levels were chosen in order to clearly determine the effect of each factor on the process.

After the first week of the optimization studies, it was discovered that there were problems with some of the selected level values. One problem was the initial L-cysteine concentration set at 20 wt%. Although the solubility of L-cysteine in water is high (150 mg/ml), it was very difficult to completely dissolve the solid at the 20 wt% level. Once the L-cysteine was completely dissolved into solution, after a few hours solid crystals would begin to appear on the surface of the PET sample. Therefore, the new high level was set at 2 wt%. Other problems were with the ethylenediamine reaction time and concentration. It was discovered that at the initial high level ethylenediamine concentration of 90 vol% and the initial high level reaction time of 4 days, the highly basic solution disintegrated the PET sample. A separate study was performed to test the effect of various ethylenediamine concentrations on the PET sample. PET samples (1 cm x 3 cm) were placed into the following ethylenediamine concentrations for 24 hours and then analyzed using fluorescence microscopy: 0, 10, 20, 30, 40, 50, 60, 70, 80, 90, and 100 vol%. During the 24-hour reaction time, the samples were placed in a reciprocating water bath at a temperature of 40°C and 130 cycles. The time of 24 hours was selected due the following reasons: 1) this was the time period set for the mean level and it

seemed to be successful, 2) at 8 hours there was little sign that ethylenediamine had reacted with PET, and 3) at 3 days most concentrations of ethylenediamine had done some damage to the surface of PET. An amine-specific fluorescent probe, Oregon Green® 488 carboxylic acid, succinimidyl ester *5-isomer*, was used to analyze the surface coverage of ethylenediamine on PET. After the samples reacted with the ethylenediamine, they were rinsed well, and then placed in a 27.5 μ M Oregon Green® 488 solution in 50 mM potassium phosphate buffer (pH ~ 9) and shaken for one hour to allow the fluorescent probe to react with the amine groups on the PET surface. The samples were rinsed with water and kept in the dark until analysis, which directly followed. The surface of each sample was examined by using an argon laser-scanning microscope (Leica TCS SP2, Exton, PA) in confocal mode with a 10.0 x 40.0 oil immersion objective lens. The filter set was set at 488 nm excitation and 515 nm emission. After reviewing the results from this study (shown later in the chapter), the low, and high levels for the ethylenediamine concentration were set at 30 vol% and 70 vol%, respectively, and the low and high levels for the ethylenediamine reaction time were set at 8 hours and 3 days, respectively.

To measure the amount of L-cysteine attached to the surface of each PET sample of the optimization studies, the fluorescence microscopy and chemiluminescence measurement methods described in Sections 3.2.3 and 3.2.6, respectively, were utilized. XPS was not used at this point due to the high analysis cost. Three 1 cm x 1 cm pieces were cut from each 1 cm x 3 cm PET sample in the optimization study, in order to use a 1 cm x 1 cm piece of each sample in each measurement method. All samples were kept in

the glove box under a N₂ atmosphere and covered to prevent exposure to damaging light until ready for analysis.

Chemiluminescence Method 1, described in Section 3.2.6, was used to measure the amount of L-cysteine on the samples. This method was selected because it was shown to accurately measure L-cysteine in solution (Chapter 3) and it has been the most used method in past research to measure the amount of L-cysteine attached to PET. To break off and nitrosate L-cysteine on each sample, each sample was placed in an amber vial containing 1 ml of a 0.5 M HCl solution initially containing 40 μM NO₂⁻. A higher concentration of NO₂⁻ was used in the nitrosation of PET-Cys in order to ensure that there would be an excess of NO₂⁻ for complete nitrosation. The vials were sealed and nitrosation was allowed to proceed for 1 hour, after which the amount of nitrosated L-cysteine in the solution surrounding the each sample was measured by using the same protocol described in Section 3.2.6.

To qualitative assess the amount of L-cysteine on the PET samples by using fluorescence microscopy, the fluorescent probe 5-IAF was used in a method similar to that described in Section 3.2.3. Each sample and a blank PET sample (control) were placed into an amber vial with 4 ml of 133 μM 5-IAF solution in a 50 μM phosphate buffer (pH ~ 8). The vials were sealed and shaken for two hours. The samples were rinsed with water and kept in the dark until analysis. The surface of each sample was examined by using an argon laser-scanning microscope (Leica TCS SP2, Exton, PA) in confocal mode with a 10.0 x 40.0 oil immersion objective lens. The filter set was set at 488 nm excitation and 515 nm emission. The gain for the argon laser was set so that the mean intensity from the blank PET sample was zero. The mean intensity of each sample

was measured keeping the gain setting constant. The mean intensities could then be compared and contrasted among the samples.

The advantage of using a Plackett-Burman fractional factorial design is that it allows one to investigate the effect of many factors on a process without having to perform excessive experiments. The results from the initial design can show which factors are the most important and can lead to a more specialized design. Using the results from the first design, the ethylenediamine reaction time and concentration were set constant at 24 hours and 40 vol%, respectively, and the glutaraldehyde reaction time was set constant at 15 minutes. A 2-level, 3-factor, and 8-run complete factorial design varying the other factors of glutaraldehyde concentration and L-cysteine reaction time and concentration was used to further optimize the modification process of adding L-cysteine to PET and is shown in Table 4.2. For this design, only the Chemiluminescence Method 1, described previously, was used to measure the amount of L-cysteine on the surface of the samples. After optimizing the process to attach L-cysteine to PET, a sample was prepared and analyzed by using the XPS measurement method in order to compare the XPS results with those from the optimized process using 2-iminothiolane and cysteine polypeptide.

4.2.4 Optimization of 2-Iminothiolane onto PET Surface

2-Iminothiolane has been used in research to introduce thiol groups in proteins and to attach thiol groups to surfaces (Phaneuf et al., 1997; Weber et al., 2000). 2-Iminothiolane is a thiolating agent for primary amines. It was selected to be attached to the surface of PET for the following reasons:

TABLE 4.2

Full Factorial Design for Optimizing the Process of Attaching L-Cysteine to the Surface of PET by Varying Glutaraldehyde Concentration and L-Cysteine Reaction Time and Concentration

Run Number	Factors		
	Glutaraldehyde Concentration	L-Cysteine Reaction Time	L-Cysteine Concentration
1	0.02 vol%	1 hour	0.0002 wt%
2	0.02 vol%	1 hour	2 wt%
3	0.02 vol%	4 days	0.0002 wt%
4	0.02 vol%	4 days	2 wt%
5	0.2 vol%	1 hour	0.0002 wt%
6	0.2 vol%	1 hour	2 wt%
7	0.2 vol%	4 days	0.0002 wt%
8	0.2 vol%	4 days	2 wt%

- It can be attached directly to the amine group of ethylenediamine on the polymer, thus removing the extra linkage of glutaraldehyde and resulting in a shorter chain length extending from the polymer. Therefore, the effect of chain length can be investigated by comparing the shorter chain length of this system to the longer chain length of the L-cysteine residue system. This was done by comparing which system produced the most thiol groups on the surface and which system prevented platelet attachment the best (Chapter 5). Also, by not using the glutaraldehyde linkage, this is one less step in the optimization of the modification process.
- It remains in a stable ring formation at low pH values, which at pH 7 – 10 the ring opens and reacts by amidine bond to present the free thiol. This makes 2-Iminothiolane easier to store in solution than free L-cysteine because it cannot form disulfide linkages while in its ring form.
- It has a small molecular weight of 137.6, which is similar to that of L-cysteine of 121.1. As a result, the transnitrosation properties of 2-iminothiolane may also be similar to those of L-cysteine.

The reaction scheme to attach 2-iminothiolane to the surface of PET is shown in Figure 4.2.

To optimize the modification process of attaching 2-iminothiolane to the surface of PET, a 3-level, 2-factor, and 9-run complete factorial design was used, as shown in Table 4.3. Since the optimal ethylenediamine concentration and reaction time were determined from the optimization of attaching L-cysteine to the surface of PET, 40 vol% and 24 hours were used, respectively. The 2-iminothiolane concentration and reaction

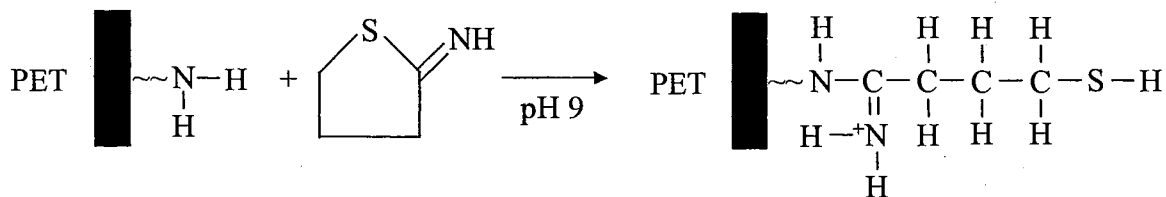
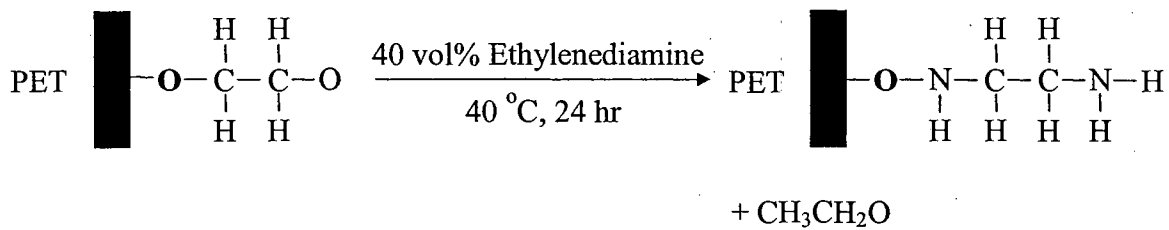


Figure 4.2 Reaction schemes of immobilizing 2-iminothiolane onto the surface of polyethylene terephthalate (PET) by first adding an amine group by the use of ethylenediamine.

TABLE 4.3

Full Factorial Design for Optimizing the Process of Attaching
2-Iminothiolane to the Surface of PET

Run Number	Factors	
	2-Iminothiolane Reaction Time	2-Iminothiolane Concentration
1	1 hour	16.5 nM
2	1 hour	16.5 μ M
3	1 hour	1.65 mM
4	24 hours	16.5 nM
5	24 hours	16.5 μ M
6	24 hours	1.65 mM
7	4 days	16.5 nM
8	4 days	16.5 μ M
9	4 days	1.65 mM

time factors were the only factors varied; therefore, a 3-level design was used in order to get more information about the effect of the factors on the optimization process. For the 2-iminothiolane reaction time, past studies had varied the reaction time from 15 minutes to 24 hours (Weber et al., 2000). Therefore, reaction times of 1 hour, 24 hours, and 4 days were selected in order to measure the effect of within the range of past studies (1 hour and 24 hours) and to go beyond the range (4 days). 2-Iminothiolane concentrations for the optimization study were chosen to be similar to the ones used in the optimization study with L-cysteine. The L-cysteine molar concentrations used in the optimization study varied from 16.5 nM to 0.165 mM. The 2-iminothiolane molar concentrations were varied from 16.5 nM to 1.65 mM. A higher concentration of 2-iminothiolane was used since it dissolves easier in water than L-cysteine and this concentration is still within the solubility limit for 2-iminothiolane (100 mg/ml). The pH of the 2-iminothiolane solutions prepared in deoxygenated water (pH ~ 4) was adjusted to 7.5 by using sodium hydroxide solutions, just prior to its reaction with ethylenediamine on the polymer surface.

To measure the amount of 2-iminothiolane attached to the surface of each PET sample of the optimization studies, the XPS and Chemiluminescence Method 1 measurement methods described in Sections 3.2.4 and 3.2.6 were utilized, respectively. The results from the L-cysteine optimization studies (see Results section) show that it was difficult to use fluorescence microscopy to quantify the amount of thiol group on the surface of the sample, so it was not used in further optimization studies. Three 1 cm x 1 cm pieces were cut from each 1 cm x 3 cm PET sample in the optimization study, in order to use a 1 cm x 1 cm piece of each sample in each measurement method. All

samples were kept in the glove box under a N₂ atmosphere and covered to prevent exposure to damaging light until ready for analysis. Since XPS analysis is costly, the modified samples from the optimization study were first analyzed by the chemiluminescence method. Chemiluminescence Method 1 was used to measure the amount of 2-iminothiolane on the surface of the modified PET samples. The experimental procedures used were the same as those described above to measure the amount of L-cysteine. The results of the analysis (see Results section) revealed very little or no free thiol groups attached to the surface of the 2-iminothiolane-modified PET samples. After reviewing other studies that used 2-iminothiolane to introduce free thiol groups to surfaces, some changes were made to the experimental design (Weber et al., 2000). First, the pH of the 2-iminothiolane solution may not have been high enough to open the ring in order for it to react by amidine bond to expose the free thiol group. Therefore, the pH of the 2-iminothiolane solutions was raised to 9 to ensure more open rings and exposed free thiol groups. In order to control the pH of the solution better, the 2-iminothiolane solutions were prepared in 0.001 M Trizma® base buffer and the pH was adjusted by using sodium hydroxide solutions. The next important change to the optimization design involved the concentration of the 2-iminothiolane solutions. Other studies used higher concentrations to attach 2-iminothiolane onto surfaces; therefore, the concentrations in the factorial design were proportionally increased to 50 nM, 50 μM, and 50 mM (Weber et al., 2000). The last change involved the reaction time for 2-iminothiolane. Since there were not any significant changes in the amount of 2-iminothiolane attached to the surface after 24 hours or 4 days shown in the previous optimization study or other studies shown in literature (Weber et al., 2000), the high level

reaction time was decreased from 4 days to 3 days in order to decrease the amount of time to complete the optimization study. The improved factorial design used to optimize the process of attaching 2-iminothiolane to the surface of PET is shown in Table 4.4.

Modified samples from the new factorial design were then analyzed by using the Chemiluminescence Method 1 and by XPS. Samples, 1 cm x 1 cm samples cut from the original 3 cm x 3 cm modified samples, were sent to the XPS facilities at the Chemistry Department at Lehigh University (Bethlehem, PA) to be analyzed. The analysis reveals the atomic percent of sulfur on each sample that can be used to compare the amount of thiol group on each sample, since 2-iminothiolane is the only group on the surface that contains sulfur.

4.2.5 Optimization of Cysteine Polypeptide onto PET Surface

A cysteine polypeptide was chosen to be attached to the surface of PET in order to add a greater number of thiol groups to the surface in long, linear chains. Initially, the goal was to attach as many cysteine residues as possible in various chain lengths. After consulting many peptide synthesis facilities, both commercial and academic, it was discovered that L-cysteine residues can become very unstable in long, linear chains. Many cysteine residues within one polypeptide are susceptible to oxidation leading to the formation of disulfide linkages. Excessive disulfide linking can lead to an extensive crosslinking of chains either within themselves or with other chains that can eventually result in the peptide precipitating out of solution. Therefore, there is a limitation to the number of cysteine residues that can be added to one peptide, and it is better to put “spacer” residues between the cysteine residues in order to prevent disulfide linkages. However, there may still be crosslinking between separate chains. A polypeptide with

TABLE 4.4

Improved Factorial Design for Optimizing the Process of
Attaching 2-Iminothiolane to the Surface of PET

Run Number	Factors	
	2-Iminothiolane Reaction Time	2-Iminothiolane Concentration
1	1 hour	50 nM
2	1 hour	50 μ M
3	1 hour	50 mM
4	24 hours	50 nM
5	24 hours	50 μ M
6	24 hours	50 mM
7	3 days	50 nM
8	3 days	50 μ M
9	3 days	50 mM

the sequence of Cys-Gly-Cys-Gly-Cys was selected and the Molecular Biology Resource Facility at the University of Oklahoma Health Sciences Center (Oklahoma City, OK) synthesized and purified the peptide. The polypeptide was made under acidic conditions and in a reducing solution in order to keep the cysteine residues from becoming oxidized. The polypeptide was lyophilized and sealed under argon prior to shipping. The peptide was kept on ice during shipping and stored in a -86°C freezer until ready for use in order to keep it stable. Three cysteine residues were selected because this is believed to be the maximum number of cysteine residues that can be added to a single polypeptide without causing significant disulfide linkages within the polypeptide chain (Jackson, 2002). Glycine was chosen to be the spacer residue because it is a very small and unreactive molecule that has also been used in past studies as a control group that can be attached to the surface of PET in the same method as L-cysteine. The reaction scheme for attaching the cysteine polypeptide to PET is similar to that shown in Figure 4.1 for attaching L-cysteine to PET, the only difference is that the single L-cysteine residue is replaced with the cysteine polypeptide. Due to the high cost and the limited amount of cysteine polypeptide that can be synthesized at a time, smaller PET samples of 1 cm x 2 cm and therefore smaller volumes of solutions were used in the optimization studies.

A 3-level, 2-factor, 9-run complete factorial design was used to optimize the process of attaching the cysteine polypeptide to the surface of PET. The optimal reaction times and concentrations for ethylenediamine (24 hours and 40 vol%, respectively) and glutaraldehyde (15 minutes and 0.02 vol%, respectively) determined from the optimization of attaching L-cysteine to the surface of PET were used in this design and only the polypeptide concentration and reaction time were varied, as shown in Table 4.5.

TABLE 4.5

Full Factorial Design for Optimizing the Process of Attaching
Cysteine Polypeptide to the Surface of PET

Run Number	Factors	
	Cysteine Polypeptide Reaction Time	Cysteine Polypeptide Concentration
1	1 hour	14.5 nM
2	1 hour	14.5 μ M
3	1 hour	14.5 mM
4	24 hours	14.5 nM
5	24 hours	14.5 μ M
6	24 hours	14.5 mM
7	3 days	14.5 nM
8	3 days	14.5 μ M
9	3 days	14.5 mM

The cysteine polypeptide concentration levels and reaction time levels selected are similar to those seen in the factorial design of optimizing the process to attach 2-iminothiolane to PET. The cysteine polypeptide solutions were prepared in deoxygenated water and the pH adjusted to 7 by adding sodium hydroxide solution. The modified samples were analyzed via the XPS and Chemiluminescence Method 1, using the same procedures as previously described in Sections 3.2.4 and 3.2.6, respectively. Two 1 cm x 1 cm pieces were cut from each 1 cm x 2 cm PET sample in the optimization study in order to use a 1 cm x 1 cm piece of each sample in each measurement method. All samples were kept in the glove box under a N₂ atmosphere and covered to prevent exposure to damaging light until ready for analysis.

4.3 Results

4.3.1 Optimization of L-Cysteine onto PET Surface

Analysis of PET Samples in Ethylenediamine Solutions

PET samples were reacted with the following concentrations of ethylenediamine for 24 hours: 0, 10, 20, 30, 40, 50, 60, 70, 80, 90, and 100 vol%. At the 70 vol% concentration and all higher concentrations, the PET samples were completely dissolved by the ethylenediamine solution. The ethylenediamine on all of the remaining samples was reacted with the fluorescent probe Oregon Green® 488 and was analyzed by using fluorescent microscopy. Figure 4.3 shows the scans of each PET sample that was reacted with the different concentrations of ethylenediamine. A lighter scan is indicative of the more fluorescence on the sample. Thus, the scans that are darker shades (black) show very little to no fluorescence on the samples.

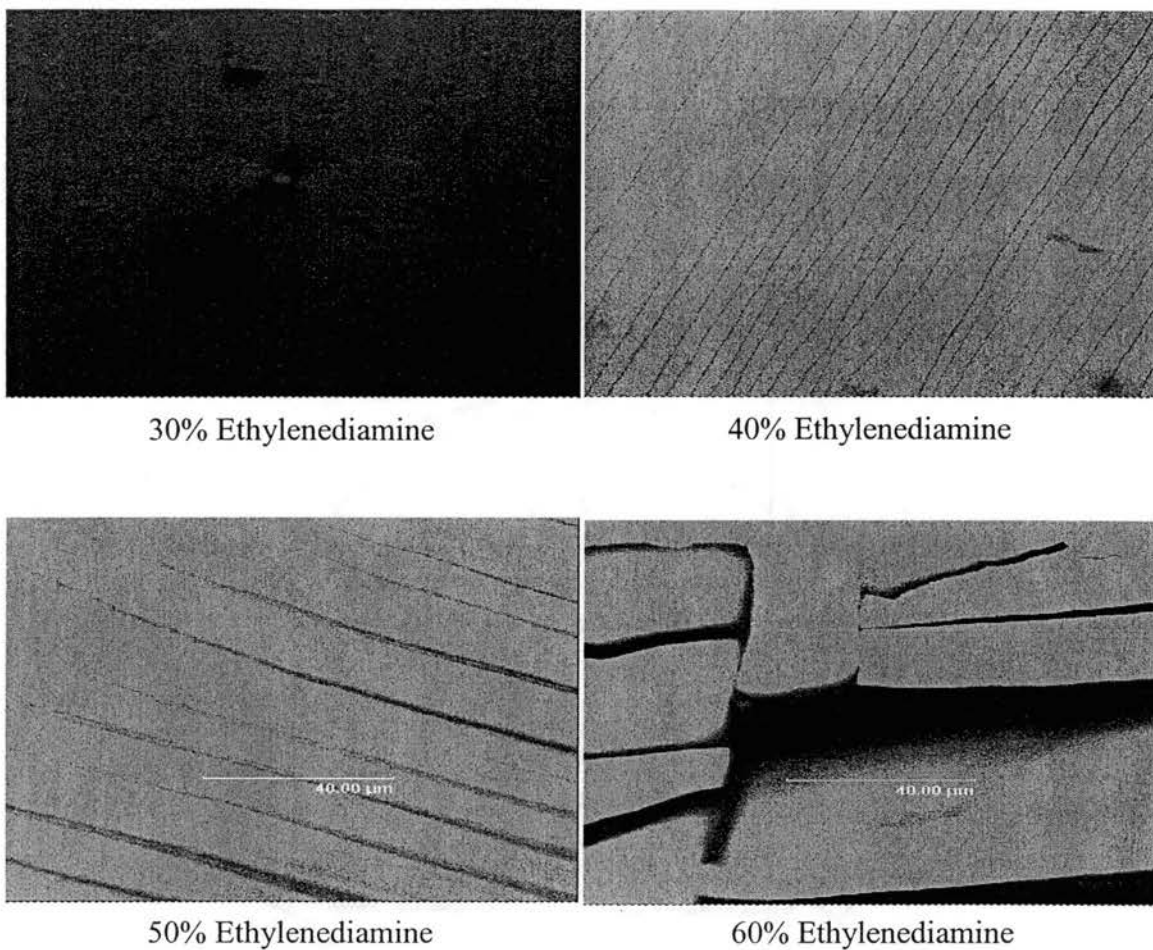


Figure 4.3 Fluorescence microscopy analysis of PET samples in various concentrations of ethylenediamine solutions. The gain setting was constant for all scans. Scans are shown at 400x magnification.

In order to compare the amount of fluorescence on all of the samples, the gain setting on the argon laser-scanning microscope was set constant for the analysis of each sample. There was no detectable fluorescence on the samples that were in the 0, 10, and 20 vol% ethylenediamine solutions (not shown in Figure 4.3). Thus, the concentrations were not high enough for the PET samples to undergo aminolysis. The scan of the PET sample that was in the 30 vol% ethylenediamine solution begins to show slight fluorescence on the surface. Although the fluorescence is slight indicating only a small amount of surface coverage of ethylenediamine, coverage does seem to be evenly distributed on the surface. The scans taken of the samples in the 40, 50, and 60 vol% ethylenediamine solutions show bright fluorescence evenly covering the surface. This indicates that at these concentrations, the surface of the samples undergo complete aminolysis. However, there are significant differences in the appearance of the physical properties of these samples that are better seen in Figure 4.4.

For the analysis of the physical characteristics of the surface of the samples shown in Figure 4.4, the gain setting on the argon laser-scanning microscope was adjusted for each sample, in order to acquire the best quality image of the surface. Therefore, the contrast of the fluorescence in the scans is not indicative of the amount of ethylenediamine on the samples, as shown previously in Figure 4.3. The scan for the sample in the 30 vol% solution shows a relatively smooth surface compared to the scans of the surfaces of the samples that were in the higher concentration solutions. Starting with the scan of the sample in the 40 vol% solution, there appears to be parallel striations on the surface. These striations were also seen in the fluorescence microscopy analysis of the samples used in each step of the process of attaching L-cysteine to the surface in

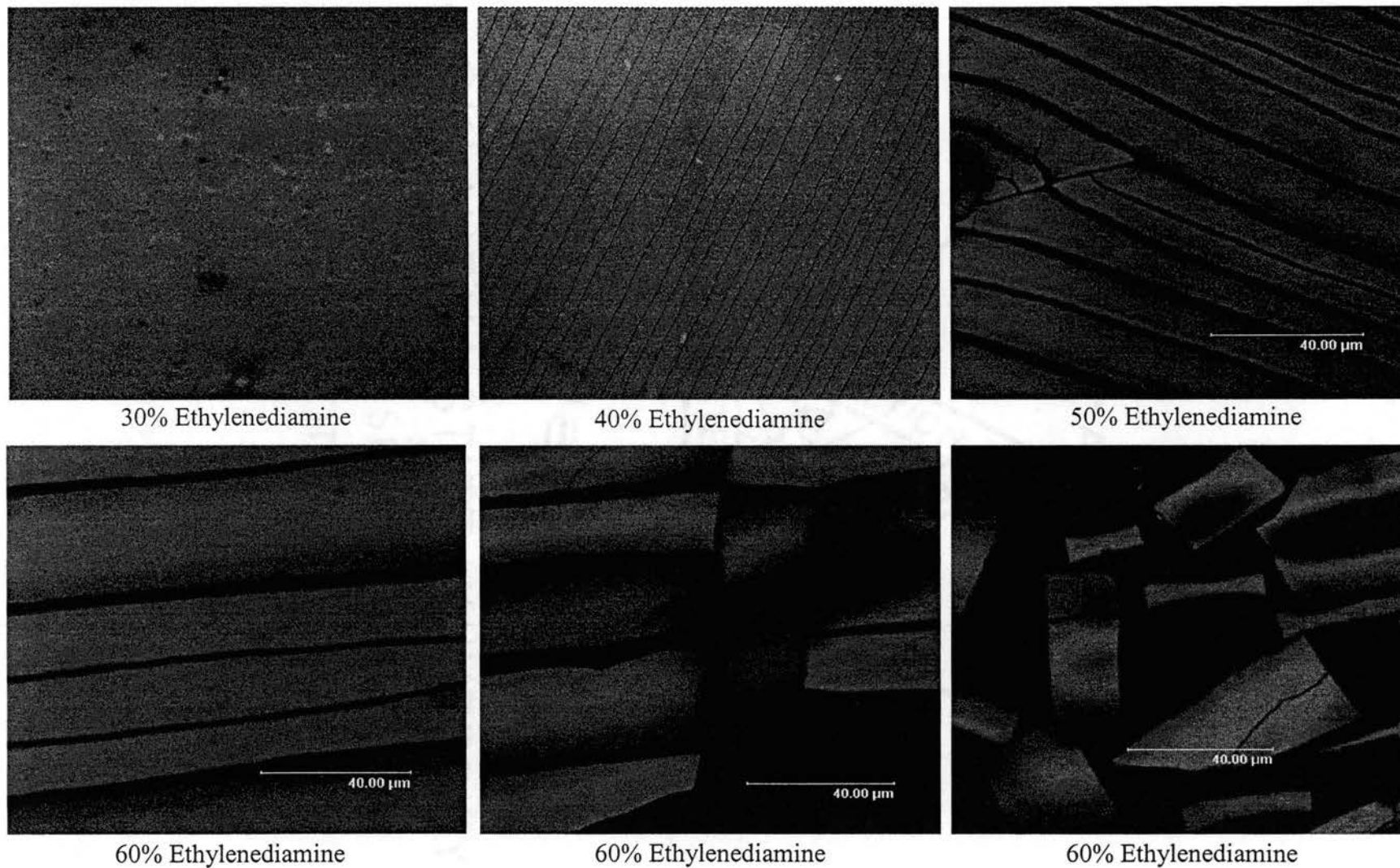


Figure 4.4 Fluorescence microscopy analysis of the effects of various concentrations of ethylenediamine on the physical properties of the surface of PET. The gain setting varied for each scan. Scans are shown at 400x magnification.

Chapter 3. It is believed that these striations are due to the fabrication process of the PET films, since they were also seen in the scanning electron microscope analysis performed by DuPont (shown in Figure 3.3). It appears that ethylenediamine reacts with the surface of PET along these striations. The thin black lines also seen in the scan of the sample in the 40 vol% solution are believed to be very small cracks in the surface where the ethylenediamine begin to break down the surface.

These cracks become wider in the scans of the samples in the 50 and 60 vol% solutions. The sample in the 60 vol% solution begins to break apart even further, with large gaps on the surface. There are three scans of the sample that was in the 60 vol% solution that were taken at different areas on the sample. At some points on the sample there is extensive surface damage, where the sample is beginning to break apart, similar to those samples that were in the higher concentration solutions. After reviewing the surface analysis of the samples in the various concentrations of ethylenediamine, a concentration of 40 vol% was selected for the remainder of the optimization studies. This concentration was chosen because it shows good surface coverage of ethylenediamine with minimal damage to the surface. The 50 vol% solution is believed to lead to even more coverage of ethylenediamine on the surface, but at the expense of extensive surface damage. Even though the physical properties of PET are not directly investigated in this research, it still must be considered for future applications of the design.

Analysis of Plackett-Burman Factorial Design

The results of the chemiluminescence and fluorescence analyses of the Plackett-Burman factorial design for L-cysteine are shown in Figures 4.5 and 4.6, respectively.

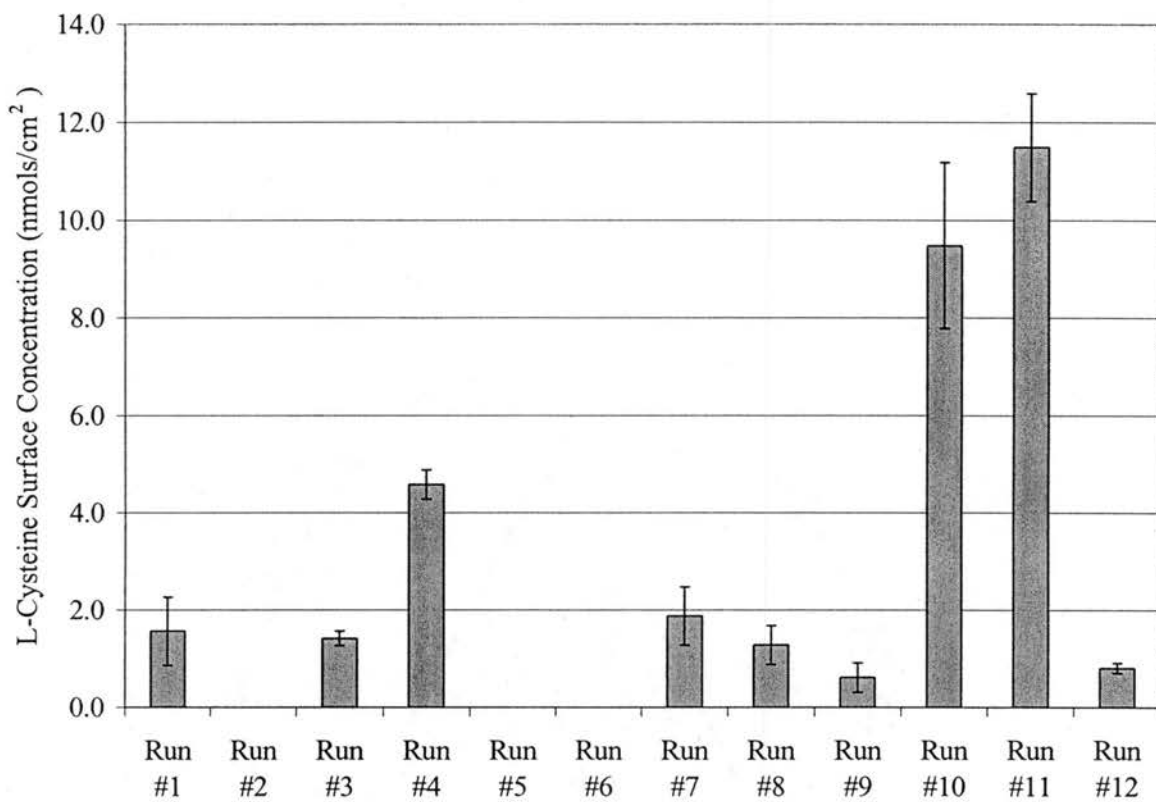


Figure 4.5 L-cysteine surface concentrations on the PET samples from the Plackett-Burman factorial design for optimizing the process of attaching L-cysteine to the surface of PET, as determined by chemiluminescence analysis. Data shown are mean values \pm standard deviation (n=3).

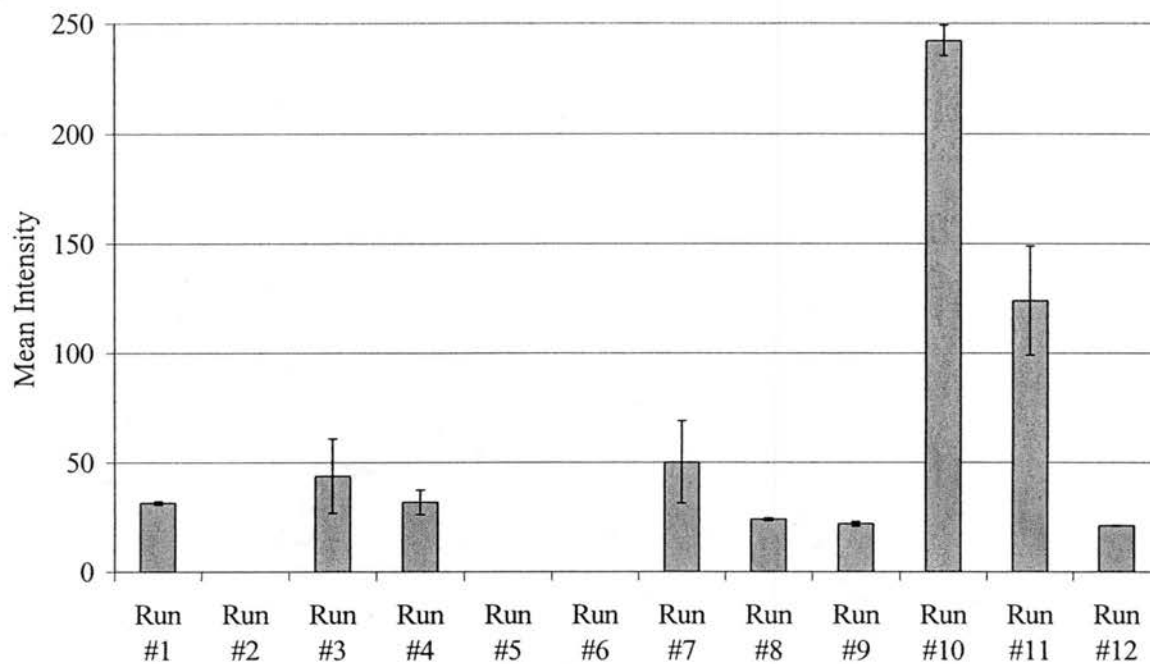


Figure 4.6 Mean intensity of fluorescence on the PET samples from the Plackett-Burman factorial design for optimizing the process of attaching L-cysteine to the surface of PET, as determined by chemiluminescence analysis. Data shown are mean values \pm standard deviation (n=3).

There are no results for the analyses of the samples from runs 2, 5, and 6 since the samples were destroyed due to the high reaction time and concentration of the ethylenediamine step. This was also shown in the results from the study investigating the effects of different concentrations of ethylenediamine on the surface of PET, described above; therefore the same effects were expected in the Plackett-Burman factorial design. The high levels were chosen in order to measure the effect when paired with a lower level, such as a high reaction time with a low concentration. For the remaining samples of the other runs, the results from the chemiluminescence analysis show that runs 10 and 11 produced samples with the most L-cysteine attached to the surface with 9.5 and 11.5 nmol/cm², respectively. Conversely, samples from runs 9 and 12 had the least amount of L-cysteine attached to the surface with 0.6 and 0.8 nmol/cm², respectively. This was expected from run 12 since all the factors for this run are set at the low levels. By using the other extremes the following conclusions can be made: 1) the samples with more L-cysteine attached to the surface had low levels for glutaraldehyde reaction time and concentration and a high level for L-cysteine concentration, and 2) the samples with less L-cysteine attached to the surface had low levels for ethylenediamine reaction time and concentration and a high level for glutaraldehyde concentration. These conclusions are all based on the assumption that there is no interaction between any of the factors; however, there may be interactions and the outcomes may be due to more of a combination of factors.

The results from the fluorescence analysis are inconclusive. Although some trends in the results seem to mimic those seen for the chemiluminescence analysis (especially for runs 10 and 11), there is too much variance in the method to be able to

compare the samples quantitatively. Some problems with the method include the following:

- Stability of the fluorescent probe: the fluorescence from the samples fades quickly and it is difficult to compare the amount of fading from each sample prior to analysis.
- Consistency in intensity measurements: due to time constraints, even though all of the samples were modified and analyzed within a certain time period, samples were analyzed on different days. The intensity of the laser on the scanning microscope decreases slightly after each use and may affect the intensity reading for samples analyzed on different days.
- Detection limits: some of the samples with less L-cysteine attached to the surface had very low intensities that were difficult to detect; therefore, it was difficult to compare the samples with the low intensities.

Due to the problems with the fluorescence microscopy analysis, it was not a useful measurement method compared to the amount of analysis time and cost and therefore was not used in the remaining optimization studies. Therefore, XPS was used in the remaining optimization studies as another measurement method to compare samples.

Table 4.6 shows the main effects of each of the six factors on the optimization process, determined by using Equation 4.2 and the results from the chemiluminescence analysis. Due to the inconclusive results from the fluorescence microscopy analysis, the main effects were not calculated based on the results of this method. The main effects are interpreted to mean that the net effect of increasing the factor level, averaged over all

TABLE 4.6

The Effect of the Factors in the Plackett-Burman Factorial Design for Optimizing the Process of Attaching L-Cysteine to the Surface of PET (Based on Mean L-Cysteine Concentrations Determined by Chemiluminescence Analysis)

Factor	Main Effect
Ethylenediamine Reaction Time (A)	-1.0
Ethylenediamine Concentration (B)	-0.8
Glutaraldehyde Reaction Time (C)	-3.4
Glutaraldehyde Concentration (D)	-5.0
L-Cysteine Reaction Time (E)	-3.0
L-Cysteine Concentration (F)	+8.1

other factor levels from low to high, is to increase or decrease the response, depending on the magnitude and direction of the main effect value of the factor. The magnitude of the main effect can be related to its significance in the optimization study. The greater the magnitude, the more influence it has on the optimization process. The sign of the main effect is related to the direction the level should be increased or decreased to influence the optimization process.

Taking all of this into consideration when interpreting the results shown in Table 4.6 for the main effects determined from the chemiluminescence analysis, the L-cysteine concentration has the most influence in the optimization study. It is also shown that the L-cysteine concentration has a positive effect, which means that the high level L-cysteine concentration results in more L-cysteine attached to the surface of the PET sample than the low level L-cysteine concentration. These findings are intuitive and were expected for the optimization process.

Another factor that is shown to have a large effect on the optimization process is the glutaraldehyde concentration. This factor has a negative effect, which means that the low level glutaraldehyde concentration results in more L-cysteine attached to the surface of the PET sample than the high level glutaraldehyde concentration. It is believed that this is due to the tendency of glutaraldehyde to crosslink at higher concentrations, resulting in few sites for L-cysteine to react. This topic was also discussed in the previous chapter during the results from the XPS analysis of the process to attach L-cysteine to the surface of PET.

The factors that seem to have the least effect on the optimization process are the ethylenediamine reaction time and concentration. Unless the high levels or low levels of

each were used simultaneously, the limits of the factors were close enough not to have a significant effect on the optimization process. Therefore, considering the results from the fluorescence microscopy study of the effects of various concentrations of ethylenediamine on the surface of PET along with the results from the Plackett-Burman factorial design, the ethylenediamine reaction time and concentration levels were set constant at 24 hours and 40 vol%, respectively. In order to use a complete factorial design to further investigate changes and combinations within some of the more significant factors, without having to perform excessive experiments, one more factor needed to be held constant in order to vary the remaining three. The glutaraldehyde reaction time was selected to be held constant at 15 minutes. The reaction time was chosen because, it is believed that the glutaraldehyde concentration has a more significant effect on the optimization process, and that the L-cysteine reaction time and concentration may produce significant effects in combination with changes to the glutaraldehyde concentration.

Analysis of Complete Factorial Design

The results of the chemiluminescence analysis of the samples from the 2-level, 3-factor, and 8-run complete factorial design are shown in Figure 4.7. Runs 4 and 8 produced samples with the most L-cysteine attached to the surface with 6.1 and 6.6 nmol/cm², respectively. However, runs 2 and 6 also produced samples with a significant amount of L-cysteine on the surface relative to the samples from the remaining runs, with 4.6 nmol/cm² on each sample. Conversely, samples from runs 5 and 7 had the least amount of L-cysteine attached to the surface with 0.4 and 0.5 nmol/cm², respectively. As a result of this factorial design, the most L-cysteine measured on the modified surface

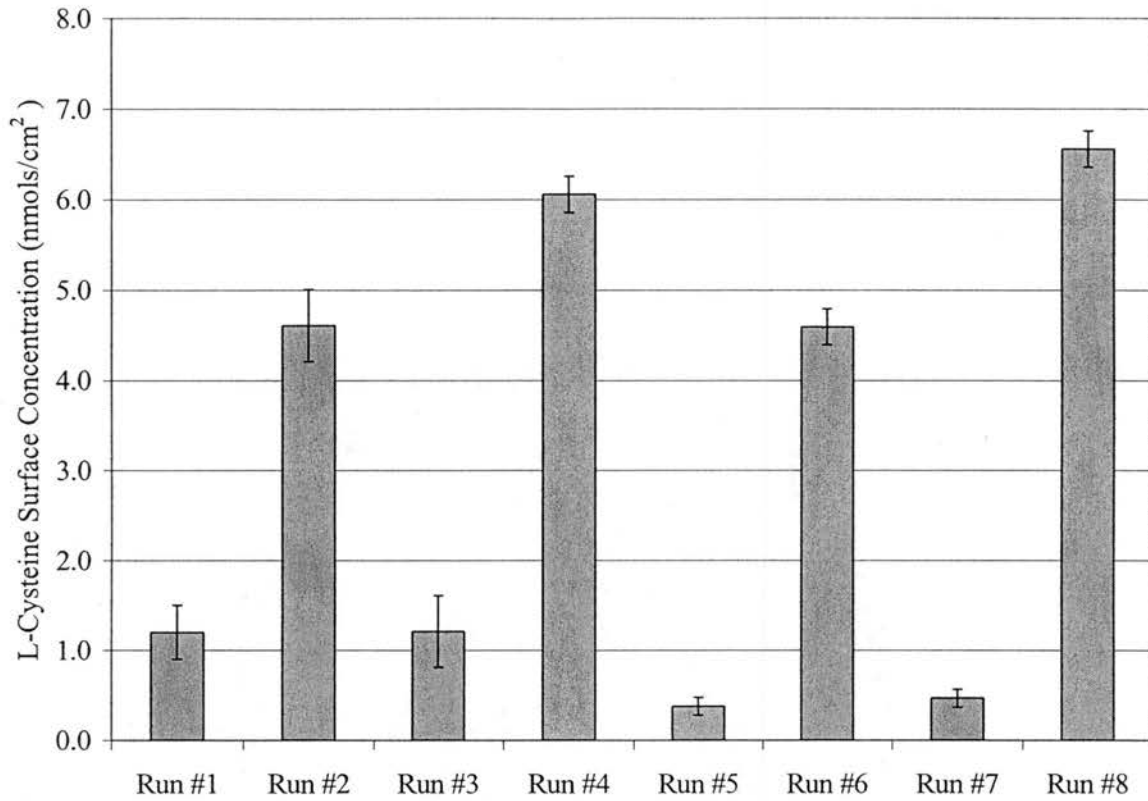


Figure 4.7 L-cysteine surface concentrations on the PET samples from the 2-level, 3-factor, and 8-run full factorial design for optimizing the process of attaching L-cysteine to the surface of PET, as determined by chemiluminescence analysis. Data shown are mean values \pm standard deviation (n=3).

was 6.6 nmol/cm^2 . This is significantly lower than the samples with the most L-cysteine measured on the surface from the Plackett-Burman factorial design, which was in the $9.5 - 11.5 \text{ nmol/cm}^2$ range. This is believed to be due to changes made to the ethylenediamine step of the modification process. For the runs in the Plackett-Burman factorial design that produced samples with high surface concentrations of L-cysteine, the samples were submitted to either high ethylenediamine concentrations or long ethylenediamine reaction times. Therefore, these factors in combination with the other optimal conditions for the runs resulted in samples with high L-cysteine surface concentrations. However, as discussed earlier, these high level ethylenediamine factors can begin to cause damage to the surface of the PET sample. So, by setting the factors for ethylenediamine to prevent surface damage to the sample, L-cysteine surface coverage may have been sacrificed.

The main effects calculated for the three factors that were varied for this complete factorial design are: 1) -0.7 for the glutaraldehyde concentration, 2) $+2.4$ for the L-cysteine reaction time, and 3) $+12.4$ for the L-cysteine concentration. Comparing the magnitudes of the main effects, the L-cysteine concentration has the most influence on the optimization process. The effect is also positive revealing that the higher level concentration causes an increase in the surface coverage of L-cysteine on the sample. The lower magnitude of the other two factors shows that they are not as significant as the L-cysteine concentration, however their sign reveals some important information. The negative effect of the glutaraldehyde concentration shows that the lower level concentration results in an increase in the surface coverage of L-cysteine on the sample,

and the positive effect of the L-cysteine reaction time shows just the opposite, an increase in the reaction time increases the surface coverage.

Analysis of the Optimal Design

After reviewing the results from both the Plackett-Burman factorial design and the complete factorial design, the following optimal factors were selected for attaching L-cysteine to the surface of PET by using the reactions shown in Figure 4.1 along with the constants described in Section 4.2.2:

- Ethylenediamine Reaction Time: 24 hours
- Ethylenediamine Concentration: 40 vol%
- Glutaraldehyde Reaction Time: 15 minutes
- Glutaraldehyde Concentration: 0.02 vol%
- L-Cysteine Reaction Time: 12 hours
- L-Cysteine Concentration: 2 wt%

For the L-cysteine reaction time, the results of the factorial designs showed that longer reaction times lead to greater L-cysteine surface coverage on the sample; therefore a reaction time greater than 1 hour was needed, but from past experience and other studies, there does not appear to be a significant difference in surface coverage after a reaction time of 12 hours (Duan and Lewis, 2002). Therefore, a L-cysteine reaction time of 12 hours was chosen instead of the 4 day time period in order to decrease the time it takes to modify samples. Any small increase in surface coverage after a reaction time of 12 hours would not be significant enough to justify the extended time.

Table 4.7 shows the results of the XPS analysis of each step of the process of attaching L-cysteine to the surface of PET, using the optimal factors. The atom% of each

TABLE 4.7

Atom% of Elements on Optimized L-Cysteine Modified PET Samples
(Comparison of Theoretical with Measured by XPS)

Sample Description	Blank PET	PET + ED	PET + ED + GA	PET + ED + GA + Cys
C's (Measured)	73.79	72.03	72.58	75.04
C's (Theoretical)	71.43	66.67	71.43	66.67
O's (Measured)	26.21	24.29	23.19	19.86
O's (Theoretical)	28.57	20.00	19.05	18.52
N's (Measured)	0	3.68	4.23	4.45
N's (Theoretical)	0	13.33	9.52	11.11
S's (Measured)	0	0	0	0.65
S's (Theoretical)	0	0	0	3.70

Abbreviations. PET = Polyethylene Terephthalate, ED = Ethylenediamine, GA = Glutaraldehyde, Cys = L-Cysteine, C = Carbon, O = Oxygen, N = Nitrogen, S = Sulfur

element measured on the surface of the optimized samples was compared to the theoretical atom% of each element on the surface, assuming a one-to-one binding of each groups as previously described in Chapter 3. The analysis of the blank sample of PET shows the atomic% of carbon and oxygen similar to the theoretical amounts. The analysis of the sample with ethylenediamine shows a lower nitrogen content than expected when compared to the theoretical amounts (approximately 28% of the theoretical atom%). This is believed to be due to incomplete surface coverage of ethylenediamine. Since there are not any nitrogen atoms on blank PET, all the nitrogen contribution is due to the addition of ethylenediamine on the surface. This results in more open sites on the PET sample, which would also lead to an increase in the oxygen and carbon content on the surface, also shown in the table. The incomplete surface coverage of ethylenediamine must be considered when analyzing the remaining samples with glutaraldehyde attached and L-cysteine attached. The low L-cysteine content on the surface may also be attributed to fewer available reaction sites due to possible crosslinking of the glutaraldehyde residues on the surface as described in Chapter 3.

When comparing the XPS results of the optimized polymer with those from the previous modification process described in Chapter 3, the following two conclusions can be made: 1) there was less surface coverage of ethylenediamine when comparing the nitrogen content after the addition of ethylenediamine to the polymer surface, and 2) there was more surface coverage of L-cysteine when comparing the sulfur content after the addition of L-cysteine to the polymer surface. The reason that there was less surface coverage of ethylenediamine on the optimized L-cysteine modified polymer sample compared to the L-cysteine modified polymer samples described previously in Chapter 3

is believed to be due to the lower concentration of ethylenediamine used to modify the samples in the optimized modification process. The fluorescent studies analyzing the effect of ethylenediamine on the physical surface properties of the polymer (Section 4.3.1 Analysis of PET Samples in Ethylenediamine Solutions) showed that the concentration that was previously used to modify the polymer samples, described in Chapter 3, (50 vol%) was degrading the surface of the polymer. Therefore, the concentration of ethylenediamine was lowered (40 vol%) for use in the optimization studies in order to prevent surface damage. The reason there was more surface coverage of L-cysteine on the optimized L-cysteine modified polymer compared to the L-cysteine modified polymer described previously in Chapter 3 is believed to simply be due to the fact that the modification process was now optimized.

4.3.2 Optimization of 2-Iminothiolane onto PET Surface

Figure 4.8 shows the results from the chemiluminescence analysis of the initial complete factorial design used to optimize the process of attaching 2-iminothiolane to the surface of PET. The results show very little to no 2-iminothiolane attached to the surface of the samples, due to problems already discussed earlier in the chapter. One conclusion that may be made about the results is that the one hour reaction time for 2-iminothiolane is not long enough for it to react with the ethylenediamine on the surface. Runs 1, 2, and 3 produced samples that did not have any detectable 2-iminothiolane on their surfaces and these were the only runs that had the one hour 2-iminothiolane reaction time.

Figure 4.9 shows the results from the improved complete factorial design. For this design, there were detectable amounts of 2-iminothiolane on the surface of all the samples. There were three runs in the design, runs 6, 8, and 9, which produced samples

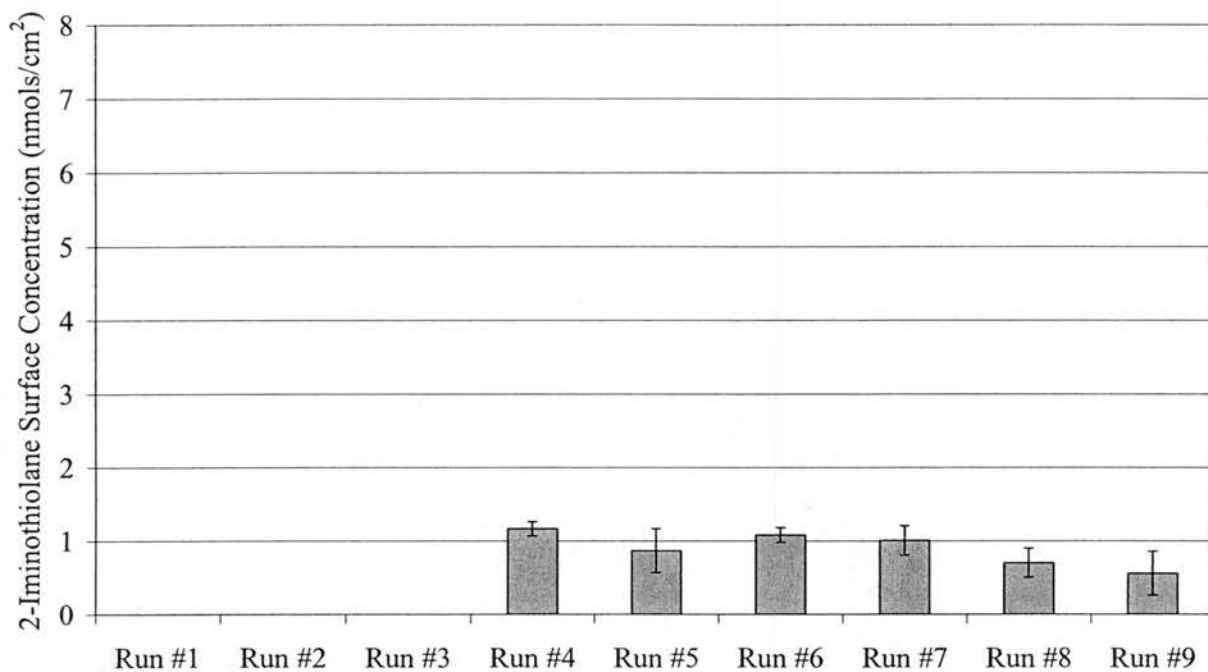


Figure 4.8 2-Iminothiolane surface concentrations on the PET samples from the initial 3-level, 2-factor, and 9-run full factorial design for optimizing the process of attaching 2-iminothiolane to the surface of PET, as determined by chemiluminescence analysis. Data shown are mean values \pm standard deviation (n=3).

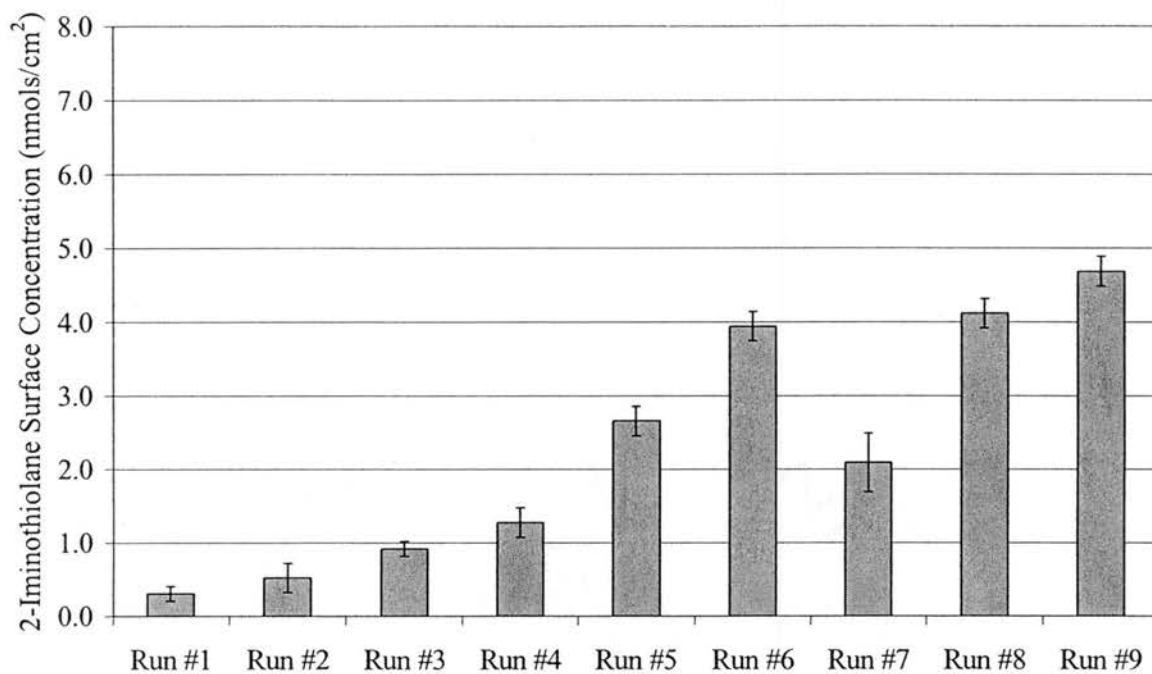


Figure 4.9 2-Iminothiolane surface concentrations on the PET samples from the improved 3-level, 2-factor, and 9-run full factorial design for optimizing the process of attaching 2-iminothiolane to the surface of PET, as determined by chemiluminescence analysis. Data shown are mean values \pm standard deviation (n=3).

with the most 2-iminothiolane on the surface with 3.9, 4.1, and 4.7 nmol/cm² on each, respectively. Samples from the first three runs, 1, 2, and 3, had the least amount of 2-iminothiolane on their surfaces. This was also seen in the results for the initial complete factorial design, and was expected due to the low 2-iminothiolane reaction time. For the runs with the longer reaction times, it appears that the higher the concentration of 2-iminothiolane used in the run, the higher the concentration of 2-iminothiolane measured on the surface. However, the reaction times may also play an important role, as seen for run 8, where the mid level concentration with the high level reaction time resulted in a high surface concentration of 2-iminothiolane.

The results from the XPS analysis of the samples from the improved factorial design are shown in Table 4.8. Even though this analysis method does not give a direct measurement for the surface concentration of 2-iminothiolane, some conclusions can be made by comparing the amount of sulfur on the surface of each sample. 2-iminothiolane is the only group on the surface that contains sulfur; therefore, the amount of 2-iminothiolane on the surface of each sample can be compared by examining the amount of sulfur on each surface. Also, the amount of nitrogen on the surface of each sample is a good indicator of the amount of ethylenediamine on the surface; however, 2-iminothiolane also contains nitrogen and contributes to the total atom% of nitrogen on the surface. The amount of nitrogen on the samples all fall within the range of 3.51 – 4.95 atom%, which is considerably lower than the theoretical atom% of nitrogen of 14.285%. The samples with the least amount of sulfur on their surfaces included those from runs 1, 4, and 7 which had the low level 2-iminothiolane concentration and run 2, which had the mid level concentration, but had the low level 2-iminothiolane reaction time. The sample

TABLE 4.8

Atom% of Elements on 2-Iminothiolane Modified PET Samples
(Comparison of Theoretical with Measured by XPS)

Run #	C's	O's	N's	S's
<i>Theoretical</i>	66.67	14.285	14.285	4.76
1	75.12	20.97	3.76	0.14
2	76.41	19.37	4.04	0.18
3	73.60	20.40	4.91	1.10
4	77.48	18.87	3.51	0.14
5	76.13	18.87	4.44	0.56
6	75.54	19.29	3.98	1.19
7	74.64	20.24	4.95	0.16
8	76.90	18.59	4.09	0.42
9	75.27	19.82	3.61	1.29

from run 3 with the low level 2-iminothiolane reaction time had a relatively high amount of sulfur on the surface. This could be due to the high level 2-iminothiolane concentration in this run and/or this sample had a high atom% of nitrogen on its surface compared to the other samples, indicating it had more ethylenediamine on the surface promoting more reaction sites for the 2-iminothiolane. The sample from run 7 also had a high atom% of nitrogen on its surface, however it had a low atom% of sulfur on its surface. This is believed to be due to the low level 2-iminothiolane concentration in this run. The samples with the greatest amount of sulfur on their surfaces are those from runs 3, 6, and 9, which all included the high level 2-iminothiolane concentration in their runs.

When comparing the XPS analysis of the samples from the optimization study with the theoretical values, there are significant differences. All samples had higher carbon and oxygen content compared to the theoretical values. Also, all the samples had lower nitrogen and sulfur content compared to the theoretical values. The lower atom% of nitrogen is indicative of a 3:1 ratio of PET:ethylenediamine, as seen from the XPS studies in Chapter 3. An incomplete coverage of ethylenediamine on the surface resulting in more open PET sites would also lead to higher carbon and oxygen contents on the surface, also seen in the XPS results. However, it is important to remember that the theoretical values are based on a clean surface with one-to-one binding of each molecule with perfect detection of the entire surface. It is very unlikely that all of these conditions are met in order to match measurements with the theoretical values.

Based on the results from the chemiluminescence and XPS analysis of the samples from the complete factorial designs, the following optimal factors were selected

for the process of attaching 2-iminothiolane to the surface of PET by using the reactions shown in Figure 4.2 along with the constants described in Section 4.2.2:

- 2-Iminothiolane Reaction Time: 24 hours
- 2-Iminothiolane Concentration: 50 mM

Since the results from the chemiluminescence and XPS analyses show that there is not a significant difference between the 24 hour and 3 day reactions times, the 24 hour reaction time was selected in order to decrease the amount of time to modify samples.

4.3.3 Optimization of Cysteine Polypeptide onto PET Surface

Figure 4.10 show the results from the chemiluminescence analysis of the complete factorial design for the optimization of the process of attaching the cysteine polypeptide to the surface of PET. There was not any detectable cysteine polypeptide on the surfaces of the samples from runs 1 – 4. Runs 1 – 3 all had the low level cysteine polypeptide reaction time, which indicates that the reaction time was not long enough for the cysteine polypeptide to react with the glutaraldehyde on the surface. Run 4 had the mid level reaction time, but the low level cysteine polypeptide concentration, indicating that at this low concentration, a longer reaction time was required. The dependence on reaction time is further shown in run 7 with the low level cysteine polypeptide concentration but the high level reaction, which had detectable cysteine polypeptide on its surface. Runs 6 and 9 produced samples with the greatest amount of cysteine polypeptide on their surfaces, with 2.60 and 2.52 nmols/cm², respectively. Both runs had the high level cysteine polypeptide concentration. The only difference between the runs was that run 6 had the mid level cysteine polypeptide reaction time and run 9 had the high level reaction time. There does not appear to be a significant difference in the

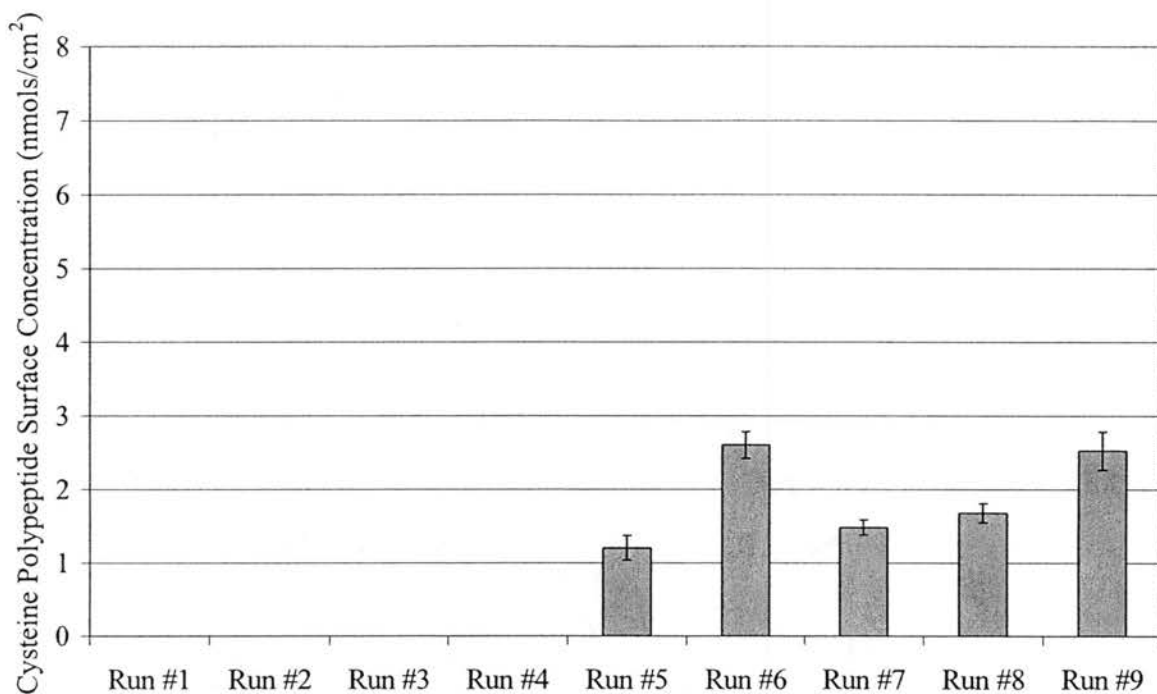


Figure 4.10 Cysteine polypeptide surface concentrations on the PET samples from the improved 3-level, 2-factor, and 9-run full factorial design for optimizing the process of attaching the cysteine polypeptide to the surface of PET, as determined by chemiluminescence analysis. Data shown are mean values \pm standard deviation (n=3).

amount of cysteine polypeptide on the surface of samples submitted to either a mid or high level reaction time, as long as the cysteine polypeptide concentration is mid to high level.

The results from the XPS analysis of the samples from the full factorial design are shown in Table 4.9. As before, sulfur is used as an indicator of the amount of cysteine polypeptide on the surface of each sample since the cysteine polypeptide is the only group on the surface that contains the sulfur atom. The results of the XPS analysis of the samples from runs 1 – 4 are the same as those from the chemiluminescence analysis, there was no detectable amount of sulfur on the samples, which can be interpreted as no detectable amount of cysteine polypeptide on the samples. The atomic% of nitrogen on the samples from runs 1 – 4 are all in the same range as the other samples from the other runs; therefore, there were available reactions sites on the surface for cysteine polypeptide, but the reaction time was not long enough. Another similarity with the results from the chemiluminescence analysis was that the samples from runs 6 and 9 had the highest atomic% of sulfur on their surfaces, signifying that these runs produced samples with the highest surface concentration of cysteine polypeptide.

Similar to the previous optimization studies, the actual measured values from the XPS analysis do not match the theoretical values shown in the table for a modified surface with one-to-one binding of each species. The trends in the measured values are also similar to those seen previously. All the samples had higher carbon content and most had higher oxygen content compared to the theoretical values. Also, all the samples had lower nitrogen and sulfur content compared to the theoretical values. Therefore, the conclusions made earlier that there is incomplete coverage of ethylenediamine and

TABLE 4.9

Atom% of Elements on Cysteine Polypeptide Modified PET Samples
(Comparison of Theoretical with Measured by XPS)

Run #	C's	O's	N's	S's
<i>Theoretical</i>	59.58	19.15	14.89	6.38
1	77.74	17.78	4.48	0
2	77.57	18.31	4.12	0
3	76.84	19.30	3.86	0
4	76.37	20.04	3.58	0
5	77.57	17.49	4.76	0.18
6	75.49	19.11	4.31	1.10
7	74.97	20.28	4.42	0.32
8	76.34	18.57	4.61	0.48
9	75.02	19.01	4.97	1.00

possible glutaraldehyde crosslinking can also be made for these sample; however, it is important to remember that the theoretical values represent the perfect conditions and may never be reached.

Based on the results from the chemiluminescence and XPS analysis of the samples from the full factorial designs, the following optimal factors were selected for the process of attaching cysteine polypeptide to the surface of PET by using the reactions shown in Figure 4.1, the only difference is that the single L-cysteine residue is replaced with the cysteine polypeptide, along with the constants described in Section 4.2.2:

- Cysteine Polypeptide Reaction Time: 24 hours
- Cysteine Polypeptide Concentration: 14.5 mM

Since the results from the chemiluminescence and XPS analyses show that there is not a significant difference between the 24 hour and 3 day reactions times, the 24 hour reaction time was selected in order to decrease the amount of time to modify samples.

4.4 Discussion

The Plackett-Burman factorial design was shown to be a useful tool in the optimization of the process to modify the surface of PET. Several factors were investigated at one time without having to perform an excessive number of experiments. Even though this factorial design did not directly result in the optimal process, it did narrow the range of factors to be further investigated. This was done by determining the effect of each factor on the process. By finding the factors that had the most effect on the process, a full factorial design was used to further study the effect of different levels on the process and among each other. This strategy was used for the optimization of the

process of attaching L-cysteine to the surface of PET. From the initial Plackett-Burman design it was discovered immediately that the ethylenediamine and L-cysteine concentrations were important. Samples disintegrated after being in the high level ethylenediamine concentration, and it was difficult to prepare the high level L-cysteine concentration because L-cysteine would not completely dissolve in solution and some solid crystals would begin to form on the surface of the PET sample. These discoveries led to additional studies to investigate the best concentration ranges to use for the ethylenediamine and L-cysteine factors in the factorial design. With the new findings, changes were made to the initial Plackett-Burman factorial design and from the improved design it was discovered that the negative effects of the glutaraldehyde concentration and L-cysteine reaction time and the positive effect of the L-cysteine concentration were the most significant factors in the process and were investigated further in a complete factorial design. Finally, the optimal conditions for the process of attaching L-cysteine to the surface of PET were determined after reviewing the results from all of the optimization studies.

Another important discovery made during the optimization of L-cysteine was that even though fluorescence microscopy was a good qualitative method to investigate the physical properties of a surface, it failed as a method to quantitatively measure the amount of L-cysteine on the surface of the samples. This problem was due to several reasons discussed earlier, the most important related to the stability of the fluorescent probe and the difficulty in accurately quantifying the amount of fluorescence on each sample. However, with improved measurement techniques, it is believed that in the

future this method will be an important analysis tool for investigating surfaces, since it could reveal important data both visually and quantitatively.

XPS was chosen as a better method to analyze the samples from the optimization studies. Currently this is a very expensive analysis method and the data from the analysis can be difficult to interpret since the method only measures the atom% of elements on a surface and not molar surface concentrations. Another problem is that the current XPS method does not reveal the type of bonding occurring or the form of the molecule on the surface. Therefore, it is difficult to determine if the thiol groups attached to the surface are in their oxidized or reduced forms, since XPS does not detect thiols, but only the sulfur atom in the thiol group. More detailed XPS analysis techniques can be used to determine the type of bonding and the form of groups on surfaces, but the analysis cost is even higher and the method is not always accurate. XPS is still a valuable method for determining if a specific atom is on a surface, making it one of the most popular methods for characterizing a surface.

The optimization study using 2-iminothiolane was simplified by using the results from the optimization study with L-cysteine (i.e. using the optimal ethylenediamine conditions). A complete factorial design was used to investigate the factors of 2-iminothiolane reaction time and concentration. The first optimization study was unsuccessful due to problems with the 2-iminothiolane solutions. It was discovered that the pH of the solution was not high enough to break the ring formation in 2-iminothiolane, allowing the ring to react via an amidine bond to ethylenediamine on the polymer surface and to expose the free thiol group. Changes were made to the experimental design and the complete factorial design was repeated. The samples were

analyzed by both chemiluminescence and XPS methods to determine the optimal conditions for the process of attaching 2-iminothiolane to the surface of PET.

The optimization study using cysteine polypeptide was also simplified by using the results from the optimization study with L-cysteine. The optimal factors for the ethylenediamine and glutaraldehyde steps, determined earlier, were used and the cysteine polypeptide reaction time and concentration factors were varied in a complete factorial design. The samples were analyzed by both chemiluminescence and XPS methods to determine the optimal conditions for the process of attaching cysteine polypeptide to the surface of PET.

When comparing the surface concentrations of thiol groups from each of the optimized processes determined from the chemiluminescence analysis method, the amount of thiol groups on the surface increased in order with the following groups: cysteine polypeptide < 2-iminothiolane < L-cysteine. When considering the solution concentration of each thiol group used in the optimization studies, the 2-iminothiolane concentration was higher than that of L-cysteine and the cysteine polypeptide, showing that the higher thiol solution concentration does not always result in a higher thiol surface concentration. The high level concentration factors for each were set due to specific reasons based on either past studies or availability, as described previously. For example, in the optimization of L-cysteine, when the low level L-cysteine concentration was used (16.5 μ M), in some cases the resulting thiol concentration on the surface of the samples was higher than that in the other optimization studies using the high level thiol concentrations of 50 mM for 2-iminothiolane and 14.5 mM for the cysteine polypeptide in the optimization process.

Other possible explanations for the lower surface concentrations of cysteine polypeptide and 2-iminothiolane on the samples include:

- The surface concentration of cysteine polypeptide on the samples may be low due to disulfide linkages between the cysteine residues on the peptide chain. The chemiluminescence method only measures thiols in their reduced form because they must first be nitrosated prior to measurement; therefore, the surface concentration of cysteine polypeptide may be higher than that measured by the chemiluminescence method.
- The surface concentration of 2-iminothiolane on the samples may be low due to problems with breaking the ring formation of the molecule so it can react with ethylenediamine on the surface. Also, 2-iminothiolane may return to its ring formation under the acidic conditions used during the nitrosation process of the chemiluminescence method, leaving it unable to be detected by the chemiluminescence method.

When comparing the surface concentrations of thiol groups from each of the optimized processes determined from the XPS analysis method, by comparing the atom% of sulfur on the surface, the results varied differently than those from the chemiluminescence analysis. The optimized 2-iminothiolane and cysteine polypeptide samples both had a higher atom% of sulfur on their surfaces compared to the optimized L-cysteine sample; however, the theoretical values indicate that they should have a higher atom% of sulfur on their surfaces compared to the L-cysteine sample, 4.76 and 6.38 atom% compared to 3.70 atom%, respectively. Compared to the theoretical atom% of sulfur, the optimized 2-iminothiolane sample did have approximately 1.5 times as much

sulfur on its surface compared to the optimized L-cysteine and cysteine polypeptide samples. This inconsistency in the analysis of the 2-iminothiolane optimized sample between the two analysis methods may be due to what is actually measured by each method. The chemiluminescence method only measures thiols in their reduced state, since the thiols must be nitrosated prior to measurement in the reducing solutions. XPS does not measure thiols directly; instead it measures the atomic percentage of sulfur on the surface, regardless of the thiol oxidation state or the possibility of disulfide bonding. Therefore, there may be more 2-iminothiolane on the surface of the optimized polymer compared to L-cysteine or the cysteine polypeptide, but, as shown by the chemiluminescence analysis, only a fraction is in its reduced state. The thiol group must be in its reduced state in order for it to become nitrosated by transnitrosation and to release NO into the surrounding area to prevent platelet attachment to the modified surface.

Once the processes to modify the polymer with the three thiol groups (L-cysteine, 2-iminothiolane, and cysteine polypeptide) were optimized, the next step was to use the optimized polymers in experiments with platelets. Studying the optimized polymers with platelets tested the hypothesis that the addition of more L-cysteine sites or different L-cysteine-containing moieties on the polymer will increase the NO-release rate per unit area and lead to a greater inhibition of platelet deposition on the modified polymer. The studies were performed to test if the optimized polymers prevented platelet attachment to the surface better than the L-cysteine modified polymers used in past research (Section 2.5.3) and which group attached to the surface of the polymer prevented platelet attachment the best under the experimental conditions.

CHAPTER 5

UTILIZATION OF THE OPTIMIZED POLYMERS IN AN IN VITRO SYSTEM WITH PLATELETS

5.1 Introduction

The hypothesis was that the optimized polymers will significantly decrease platelet attachment to the polymer surface compared to control samples. This study is the first step in the process to investigate the utilization of the optimized polymers and the mechanisms by which they function. The main purpose of this study is to investigate how well the optimized polymers prevent platelet attachment to their surfaces under controlled conditions. Once it is determined how well these optimized polymers prevent platelet attachment to their surfaces, further studies may be performed to investigate the exact mechanisms and components involved. As described previously, the modified polymer inhibits platelet attachment by utilizing naturally occurring nitrosothiols in the plasma that can transfer nitric oxide (NO) to the attached thiol on the modified polymer. It has also been shown that there are other plasma components, such as metal ions that promote the release of NO from nitrosothiols (Singh et al., 1996). Therefore, nitrosothiols must be present with the platelets in order for the modified polymer to inhibit platelet attachment.

Slit flow chambers are commonly used in research to study the interactions between a surface and a flowing solution or suspension (Azeredo et al., 2003; Chotard-

Ghodsnia et al., 2002; Ruel et al., 1995; van Kooten et al., 1992). A specific type of slit-flow chamber is a parallel plate flow chamber. In a parallel flow chamber, a solution or suspension flows through a thin slit between two parallel plates. The surface under investigation may be either the surface of the plate itself or a thin film placed between the two plates. The parallel plate flow chamber design used for this study is similar to the one used in past studies and is shown in Figure 5.1 (Duan and Lewis, 2002; Ramamurthi and Lewis, 1998).

Several established techniques can be used to measure the amount of platelet deposition on surfaces. Some of the more common techniques include: 1) scanning electron microscopy (SEM) (Dadsetan et al., 2001; de Brito Alves et al., 2003), 2) fluorescent microscopy (Adams and Feuerstein, 1980; Baker et al., 1997), and 3) radiolabeling (Datz, 1986; Desai and Thakur, 1986). Each technique may also have several different ways of operation. All of these techniques are well established and each has been shown to adequately measure platelets on surfaces. For this study, fluorescent microscopy and radiolabeling were selected to measure the amount of platelet deposition on the modified polymers. The SEM technique was not selected due to its high cost. Similar to SEM, fluorescent microscopy can also visually show platelet deposition on the surface, but at a much lower cost.

Several fluorescent probes can be used to label platelets in order to view the platelets with a fluorescence microscope. The ideal method involves a label that is detectable with a high level of sensitivity, is stable over the lifespan of the platelet, and does not alter the normal functional and survival characteristics of the cells. 5-Chloromethylfluorescein diacetate (CMFDA) is one probe that is used to label platelets.

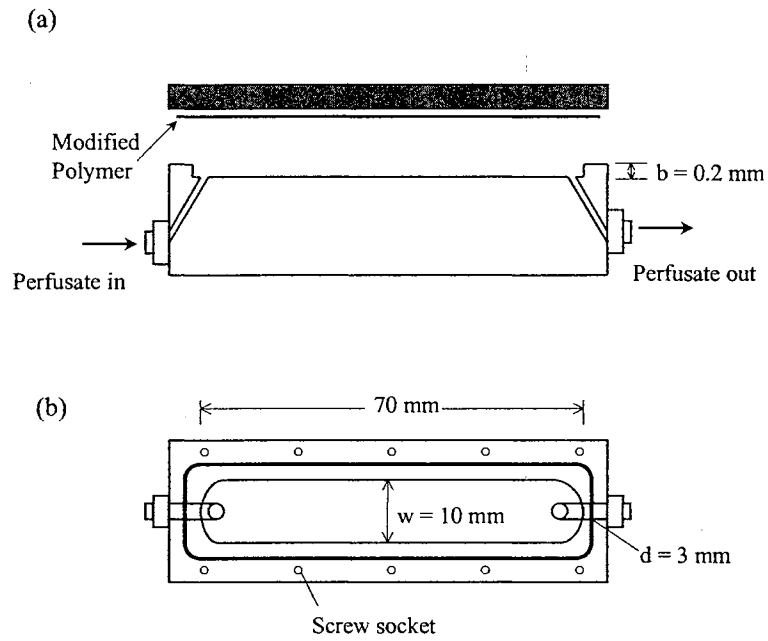


Figure 5.1 Parallel plate flow chamber used to test platelet deposition on the optimized polymers. (a) Side view. (b) Top view. Figure from Duan, 2001.

CMFDA freely passes through cell membranes, and is a colorless, nonfluorescent compound that contains a reactive chloromethyl group. Once inside of a cell, the chloromethyl group reacts with intracellular thiols, transforming the probe into a cell-associated dye-thiol adduct. After cytosolic esterases cleave off the acetate groups of CMTDA, a brightly fluorescent product is generated. This particular probe would not be a good selection for this study because any excess probe in the platelet suspension that may come into contact with the modified polymer may also react with the free thiol groups on the surface of the modified polymers. The probe may also react with any exposed amine groups on the surface of the modified polymers, as seen earlier with the reaction of 5-IAF with ethylenediamine. Another type of probe is an antibody specific probe for platelet surface receptors that is labeled with a fluorochrome. This probe is very specific to platelets, and several types of fluorochromes are available.

Unfortunately, this label is very expensive and requires large amounts of the probe to ensure complete labeling of the platelets. The most common probe used to label platelets is quinacrine dihydrochloride, or better known by its common name, mepacrine.

Mepacrine accumulates rapidly and selectively into platelet dense granules. This probe was selected due to its wide use in platelet applications and its low cost.

The two most common radiolabels used to label platelets are chromium-51 (Cr-51) and indium-111 (In-111). Because of different physical and chemical natures of chromium and indium, the radionuclides are known to bind to different intracellular components. A large proportion of Cr-51 is known to bind to the nucleotides, and a small proportion of radioactivity remains in the membranes (Cunningham and Siegel, 1982). In contrast, In-111 complexes appear to bind to other cytoplasmic components with least

radioactivity on the membranes (Thakur et al., 1976). In-111 is superior over Cr-51 in labeling platelets for use *in vivo*, because the gamma emissions of Cr-51 are too low to allow external imaging. However, Cr-51 is suitable for labeling platelets to be used in experiments *in vitro*. Cr-51 also has some advantages over In-111 including a longer life span and unlike Cr-51, there is a small spontaneous release of In-111 from labeled platelets. Therefore, Cr-51 was selected to be used to radiolabel the platelets in the study with the modified polymers.

For this study, the following four solutions were used in the perfusion experiments with the optimized polymers:

- **Solution A:** A labeled platelet suspension in buffer solution
- **Solution B:** A labeled platelet suspension in a buffer solution containing 7 μM nitrosated bovine serum albumin (BSANO). This is the typical concentration of nitrosated albumin in human blood) (Stamler et al., 1992a). Bovine serum albumin (BSA) was used instead of human serum albumin (HSA) because BSA is less costly and has been shown to have identical transnitrosation properties as that of HSA (Scorza et al., 1997).
- **Solution C:** A labeled platelet suspension in a plasma solution
- **Solution D:** A labeled platelet suspension in whole blood solution

Each of the solutions described above will be used in order to study the effect of different constituents and possible mechanisms the modified polymers may be utilizing to inhibit platelet deposition. Solution A will be used to measure the effect of platelet deposition on the modified polymer in the absence of nitrosothiols. It is believed that the modified polymers prevent platelet deposition by the transfer of NO from nitrosothiols in

the plasma to the thiol group on the modified polymer and then the NO is released from the polymer into the surroundings to prevent platelet deposition. Therefore, if no nitrosothiols are available, then the modified polymers should not be able to inhibit platelet deposition and platelet deposition should be similar to that on the control sample. Solution B is used to investigate if nitrosated albumin is the primary plasma constituent needed to freely transfer NO to the thiol group on the modified polymers to prevent platelet deposition. Even though nitrosated albumin makes up the largest quantity of nitrosothiols in plasma, it is believed that there are other constituents in the plasma that are needed for the transfer of NO between nitrosothiols and for the release of NO from nitrosothiols, such as metal chelators like Cu^+ . Therefore, the amount of platelet inhibition by using solution B can be compared to the amount by using solutions C or D that contain all of the plasma constituents. Finally, solutions C and D can be used to compare the difference in platelet deposition on the modified polymers without and with the presence of red blood cells, respectively. Hemoglobin found in red blood cells in whole blood has been shown to react readily with NO in solution and take part in transnitrosation between circulating nitrosothiols (Winterbourn, 1990). Therefore, by comparing the results of platelet inhibition on modified polymers by using solutions C and D, the effects of hemoglobin on the transnitrosation, NO release, and platelet deposition process can be assessed.

5.2 Materials and Methods

5.2.1 Reagents

Sodium nitrite was purchased from Fisher Scientific (Fairlawn, NJ). Phosphate buffered saline (PBS, pH 7.4) was obtained from Life Technologies (Gaithersburg, MD).

Polyethylene terephthalate (PET) (thickness = 0.2 mm) was supplied by DuPont (Hopewell, VA). Bovine serum albumin (BSA), citrate-dextrose solution (ACD), ethylenediamine, glutaraldehyde (GA), glycine, HEPES, 2-iminothiolane hydrochloride, iodine, L-cysteine, quinacrine dihydrochloride (mepacrine), Trizma® base (tris[hydroxymethyl]aminomethane), Tyrode's salts, and all the other reagents were purchased from Sigma Chemical Co. (St. Louis, MO). The L-cysteine polypeptide (Cys-Gly-Cys-Gly-Cys) and the glycine polypeptide (Gly-Gly-Gly-Gly-Gly) were purchased from the Molecular Biology Resource Facility (Norman, OK). Chromium-51 was purchased from Amersham Biosciences (Arlington Heights, IL). All water used was of HPLC-grade quality and was deoxygenated by bubbling nitrogen in the water prior to use.

5.2.2 Preparation of Platelets for Use in Perfusion Studies

Platelet Isolation

Human platelets are among the most widely studied cells in the body. A vast number of investigators are presently isolating and successfully using platelets in studies; however, the methods used in these studies vary radically. Some important points in the methods that vary among the studies and that were considered for the platelet preparation for this study are listed below.

- Many drugs are known to interfere with platelet function and therefore, it is crucial to ensure that potential blood donors have not ingested such drugs during the previous 14 days. These drugs include antiplatelet drugs, such as aspirin, and other non-steroidal anti-inflammatory drugs and antihistamines.

- Several anticoagulants are available. The choice of anticoagulant depends on what aspect of platelet function is to be examined. Heparin has been widely used as an anticoagulant; however, some heparin preparations cause platelet aggregation and it prevents platelets from aggregating in an irreversible manner. Inhibition of coagulation by chelating divalent cations, such as ethylenediaminetetraacetic acid (EDTA), has also been widely used, but is not ideal as it both affects cell surface adhesive receptors and may deplete intracellular calcium stores. Any of the three citric acid based anticoagulants can be used without effecting normal platelet function, which includes sodium citrate, citrate-citric acid-dextrose (CCD), and acid-citric acid-dextrose (ACD). ACD was selected to be used in the platelet isolation procedures.
- There are many different types of buffers used to wash and store platelets. Ideally, the buffer mimics the properties of the natural medium for platelets, plasma, including a balance of salts and the addition of important proteins. Some of the more common types of buffers used with platelets are 1) Tyrode's balance salt solution, 2) Eagle's minimal essential medium, and 3) buffered saline glucose citrate (BSGC). All seem to work equally well in preserving the function of plates in solution for washing and storing purposes. Tyrode's balance salt solution was chosen to be used in the platelet studies.
- The aggregation of platelets in solution is pH dependent. The recovery of platelets is higher if the pH of the solution is slightly acidic. This is due to a decrease in platelet adhesiveness and aggregation. Repeated centrifugation releases ADP from the red blood cells, increasing platelet adhesiveness.

Acidification affects the electrostatic forces at the platelet's surface, inhibiting the effect of ADP. Acidity also reduces the metabolism of ATP to ADP (Flatow and Freireich, 1966). Studies have shown that platelet aggregation caused by centrifugation occurs at a pH above 6.3 (Aster and Jandl, 1964). Therefore, ACD was added to each platelet solution that was centrifuged in a quantity sufficient to keep the pH below 6.3. The amount of ACD added depended on the type of platelet solution and the volume of the solution.

- The type and number of platelets isolated are dependent on the centrifugation method used in the process. Ideal centrifugation conditions for the production of platelet rich plasma (PRP) are 1750 to 2700 g-min (Woods et al., 1976). At higher forces, too many platelets are lost, whereas lower forces result in excessive red blood cell contamination. The duration of centrifugation can affect the age of the platelets recovered. With longer centrifugation times, the younger platelets, which are more adhesive than older ones, tend to sediment out of the PRP (McBride, 1968). Optimal conditions for production of the platelet pellet are 10,000 to 20,000 g-min (Mathias and Welch, 1984) and were used during platelet isolation procedures.
- The type and amount of agitation affects platelet aggregation properties. A study between a tumbler and a horizontal type agitator showed that the tumbler agitator did more damage to the platelets than the horizontal tumbler under the same experimental conditions. Also, excessive agitation (> one hour) can damage platelets (Bannai et al., 1985). A horizontal tumbler was

used for the platelet labeling procedures and agitation times did not exceed one hour.

- Platelet aggregation and deaggregation are temperature dependent. The rate of aggregation is less at 20°C (~ room temperature) than at 37°C (~physiological temperature), and ADP does not cause aggregation at 0°C except when high concentrations of the nucleotide are used. Thus, platelet solutions were prepared and stored at lower temperatures (~ 4°C) and then the temperature was raised to 37°C for use in the platelet studies.

The methods used to obtain and isolate the platelets used in this study were approved by the Institutional Review Board for Human Research at Oklahoma State University, Stillwater, OK. Blood was solicited from healthy individuals 18 years old or older. Informed consent was obtained from all donors. The protocol used to isolate platelets and prepare them for the perfusion studies with the optimized polymers is shown in the steps below:

1. Human blood was drawn from paid research donors by trained medical technicians at the Student Health Center at Oklahoma State University by venipuncture in volumes not exceeding 30 ml per drawing. Blood volume from two donors was used for each experiment in order to isolate a sufficient number of platelets. Blood samples from individual donors were kept separate in order to avoid any adverse effects, such as complement activation. Blood was not drawn from a single subject any more than twice a week. The initial 2-3 ml of blood was discarded to prevent the blood from clotting, since the initial small volume of blood is rich in clotting factors. The rest of the

blood sample was drawn into six 5 ml tubes, each containing an anticoagulant (1 part of 0.105 M of trisodium citrate per 9 parts of whole blood). The samples were stored on ice in a sealed container for transport back to the laboratory. Platelet preparation took place within 30 minutes of obtaining the blood samples.

2. Once back at the laboratory, samples were divided equally by volume into six 15 ml centrifuge tubes (~9 ml per tube). Once again, blood samples from individual donors were kept separate. The blood samples were centrifuged at 200x g for 10 minutes to separate the red blood cells from the platelet rich plasma (PRP). The heavier red blood cells migrated to the bottom of the centrifuged tubes leaving the lighter PRP on top.
3. The PRP was removed from each tube, combined, and divided equally by volume between two 15 ml centrifuge tubes (~8-13 ml), ensuring that samples from individual donors were kept separate. The tubes containing the red blood cells were stored at 4 °C until ready for use in the perfusion studies. The anticoagulant ACD was added to each tube containing the PRP (1:10 v/v) in order to prevent platelet aggregation during centrifugation. The samples were centrifuged at 500x g for 15 minutes to separate the platelets from the plasma solution. The platelets migrated to the bottom of the centrifuge tube and formed a pellet in the platelet poor plasma (PPP) solution.
4. The PPP solution was carefully removed from each tube, in order to avoid disturbing the platelet pellet. The PPP was placed in a centrifuge tube and stored at 4 °C until ready for use in the perfusion studies. The platelet pellet

was gently resuspended in ~10 ml of a sterile-filtered HEPES-buffered Tyrode's solution (8.0 g NaCl, 2.38 g HEPES, 1.0 g D-glucose, 1.0 g NaHCO₃, 0.2 g KCl, 0.2 g CaCl, 0.1 g MgCl, 0.05 g NaH₂PO₄•H₂O in 1.0 L HPLC-grade water, pH 7.4). At first, ACD was added to each at a 1:10 v/v ratio, but after the next centrifugation step, the platelets aggregated in solution. It was determined that the pH of the platelet solution was too high for centrifugation (pH 6.2). Therefore, ACD was added to Tyrode's buffer at a 1.25:10 v/v ratio in order to lower the pH to 6.0. This ratio of ACD was added to Tyrode's buffer during all wash steps and storage of the platelets, in order to prevent aggregation.

Platelet Counting

Once the platelets were isolated, they were counted by using phase microscopy. A 1% ammonium oxalate solution was prepared in HPLC-grade water and sterile filtered. To a 1.5 ml microcentrifuge tube, 50 µL of the platelet suspension was added to 950 µL of 1% ammonium oxalate and mixed thoroughly. The ammonium oxalate stimulated the lysis of any remaining red blood cells in the platelet suspension that could possibly interfere with the platelet count. Approximately 20 µL of the suspension was added to one side of a haemocytometer and allowed to settle for 15 minutes to ensure even distribution of the platelets on the counting surface. The haemocytometer was examined under a phase microscope (400x magnification), and a 5 x 5 grid was used to count the platelets. Platelets were counted from five blocks in the grid (the four corners and the middle) and an average platelet count was determined by taking the average of the counts from the five blocks. Each block also had its own 4 x 4 grid to aid in the counting of the

platelets. Figure 5.2 shows an example of the platelets spread over one of the 5 x 5 counting grids. The smaller spheres that make up the majority of the cells shown in the image are the platelets, and the few larger spheres seen sporadically in the image are red blood cells. As shown in Figure 5.2, some of the platelets were already forming aggregates on the surface of the haemocytometer after only five minutes due to platelet activation. The modified polymers should decrease the number of platelets or prevent platelets from becoming activated and attaching to the modified surface. The volume within one grid was 10^{-4} ml (determined by manufacturer). Therefore, the platelet concentration was calculated by taking the average platelet count within one grid divided by the volume for that grid. The concentration of the original 10 ml platelet suspension was determined by correcting for the dilution of the sample in the ammonium oxalate solution. After counting the platelets in each solution, the platelets from each donor were mixed and then equally divided by volume between two tubes, prior to labeling.

Platelet Labeling

Platelets were labeled with either the fluorescent label mepacrine or the radiolabel Cr-51, prior to their use in the perfusion studies. The labeling process took place after the isolation and counting procedures. The steps, used to label the platelets with either mepacrine or Cr-51, are described below.

1. The platelet suspensions were centrifuged at 500x g for 15 minutes and the Tyrode's buffer solution gently removed so to not disturb the platelet pellet.
 - To label the platelets with the fluorescent probe, the platelets were resuspended in 10 ml of a 10 μ M mepacrine solution prepared in Tyrode's buffer with ACD.

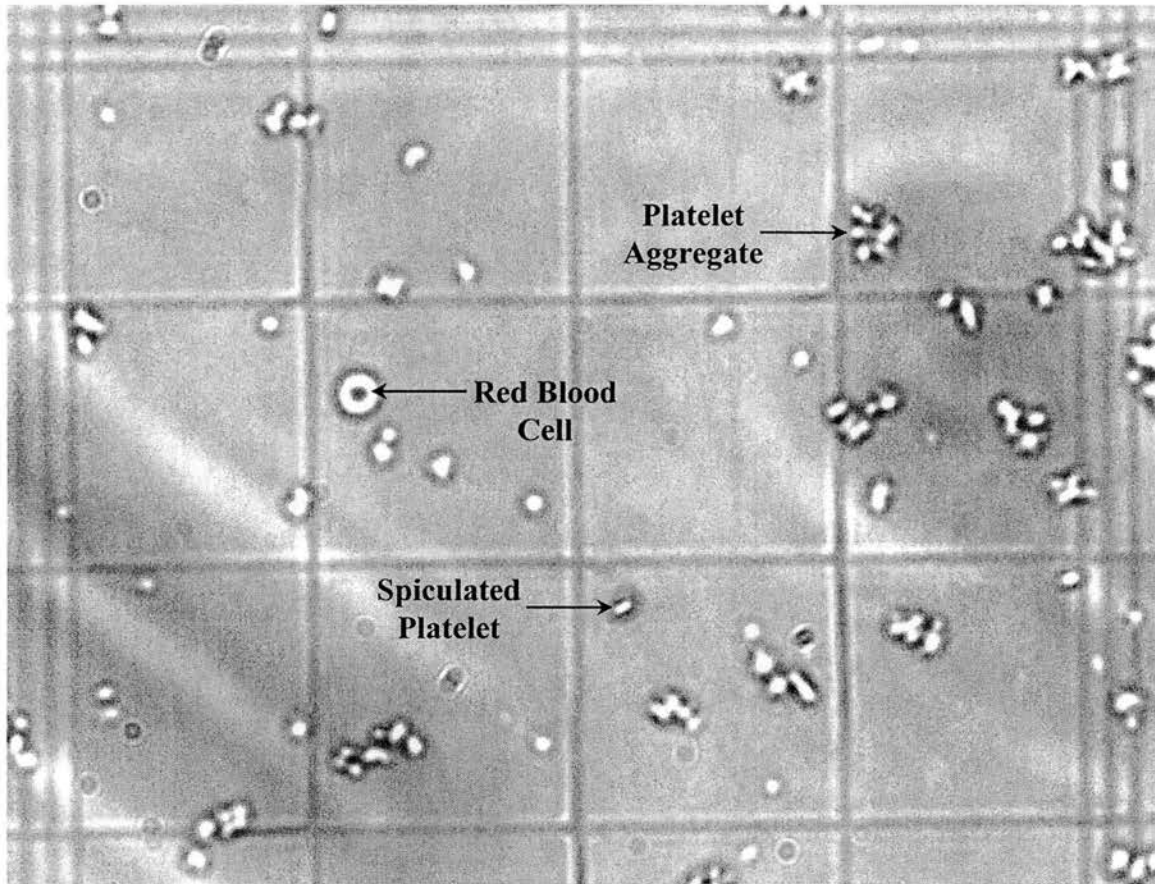


Figure 5.2 An example of one of the 5 x 5 grids (outlined by the triple lines) on the haemocytometer used to count platelets by phase microscopy. Sample at 400x magnification.

- To label the platelets with the radiolabel, the platelets were resuspended with Cr-51 (100 μCi per 15×10^9 platelets) in Tyrode's buffer with ACD. The volume of Cr-51 added to the platelet solution was determined by the following expression, based on the specific activity of the Cr-51 solution.

$$\text{Vol. of Cr-51 added } (\mu\text{L}) = \frac{VC}{\text{S.A.}} \frac{(100 \mu\text{Ci})}{(15 \times 10^9 \text{ platelets})} \quad \text{Eq. 5.1}$$

where,

V = the volume of the platelet suspension (ml)

C = the concentration of the platelet solution (platelets/ml)

S.A. = the specific activity of Cr-51 ($\mu\text{Ci/ml}$)

The specific activity of Cr-51 was calculated according to the following:

$$\text{S.A. } (\mu\text{Ci/ml}) = N_0 (\mu\text{Ci/ml}) \times \exp\left(\frac{-0.693 \times T}{T_{1/2}}\right) \quad \text{Eq. 5.2}$$

where,

N_0 = initial specific activity of Cr-51 (supplied by manufacturer)

T = the time since the determination of N_0 (days)

$T_{1/2}$ = the half-life of Cr-51 (26.6 days)

2. Each centrifuge tube was attached to a horizontal rotating plate and was gently rotated at the lowest setting for 30 minutes.
3. The platelet suspensions were centrifuged at 500x g for 15 minutes and the mepacrine or Cr-51 solution gently removed.

4. To remove any excess label that did not react with the platelets, the platelets were washed by resuspending them in 10 ml of Tyrode's buffer with ACD. The suspensions were centrifuged at 500x g for 15 minutes and the wash solution gently removed. This wash step was repeated to ensure complete removal of any excess label.

All steps of the fluorescent labeling procedure were done in the dark with all solutions and samples covered in order to avoid damaging light. The fluorescently labeled samples were stored and transported in a black sample box until ready for analysis.

All personnel involved in the handling of the radioisotope received training and certification by the Radiological Safety Officer (RSO) at Oklahoma State University, Stillwater, OK. All steps of the radiolabeling procedure were performed in a designated work area behind lead shielding at least 1/8 in thick, to shield from harmful gamma radiation from Cr-51. A Geiger counter was also used to survey the area where the radiolabel was used and stored. The radiolabeled samples were stored and transported in a lead-lined sample box until ready for analysis. All dry and liquid waste from the radiolabeling procedures was disposed of by the guidelines set forth by the RSO.

5.2.3 Preparation of Optimized Polymers and Control Samples

Fresh samples of the modified polymers were prepared prior to each perfusion experiment and used within 12 hours after modification. Samples modified by each of the groups described in Chapter 4 were used in the perfusion studies, including L-cysteine, 2-iminothiolane, and the cysteine polypeptide. The modified samples were prepared by using the optimized conditions determined in Chapter 4. All samples were

stored under a N₂ atmosphere until ready for use in the perfusion studies. An extra sample was prepared in each batch of modified polymers used in the perfusion studies in order to measure the average thiol surface concentration on the samples, assuming that samples from the same batch will have approximately the same thiol surface concentration. The thiol concentration on the surface of the samples was measured by using the Chemiluminescence Method 1 (see Section 3.2.6).

Control samples for the perfusion experiments included glycine-modified samples and glycine polypeptide-modified samples. The glycine-modified sample was a control sample in past studies (Duan, 2001) and was selected as a control sample for this study for the following reasons: 1) glycine (MW = 75.1) is similar in size to L-cysteine (MW = 121.1) and 2-iminothiolane (MW = 137.6), 2) the method for attaching glycine to the surface of PET is similar to that for attaching the other groups in the modification process, and 3) it does not contain a thiol group; therefore, it does not react with NO or participate in transnitrosation reactions. To prepare the glycine-modified samples, the same procedures that were used to prepare the optimized L-cysteine modified samples were used, except that glycine was substituted for L-cysteine in the last step. The glycine-modified control samples were prepared in parallel with each of the other modified samples that were used in the perfusion studies.

In order to test the effect on platelets of the size of the molecule attached to the surface of PET, such as the cysteine polypeptide, a glycine polypeptide modified sample was used as a control sample. The glycine polypeptide is a linear peptide containing five glycine residues. It is attached to the surface of PET in a method similar for attaching the

cysteine polypeptide to the surface of PET, except that the glycine polypeptide was substituted for the cysteine polypeptide in the last step.

5.2.4 Parallel Plate Perfusion Studies

As mentioned previously, there were four types of solutions that were used in the perfusion studies, 1) Tyrode's buffer solution, 2) 7 μM BSANO solution, 3) 50 vol% plasma solution, and 4) 50 vol% whole blood solution. The Tyrode's buffer solution used in the perfusion studies was the same as that used in the platelet preparation procedures. The BSANO solution was prepared ~12 hours prior to its use in the perfusion studies. To prepare the BSANO solution: 10 ml of 20 μM BSA in a 0.5 M HCL solution, initially containing 40 μM NO_2^- , was shaken for 12 hours to completely nitrosate all of the BSA. An excess of NO_2^- was used in order to ensure complete nitrosation of the BSA in the solution. Studies have shown an understoichiometric concentration of free thiols in BSA (0.53 ± 0.02 -SH/molecule) due to mixed disulfides (DeMaster et al., 1995; Stubauer et al., 1999). Other studies have shown that with excess nitrite, BSA is nitrosated to yield a stoichiometry of 0.85 ± 0.07 mol S-NO/mol BSA (Scharfstein et al., 1994). Therefore, even though steps were taken to keep BSA in its reduced form (N_2 atmosphere, no light, deoxygenated solutions, etc.) the actual concentration of BSANO may be lower than expected. Just prior to its use in the perfusion studies, the BSANO solution was neutralized by using NaOH solutions and diluted to its final concentration of 7 μM by using Tyrode's buffer. The plasma solution used in the perfusion studies was 50 vol% of the plasma saved from the platelet isolation procedure in Tyrode's buffer. The whole blood solution was prepared by mixing equal volumes of plasma and red blood cell suspension saved from the platelet isolation

procedures and preparing a 50 vol% solution in Tyrode's buffer. The plasma and whole blood suspension used for each perfusion study was isolated from only one of the two donors, ensuring that samples from individual donors were kept separate. Since the whole blood and plasma solutions contain the large red blood cells and/or large proteins, each were diluted with Tyrode's buffer in order to flow through the parallel plate flow chamber (described below) easier, allowing more platelets to make contact with the surface of the modified polymers. ACD was not added to any of the solutions used in the perfusion studies, so that it would not interfere with the natural platelet activation mechanisms. Each solution contained approximately the same number of platelets, and the solutions were heated to physiological temperature (37 °C) just prior to use in the perfusion studies. Not adding ACD to the solutions and heating the solutions to physiological temperature were done in order to mimic physiological conditions as closely as possible during the perfusion studies.

As shown previously in Figure 5.1 a parallel plate flow chamber was used to test platelet adhesion under flow conditions on the optimized samples described in Chapter 4. The flow chamber consists of two sections, the bottom plate and the top plate. The bottom, thicker plate contains a very thin flow slit (0.20 ± 0.01 mm deep, 10 mm wide, and 70 mm long) with a perfusate inlet and outlet, which are inclined at a 45° angle and have a diameter of 3 mm. The top plate is used to cover the bottom plate, to form a seal between the two plates so that the perfusate only flows through the thin slit. The two plates were sealed by using two C-clamps connected to each end of the parallel plate chamber. Pharmed® tubing (i.d. = 3mm) is connected to the perfusate inlet and outlet via polypropylene luer fittings. Pharmed® tubing is specially designed to be used in

biological applications due to its inert properties. A variable flow syringe pump (Model 74900-10, Cole Parmer, Vernon Hills, IL) was used to perfuse the platelet suspension through the chamber. Just prior to performing each perfusion study, a sample modified with one of the groups described in Chapter 4 along with a glycine-modified control sample, both approximately 1 cm x 3 cm, were wetted with buffer and attached end-to-end to the top plate of the perfusion chamber. The samples were positioned in such a way that once the top plate was sealed to the bottom plate, the samples covered the area of the thin slit and the solutions flowed over the bottom surface of each sample. The samples were slightly wider (~ 1.2 cm) than the width of the thin slit (1.0 cm), to ensure that the samples would not fall into the slit if the samples came unattached from the top plate. There was approximately 0.5 cm gap between the end of each sample and the inlet or outlet ports of the slit. To investigate if there were any entrance or exit flow effects on the placement of samples within the perfusion chamber or if the order of the samples in the perfusion chamber had an impact on the reaction of platelets with the surfaces, two glycine-modified control samples were placed end-to-end in the perfusion chamber and tested under the same conditions in the procedures described above for the perfusion studies. The order of the samples in the perfusion chamber was also varied among the runs, in order to ensure that the placement of the samples in the chamber did not affect platelet interaction with the surface of the modified polymer. Fresh polymer samples were used with each of the four test solutions. Thus, a total of eight samples (one optimized and one control for each of the four test solutions) were tested for each perfusion study. In order to perform statistical analyses, each perfusion study was also

performed in triplicate, each on a separate day. The procedures for each perfusion experiment were as follows:

- Perfused with 5 ml of Tyrode's buffer for 5 min at a flow rate of 1.0 ml/min in order to rinse the sample and to remove any contaminants from the system.
- Perfused with 10 ml of one of the test solutions containing platelets labeled with either mepacrine or Cr-51 for 10 min at a flow rate of 1.0 ml/min.
- Perfused with 10 ml of Tyrode's buffer for 10 min at a flow rate of 1.0 ml/min to remove any platelets that are not attached to the surface of the sample.

For a specific flow rate, the dimensions of the flow channel determine the shear rate. A flow rate of 1.0 ml/min was used in this study, which corresponds to a wall shear rate (γ) of 250 s^{-1} (laminar flow) according to the following equation: (Sakariassen et al., 1989)

$$\gamma \text{ (s}^{-1}\text{)} = \frac{3}{2} \frac{Q}{60wb^2} \quad \text{Eq. 5.3}$$

where,

Q = volumetric flow rate (ml/min)

w = slit width (cm)

b = half-thickness of the flow slit (cm)

This flow rate was selected in order to produce a wall shear rate that was within the physiological range.

In order to investigate if the size of the molecule attached to the surface of PET had an effect on platelet attachment, a glycine polypeptide modified sample was tested in the perfusion chamber along with a glycine-modified control sample, both 1 cm x 3 cm.

Each perfusion experiment was carried out as described above, using each of the four test solutions. The perfusion studies using the glycine polypeptide modified samples were also performed in triplicate.

5.2.5 Surface Analysis of the Modified Polymer Samples

The surfaces of the modified polymer samples used in the perfusion studies with the fluorescently labeled platelet solutions were analyzed by using an argon laser-scanning microscope (Leica TCS SP2, Exton, PA) in confocal mode with a 10.0 x 40.0 oil immersion objective lens. The filters were set at 436 nm for the excitation and 525 nm for the emission. Due to the weak signal of the fluorescent label, viewing was improved by using a mercury lamp. The surface coverage of platelets on samples was compared by counting the number of individual platelets on the surface of each sample within a certain surface area. The modified polymer samples used in the perfusion studies with the radiolabeled platelet solutions were analyzed by measuring the amount of radioactivity, measured in counts, on each sample with a COBRA-II autogamma counter (Packard Instrument Company, Meriden, CT).

The counts of each sample, either the number of fluorescently labeled platelets or amount of radioactivity, were compared as a percentage of the glycine-modified control sample paired with each during the perfusion studies. Both the analysis of the fluorescently labeled platelets and the analysis of the radiolabeled platelets were normalized based on the number of platelets in the test solution prior to perfusion over the sample.

5.3 Results

5.3.1 Preparation of Optimized Polymers and Control Samples

The analysis of the modified samples taken from each batch of the modified polymers prepared for the perfusion studies showed that the concentration of the thiol groups on the surface of each sample were similar to the measured values of the optimized samples from Chapter 4. The average thiol surface concentrations were 5.9 ± 0.5 nmols/cm², 4.3 ± 0.7 nmols/cm², and 2.3 ± 0.4 nmols/cm² for the L-cysteine, 2-iminothiolane, and cysteine polypeptide modified samples, respectively.

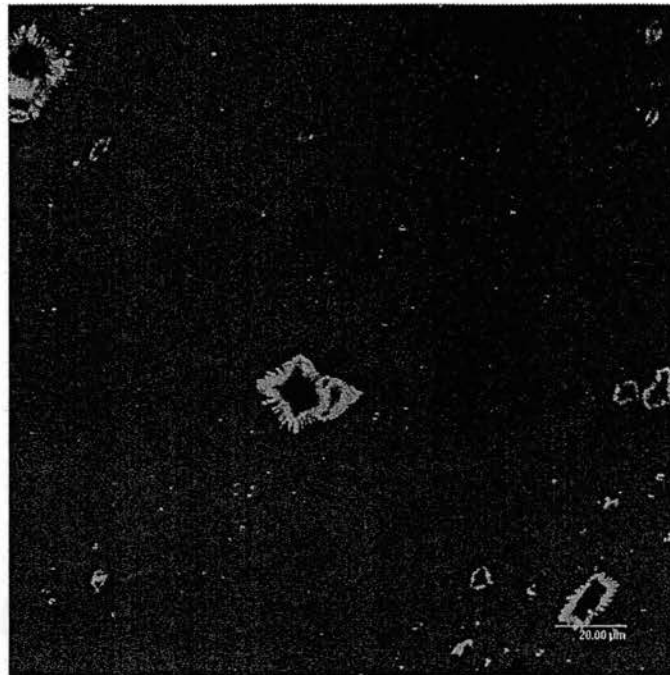
5.3.2 Parallel Plate Perfusion Studies

Analysis of Fluorescently Labeled Platelets

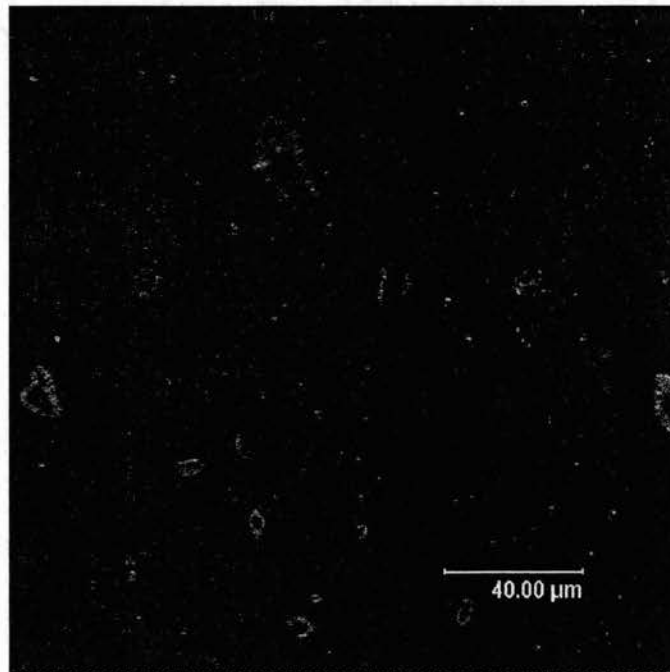
In order to compare the amount of platelet attachment on the modified samples used in the perfusion studies, the number of platelets within a given area on each sample was to be counted and compared. Unfortunately, the number of platelets on each sample could not be determined due to several problems, including: 1) aggregates on the surfaces made it difficult to determine the number of individual platelets, 2) the weak signal of the fluorescent probe made it difficult to identify some platelets, 3) the thickness of the platelet layers resulted in many different planes of focus, making it difficult to identify all of the individual platelets, and 4) because the thin polymer film was semi-transparent, it was difficult to distinguish if the platelets were only in layers on one side of the polymer or if some platelets were able to contact the surface of the polymer that was attached to the top plate and there was a fluorescent signal from these platelets passing through the sample.

Due to the difficulty of trying to perform a quantitative analysis with the samples containing the fluorescently labeled platelets, a more qualitative analysis was attempted to get some useful information from the samples. Each modified sample that was used in the perfusion study was compared side-by-side to its corresponding control sample from the study. It is still difficult to draw direct conclusions from this qualitative analysis; however, it may be possible to find trends in the data that can be useful when interpreting the data from other analysis techniques, such as the radiolabeled platelets. An important point to remember when comparing the images from the fluorescent analysis is that unlike previous studies from Chapters 3 and 4, the contrast of the fluorescence is not related to the coverage of platelets on the surface. The gain on the scanning laser microscope was adjusted in order to acquire the best possible image; therefore, some images may be brighter or darker than others. The images can only be compared by examining the number of platelets on each image.

Figures 5.3 to 5.6 show the images of the L-cysteine modified samples after their use in the perfusion studies with Tyrode's buffer, BSANO, plasma, and whole blood, respectively. In Figure 5.3, the scan of the L-cysteine modified sample was mistakenly taken at 800x magnification; therefore, the scan of the glycine modified sample was increased to 800x magnification in order to compare the two samples. All other scans of the samples were at 400x magnification. There were no significant differences in the amount of scatter of the platelets on the surfaces shown in Figures 5.3, 5.4, and 5.6 that were used in the perfusion studies with platelets in the Tyrode's buffer solution, the BSANO solution, and the whole blood solution, respectively. For the samples shown in Figure 5.5, there appears to be slightly fewer platelets attached to the surface of the L-

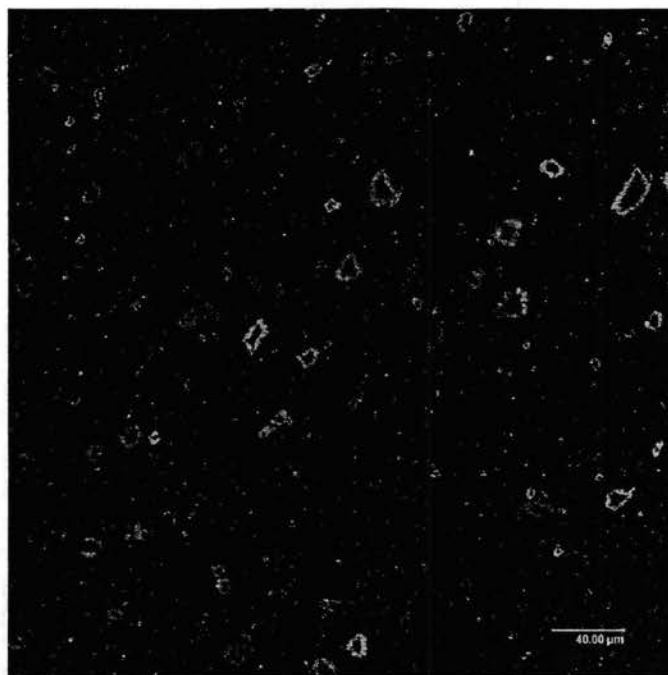


(a) L-Cysteine Modified PET

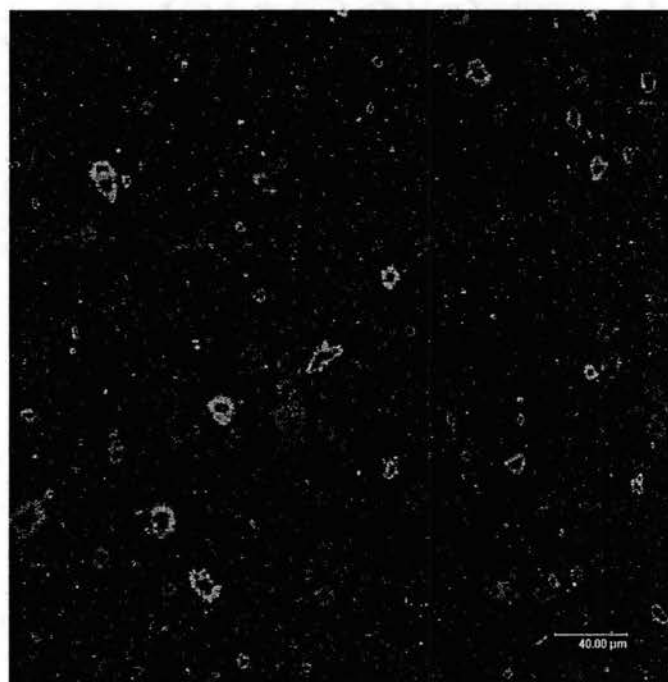


(b) Glycine Modified PET

Figure 5.3 Scans of the fluorescently labeled platelets on the surface of (a) L-cysteine modified PET and (b) glycine modified PET. Both samples were used in the perfusion study with platelets in a Tyrode's buffer solution. Scans are shown at 800x magnification.

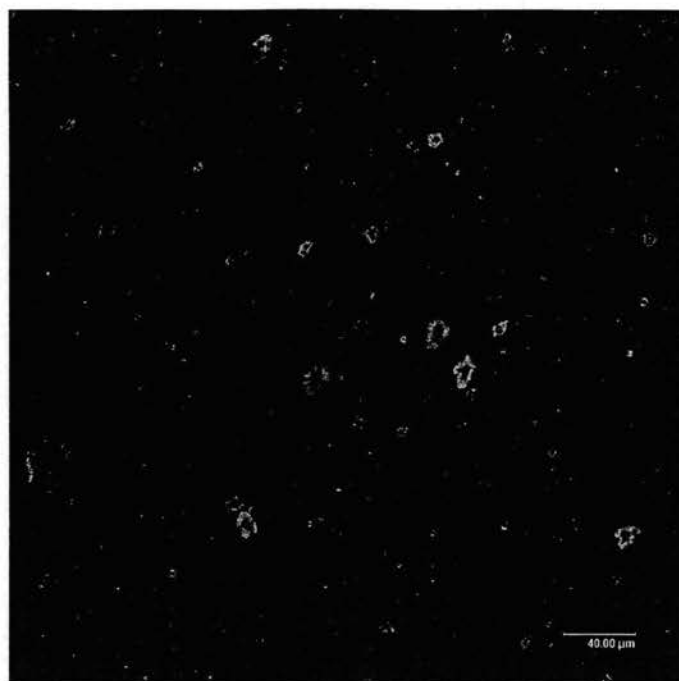


(a) L-Cysteine Modified PET

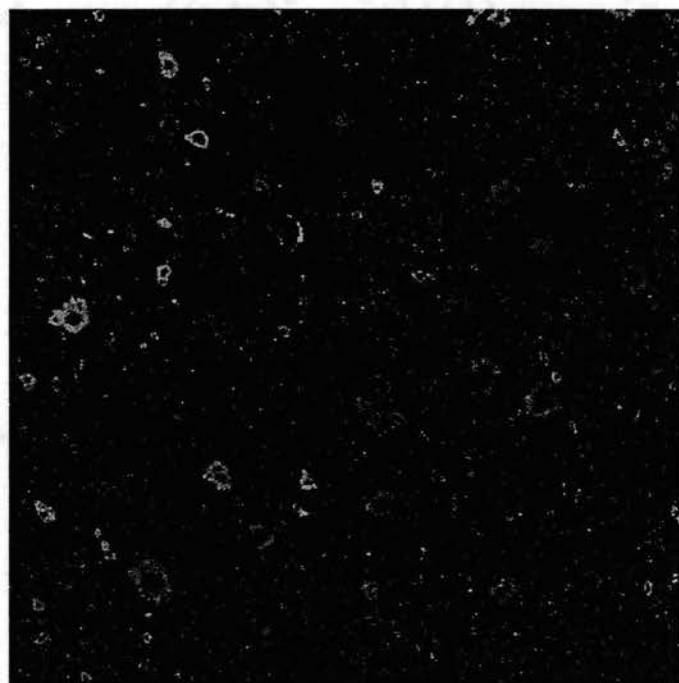


(b) Glycine Modified PET

Figure 5.4 Scans of the fluorescently labeled platelets on the surface of (a) L-cysteine modified PET and (b) glycine modified PET. Both samples were used in the perfusion study with platelets in a 7 μM BSANO solution. Scans are shown at 400x magnification.

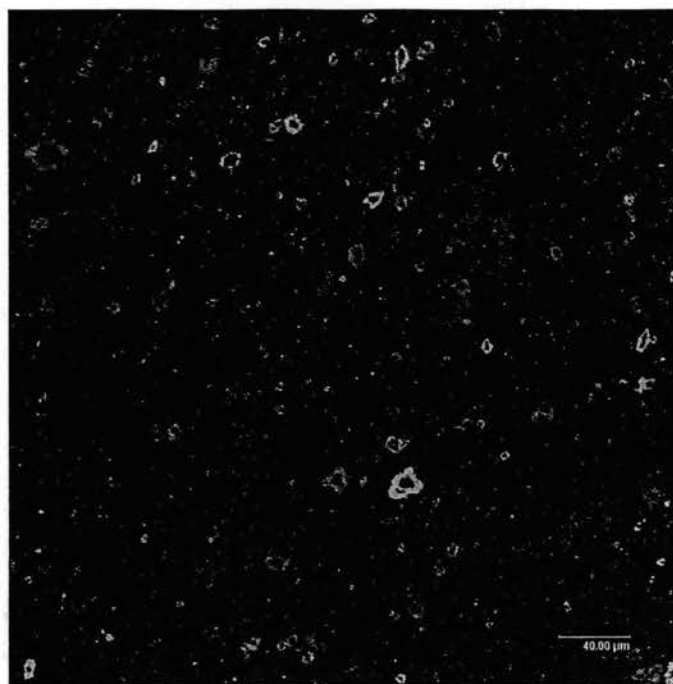


(a) L-Cysteine Modified PET

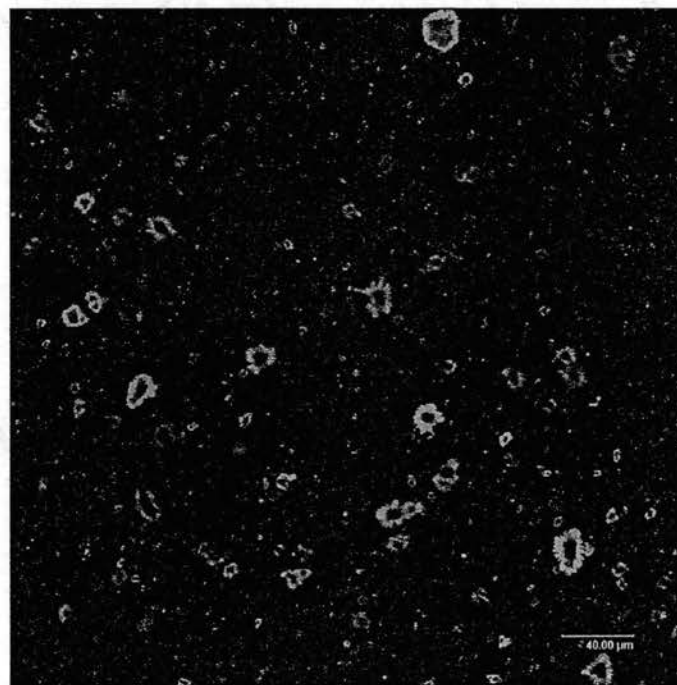


(b) Glycine Modified PET

Figure 5.5 Scans of the fluorescently labeled platelets on the surface of (a) L-cysteine modified PET and (b) glycine modified PET. Both samples were used in the perfusion study with platelets in a plasma solution. Scans are shown at 400x magnification.



(a) L-Cysteine Modified PET



(b) Glycine Modified PET

Figure 5.6 Scans of the fluorescently labeled platelets on the surface of (a) L-cysteine modified PET and (b) glycine modified PET. Both samples were used in the perfusion study with platelets in a whole blood solution. Scans are shown at 400x magnification.

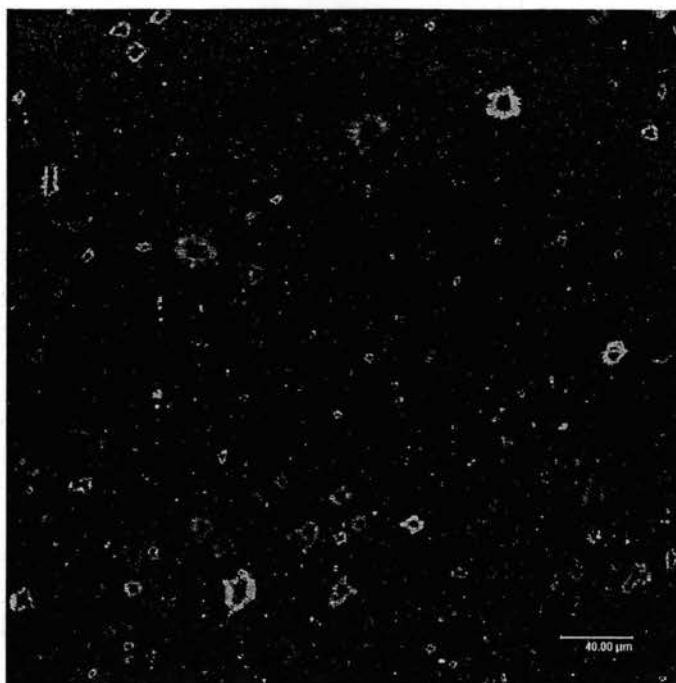
cysteine modified polymer sample compared to the glycine modified polymer control sample. These samples were used in the perfusion studies with platelets in the plasma solution. It appears that the L-cysteine modified samples may be inhibiting some platelet attachment to their surfaces when perfused with platelets in a plasma solution. However, due to problems with the accuracy of this method, further analysis must be done in order to verify this conclusion.

Figures 5.7 to 5.10 show the images of the 2-iminothiolane modified samples after their use in the perfusion studies with Tyrode's buffer, BSANO, plasma, and whole blood, respectively. There was no significant difference in the amount of scatter of the platelets on the surfaces between the samples shown in any of the figures. This was also the case for the cysteine polypeptide modified samples and the glycine polypeptide modified samples (data not shown). Due to the problems of this analysis method, it did not reveal very much useful information about the perfusion studies.

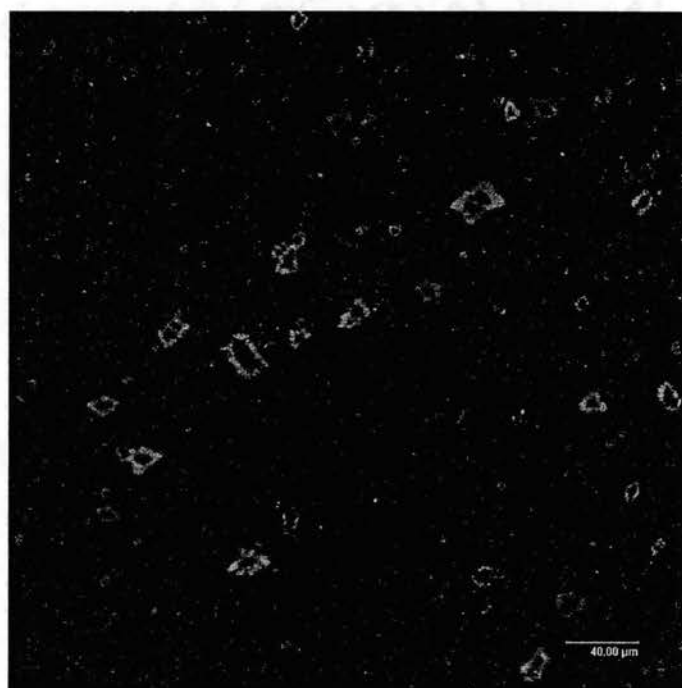
Analysis of Radiolabeled Platelets

Two glycine modified PET samples were used in the perfusion chamber with each test solution in order to investigate if the order of the sample in the chamber has an affect on platelet attachment. After measuring the radioactivity of the radiolabeled platelets attached to each sample, there was no significant difference of platelet attachment between each set of glycine modified samples.

The results from the perfusion studies using radiolabeled platelets in each of the four test solutions are shown in Figure 5.11. As shown, there was a great deal of variability in the results that can be attributed to a combination of factors including, 1) variance in the surface concentration of the thiol group on each modified polymer, 2)

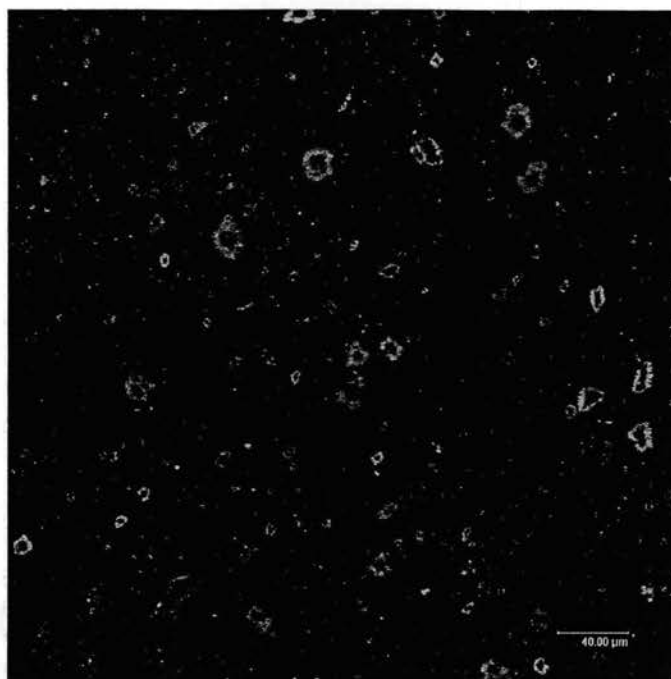


(a) 2-Iminothiolane Modified PET

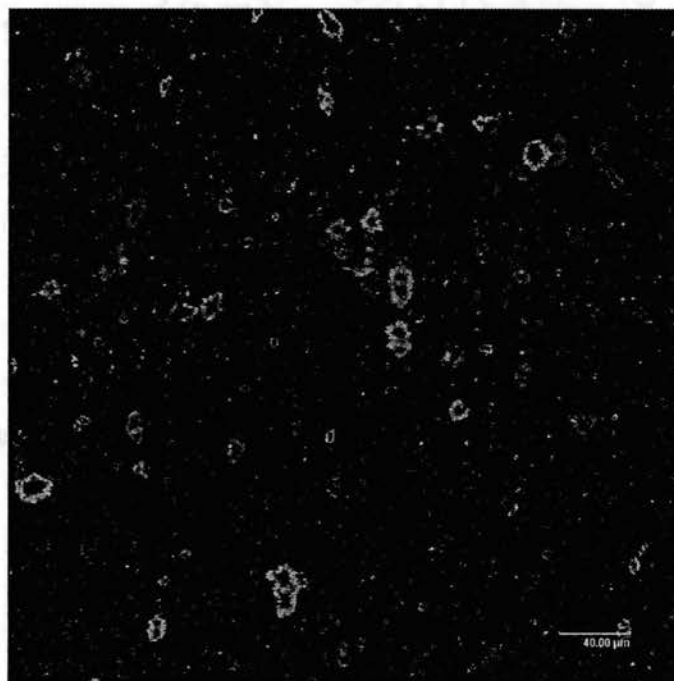


(b) Glycine Modified PET

Figure 5.7 Scans of the fluorescently labeled platelets on the surface of (a) 2-iminothiolane modified PET and (b) glycine modified PET. Both samples were used in the perfusion study with platelets in a Tyrode's buffer solution. Scans are shown at 400x magnification.

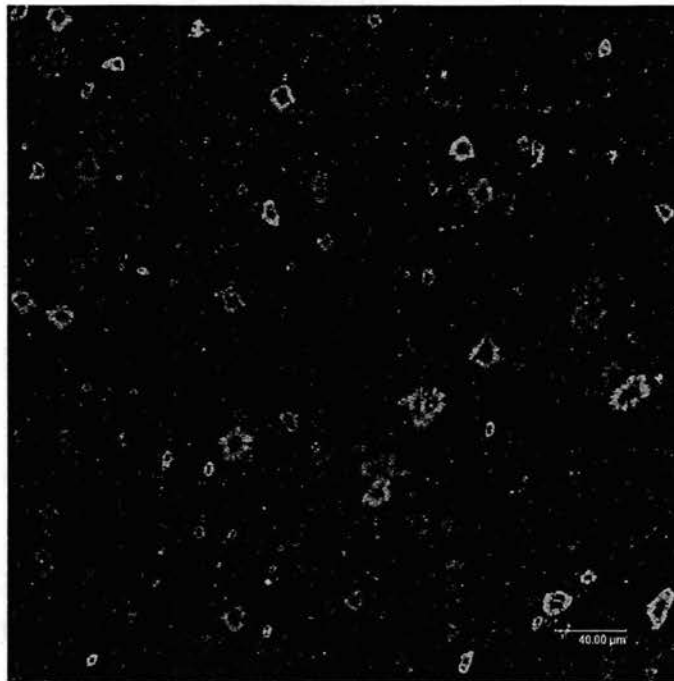


(a) 2-Iminothiolane Modified PET

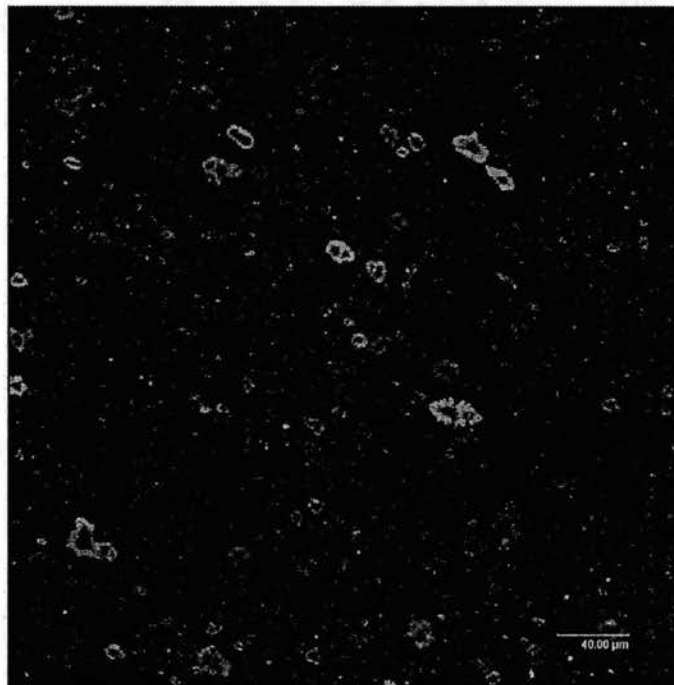


(b) Glycine Modified PET

Figure 5.8 Scans of the fluorescently labeled platelets on the surface of (a) 2-iminothiolane modified PET and (b) glycine modified PET. Both samples were used in the perfusion study with platelets in a 7 μ M BSANO solution. Scans are shown at 400x magnification.

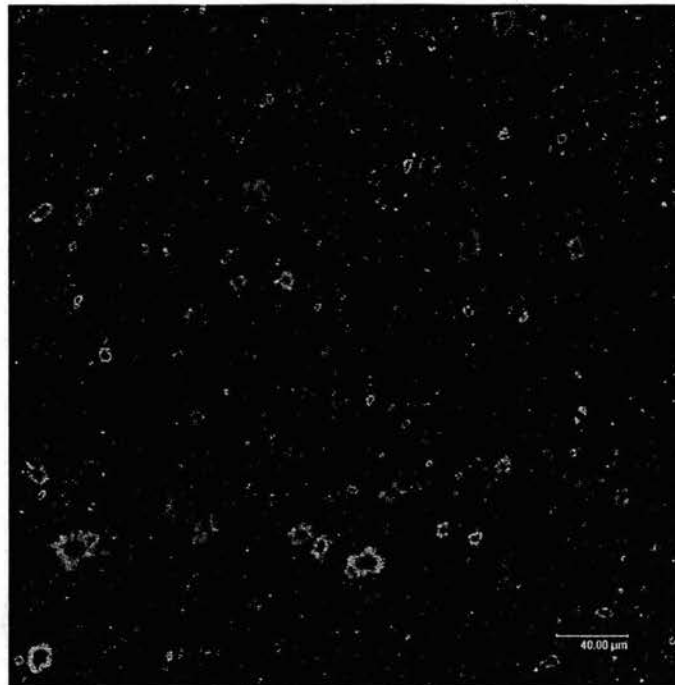


(a) 2-Iminothiolane Modified PET

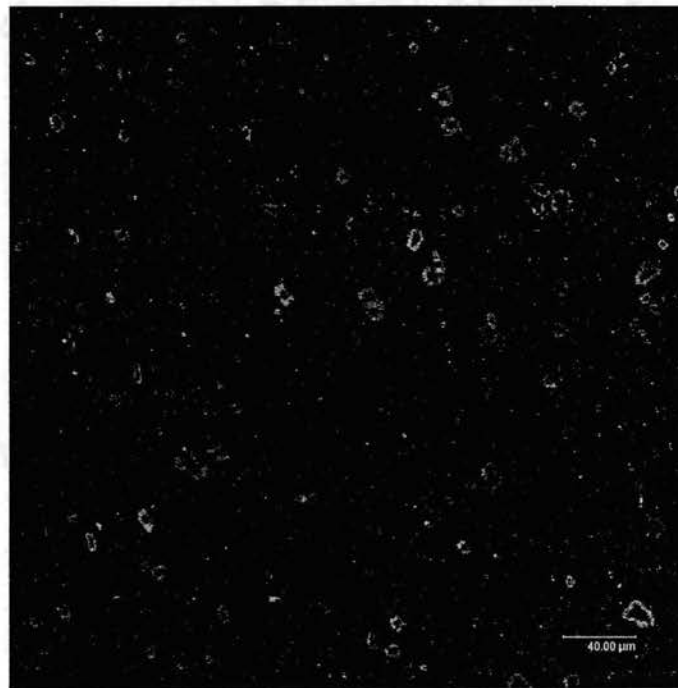


(b) Glycine Modified PET

Figure 5.9 Scans of the fluorescently labeled platelets on the surface of (a) 2-iminothiolane modified PET and (b) glycine modified PET. Both samples were used in the perfusion study with platelets in a plasma solution. Scans are shown at 400x magnification.



(a) 2-Iminothiolane Modified PET



(b) Glycine Modified PET

Figure 5.10 Scans of the fluorescently labeled platelets on the surface of (a) 2-iminothiolane modified PET and (b) glycine modified PET. Both samples were used in the perfusion study with platelets in a whole blood solution. Scans are shown at 400x magnification.

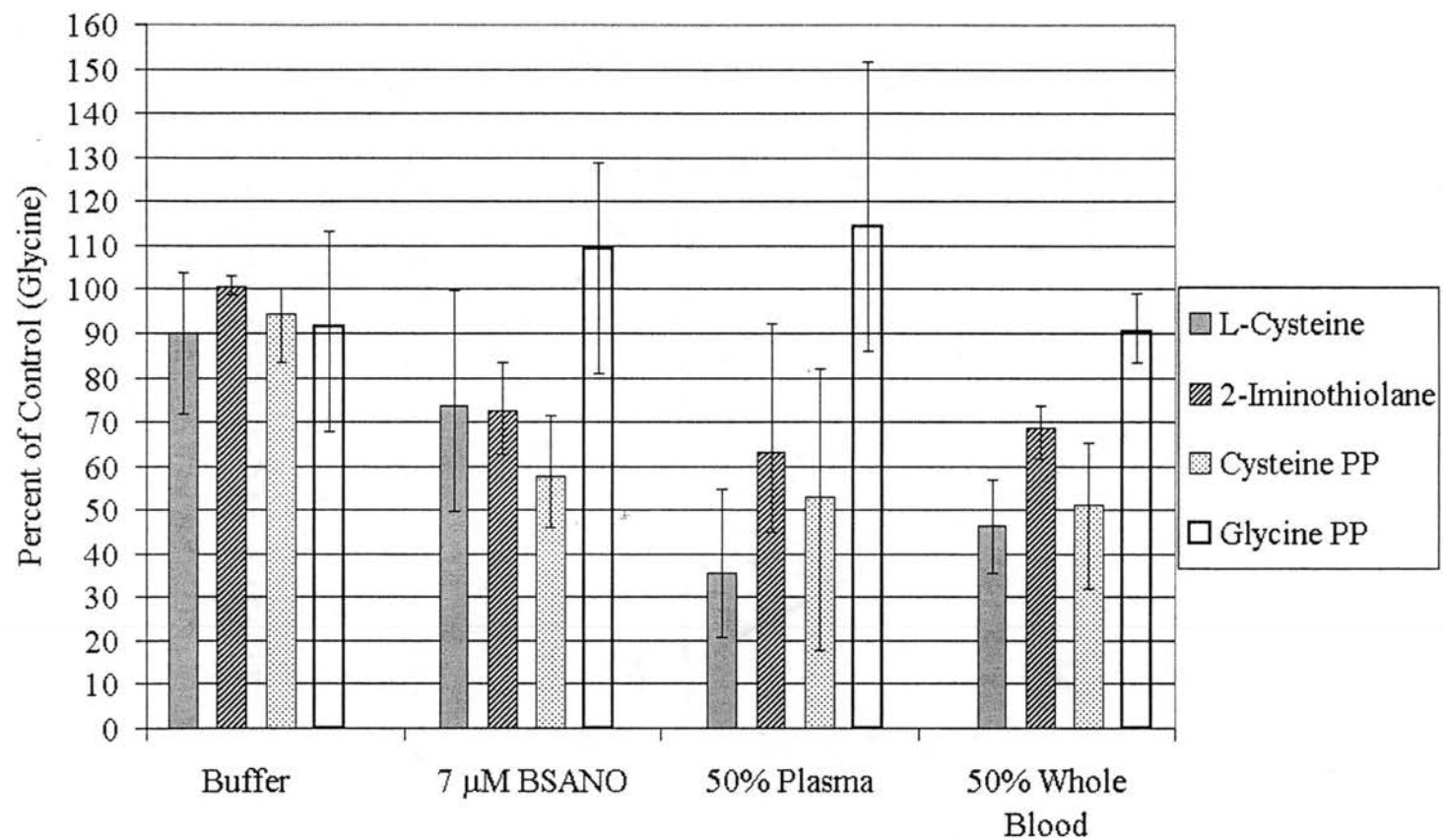


Figure 5.11 The amount of platelet attachment on the surface of each modified sample as a percent of each control sample (glycine). The amount of platelet attachment was determined by measuring the radioactivity of the radiolabeled platelets attached to each sample. Values shown are mean values \pm standard deviation (n=3).

variance in the experimental conditions, and 3) variance in the method used to measure the radiolabel on the samples. As shown previously, there can be a lot of variance between the thiol surface concentrations between samples with the same modification process. Less thiol content on the surface would lead to less NO release to inhibit platelet attachment. The perfusion experiments were performed three times for each type of modified polymer sample, in order to measure the variance in the experimental procedure. One of the major problems with biological *in vitro* experiments is the amount of variables involved that cannot be controlled or sometimes even known. For example, even though donors go through a stringent screening process, there still may exist significant differences between donors, such as differences in platelet function, differences in diets that may affect the type and amount of proteins and small molecules in their blood, and even differences in stress levels that can lead to the release of hormones or other factors into the blood that may affect platelet function. There was little variability in the method used to measure the amount of radiolabel on each sample. Standard solutions of Cr-51 were used to calibrate the gamma counter prior to measuring any of the samples and there was less than a 10% difference in the measurements.

Some conclusions about the perfusion experiment can be made by comparing the mean values of platelet attachment to the surface of each sample. Only the polymers modified with the three groups used in the optimization studies from Chapter 4 will be discussed first, saving the discussion of the glycine polypeptide modified polymer for later. When comparing the samples that were perfused with platelets in the Tyrode's buffer solution, there were no significant differences in platelet attachment between any of the samples. This was expected, since there is not any NO available in the solution to

be transferred to the surface of the modified polymers and released in order to prevent platelet attachment.

When comparing the samples that were perfused with platelets in the BSANO solution, there were decreases in platelet attachment to the surface of the modified samples. Platelet attachment was decreased by approximately 26%, 27%, and 42% for the samples modified with L-cysteine, 2-iminothiolane, and cysteine polypeptide, respectively. When these results are compared to the previous ones for the samples perfused with the platelets in Tyrode's buffer solution, it appears that the BSANO does affect platelet attachment to the surface of the modified polymers. It is believed that this is due to the transfer of NO from the BSANO to the surface of the modified polymers to be used to inhibit platelet attachment.

The most significant decreases in platelet attachment to the modified polymers were seen when comparing the samples that were perfused with platelets in the plasma solution. Platelet attachment was decreased by approximately 65%, 37%, and 47% for the samples modified with L-cysteine, 2-iminothiolane, and cysteine polypeptide, respectively. These results indicate that there may be factors other than just BSANO that are involved in the mechanisms used by the modified polymers to prevent platelet attachment.

When comparing the samples that were perfused with platelets in the whole blood solution, there were decreases in the amount of platelets attached to the surface of the modified samples. Platelet attachment was decreased by approximately 53%, 32%, and 49% for the samples modified with L-cysteine, 2-iminothiolane, and cysteine polypeptide, respectively. Platelet attachment to the modified surfaces was prevented

more when compared to the samples perfused with either the buffer solution or the BSANO solution, but less when compared to the samples perfused with the plasma solution for the L-cysteine and 2-iminothiolane modified samples. It is difficult to determine from these results if the hemoglobin in the whole blood had any effect on the mechanisms used by the modified polymers to prevent platelet attachment. It is believed that platelet attachment was higher than expected for this group, due to the higher viscosity of the solution may have trapped more platelets onto the surface. After the samples that had been perfused with the whole blood solutions were rinsed, some of the red blood cell suspension remained on the surface. All samples were rinsed with the same volume of buffer for the same amount of time in order to ensure that approximately the same number of platelets would be rinsed from the surface of each sample. However, since the whole blood solution was more viscous than the other solutions, the rinse conditions were not adequate enough to completely remove all of the red blood cell suspension, which was visually identified on the surface of the samples. Platelets could have been trapped among the red blood cells remaining on the surface, resulting in higher platelet counts for these samples. The differences between the plasma and the whole blood solutions are important to study because if the modified polymers are used *in vivo*, then they will be exposed to whole blood and not just plasma.

When comparing which optimized polymer prevents platelet attachment the best, the L-cysteine modified polymer did best when used in the plasma and whole blood solutions. From Chapter 4, the L-cysteine modified polymer was shown to have the most thiol groups attached to its surface. The hypothesis was that the addition of more L-cysteine sites or different L-cysteine-containing moieties on the polymer will increase the

NO-release rate per unit area and lead to a greater inhibition of platelet deposition on the modified polymer. Therefore, it is believed that the L-cysteine modified polymer was able to prevent platelet attachment the best because it contained the most thiol groups on its surface. The cysteine polypeptide modified polymer did the best in the BSANO solution, but did not do as well as the L-cysteine modified polymer in the plasma and whole blood solutions, especially in the plasma solution. The 2-iminothiolane modified polymer did the worst of the three modified polymers in all three solutions; however, there were still significant decreases in platelet attachment to the modified material in each of the three solutions, when compared to the control sample.

It appears that chain length (size) of the group attached to the surface does not have a significant effect on platelet inhibition. The cysteine polypeptide modified polymer in one case inhibited platelets better than a polymer modified with a smaller group (2-iminothiolane) and in another case did not inhibit platelets as well as a polymer modified with a smaller group (L-cysteine). However, 2-iminothiolane may have not prevented platelet attachment as well, due to other undetermined factors not related to its size. When comparing platelet attachment on the glycine polypeptide and the glycine modified samples, there was no significant difference between the two samples in any of the test solutions, also showing that chain length may not be a factor.

5.4 Discussion

This study was the first step in the process to investigate the utilization of the optimized polymers and the mechanisms by which they function. The main purpose was to investigate how well the optimized polymers prevent platelet attachment to their surfaces under controlled conditions. To do this, a parallel plate flow chamber was

utilized in order to measure platelet attachment on the modified polymers compared to a control sample, under flow conditions.

Four specific solutions were selected to be used in the perfusion studies in order to test for specific factors. The solution of platelets in the Tyrode's buffer served as a control solution that could be compared to the other test solutions. As expected, there were not any significant differences in platelet attachment on the modified polymers compared to the control polymers. The second solution of platelets in 7 μ M BSANO was used to investigate if nitrosated albumin is the primary plasma constituent needed to freely transfer NO to the thiol group on the modified polymers to prevent platelet deposition. The results indicated a decrease in platelet attachment on the modified polymers, suggesting that the polymers are functioning by the proposed mechanisms. The third solution of platelets in plasma was used to determine if BSANO is the only factor from plasma that is required in the mechanisms by which the modified polymers prevent platelet attachment, or if other factors found in plasma are needed. As shown by the enhanced decrease in platelet attachment on the modified polymers, it appears that there are other factors in plasma that are important and that this phenomenon should be further investigated in order to utilize these factors to further decrease and eventually prevent platelet attachment on the modified polymers. Finally, the fourth solution of platelets in whole blood was used to study the effect of hemoglobin as a possible carrier of NO to the modified polymer in order to further inhibit platelet attachment. Unfortunately, no conclusions could be made from this study due to platelet attachment was actually higher than that seen previously with the plasma solution. It is possible that the more viscous whole blood solution (more than twice as viscous as plasma) causes

more platelets to attach to the surface under flow conditions. As discussed previously, during the perfusion studies it was noticeable that the whole blood solutions were more difficult to rinse from the samples than the other solutions.

The three modified polymers that were optimized, as discussed in Chapter 4 were each used in the perfusion studies in order to compare which modification could best inhibit platelet attachment to its surface. Other factors, such as the type of group on the surface, the size of the group on the surface, and the thiol concentration on the surface were also studied to measure their possible effects on platelet attachment. Overall, platelet attachment was inhibited by the polymer modified by one of the three groups in the following order from least to greatest: 2-iminothiolane, cysteine polypeptide, and L-cysteine. L-cysteine is the smallest of the three groups that were attached to the surface and it also consistently had the highest thiol surface concentration. Cysteine polypeptide contained three cysteine residues per peptide chain and was the largest of the three groups. This modified polymer consistently had the lowest thiol surface concentration. 2-Iminothiolane was slightly larger than L-cysteine and was attached by only one linker group instead of two that were used with L-cysteine and cysteine polypeptide. This group consistently had a thiol surface concentration between that of the other two groups. The size alone of the group on the modified polymer does not seem to be significant, as shown from the results of the perfusion studies using glycine polypeptide modified samples. There was no significant difference in platelet attachment of the glycine modified sample compared to the control sample in any of the perfusion studies. At this point, it is still inconclusive if it is the type of group attached to the polymer or if it is the thiol concentration on the surface of the polymer that affects platelet attachment more.

This is due to the finding that although both L-cysteine and 2-iminothiolane modified polymers have higher thiol surface concentrations compared to cysteine polypeptide modified polymer, cysteine polypeptide modified polymer inhibited platelets better than the 2-iminothiolane modified polymer.

CHAPTER 6

CONCLUSIONS AND FUTURE WORK

The purpose of this research was to improve the haemocompatibility of blood-contacting biomaterials by modifying the surface of the material in such a way that it utilizes naturally occurring compounds and mechanisms in the body. The major driving force for this research was the need for more biocompatible materials that can be used in blood-contacting applications. According to the American Heart Association, such applications have drastically increased in the United States alone from 1979 to 2000 (Association, 2003).

Previous research demonstrated the ability to modify the surface of a biomaterial in such a way that it utilizes naturally occurring components and mechanisms that are readily available and that will not expire (Duan and Lewis, 2002). One of the naturally occurring components utilized by this design is endogenous NO bound to serum albumin in human plasma (Stamler et al., 1992a). By attaching L-cysteine to the surface of a biomaterial one of the naturally occurring mechanisms used by this design is the transfer of NO from the nitrosated serum albumin to the L-cysteine through transnitrosation (Meyer et al., 1994; Scharfstein et al., 1994). The nitrosated L-cysteine is very unstable and due to the presence of naturally present metal ions in blood (Beloso and Williams, 1997; Singh et al., 1996), NO is released from the surface and available to inhibit platelet attachment. The initial findings from the past studies laid the groundwork for this present

research. First, the concentration of NO needed to prevent platelets from attaching to a surface was determined (Ramamurthi and Lewis, 1998). Next, a design to attach L-cysteine to the surface of a polymer was developed and steps were taken to characterize the modified surface (Duan, 2001). Lastly, the modified material was tested in vitro with platelets in both at both stagnant and flow conditions (Duan, 2001). The research described in this thesis continued the work and attempted to solve any open problems from the past studies.

The objectives for this project included:

- *Surface characterization* of the modified material in order to depict changes to the surface and to accurately measure these changes.
- *Optimization* of the process to modify the biomaterial in order to maximize its effectiveness.
- *Utilization* of the modified material in a system with platelets in order to measure the effectiveness of the material to prevent platelet attachment.

There were some problems when attempting to characterize the surface of the modified material in the past research studies. There were not any methods readily available that could measure L-cysteine attached to a surface at low concentrations (< 10 nmols/cm²), and the chemiluminescence method developed by past studies showed some inconsistencies. It was also desired to have alternative methods to validate the chemiluminescence method. In Chapter 3, several measurement methods were investigated to measure thiol groups on surfaces including fluorescence microscopy, x-ray photoelectron spectroscopy (XPS), and several chemiluminescence-based assays to measure thiols on surfaces and solutions. The advantage of fluorescence microscopy was

the ability to visualize the surface coverage of the thiol group. Some disadvantages with fluorescence microscopy included the lack of specificity of the fluorescence probe and the analysis was more qualitative and did not directly produce surface molar concentrations. The advantage of XPS was that it was a highly precise and detailed analysis of only the surface of the material. The disadvantage of XPS was that it only measured the atomic percentages on the surface, which made it difficult to determine a molar surface concentration. The chemiluminescence-based assays were the most successful in measuring surface molar concentrations of thiols. The advantage of the chemiluminescence-based method was that it could accurately measure (within 1% error) molar concentrations of any thiol-containing compound with a detection limit in the pmol range. The major disadvantage to this method was that the thiol group had to be broken off of the surface and into solution prior to measurement, therefore leaving the sample unable to be reused.

In past research studies, L-cysteine modified polymer was tested in vitro with platelets in both stagnant and flow conditions in order to measure the amount of platelet attachment to the surface. Although the studies showed a significant reduction in platelet attachment to the modified material, the modified materials were unable to completely inhibit platelet attachment to the surface. It was hypothesized that the addition of more L-cysteine sites or different L-cysteine-containing moieties on the polymer will increase the NO-release rate per unit area and will increase the inhibition of platelet deposition. In Chapter 4, the optimization of the polymer modification process was performed in order to maximize the amount of thiol groups on the surface of the modified polymer. The following groups were used in the modification process: 1. L-cysteine residues, 2. a L-

cysteine containing moiety, 2-Iminothiolane, and 3. a polypeptide containing multiple cysteine residues, Cys-Gly-Cys-Gly-Cys. Multiple factorial designs were used for the optimization of the modification process, along with the measurement techniques from Chapter 3. Not only did this research show that each of the three groups could be successfully attached to PET, but it also determined the optimal conditions to attach the groups. The chemiluminescence and XPS methods were the most successful in comparing the modified samples. The fluorescent microscopy method is a useful analysis method when there are significant differences between samples, but is inconclusive when attempting to use it to compare samples with small difference, as some samples from the optimization study. When comparing the surface concentrations of thiol groups from each of the optimized processes determined from the chemiluminescence analysis method, the amount of thiol groups on the surface increased in order with the following groups: cysteine polypeptide < 2-iminothiolane < L-cysteine.

In past studies, only the L-cysteine modified polymer was tested in a perfusion chamber with platelet solutions, and the only platelet solutions that were studied were platelets in a buffer solution and platelets in a plasma solution. The studies performed in Chapter 5 were the first step in the process to investigate the utilization of the optimized polymers and the mechanisms by which they function. The main purpose was to investigate how well the optimized polymers prevent platelet attachment to their surfaces under controlled conditions. To do this, a parallel plate flow chamber was utilized in order to measure platelet attachment on the modified polymers compared to a control sample, under flow conditions. Four solutions containing either fluorescently labeled or radiolabeled platelets were used in the perfusion studies, 1) Tyrode's buffer solution, 2) 7

μM BSANO solution, 3) 50 vol% plasma solution, and 4) 50 vol% whole blood solution. It was difficult to quantify the number of platelets on the surface of the modified samples by using the fluorescently-labeled platelets; therefore, the Cr-51 labeled platelets were used to quantify the number of platelets on the modified samples by measuring the amount of radioactivity of the labeled platelets on the surface of each modified sample. The platelet perfusion studies show that components in the plasma are important in the mechanisms used by the modified polymers to prevent platelet attachment. Also shown was that the modified polymers inhibited platelets less in the whole blood solution compared to the plasma solution. Overall, platelet attachment was inhibited by the polymer modified by one of the three groups in the following order from least to greatest: 2-iminothiolane, cysteine polypeptide, and L-cysteine. The longer chain length of the glycine polypeptide modified sample did not show any significant effects on plate attachment.

In order to improve the modified polymers ability to further decrease and eventually prevent platelet attachment to their surfaces, future work must still be performed in this research area, including:

- Continue to develop more accurate methods to measure the thiol surface concentrations on the modified samples, without destroying the samples.
- Continue to attach other thiol groups to the polymers to investigate the effect on platelet attachment.
- Study the kinetics of the reactions taking place at the surface of the polymer and in the surrounding solution. First, all of the species involved in the mechanisms would need to be determined, measured, and modeled. Next, all

of the reactions taking place at the surface and in the surrounding solution would need to be determined. Finally, equilibrium rate constants for the transnitrosation reactions and the rate constants for the release of NO from thiol groups would need to be determined.

- Study the effects of storage on the modified polymers. For all of the studies in this research, samples were used within 24 hours after they were modified. Studies should be performed to determine the “shelf-life” of these modified materials and the best conditions for storage.
- Study the reusability of the modified polymers. For the studies in this research, the modified polymers were only used once. Studies should be performed to investigate if the modified polymers are still effective after repeated use.
- Study the long-term properties of the modified polymers. Modified polymers that were used in this research were only used for short-time periods. Studies should be performed to measure how long the modified polymers continue to significantly prevent platelet attachment to the surface.

REFERENCES

- Adams, G. A., and Feuerstein, I. A. (1980): Visual fluorescent and radio-isotopic evaluation of platelet accumulation and embolization. *Trans Am Soc Artif Intern Organs* **26**, 17-23.
- Aleryani, S., Milo, E., Rose, Y., and Kostka, P. (1998): Superoxide-mediated decomposition of biological S-nitrosothiols. *J Biol Chem* **273**, 6041-5.
- American Heart Association (2003): Heart Disease and Stroke Statistics, www.americanheart.org.
- Anggard, E. (1994): Nitric oxide: mediator, murderer, and medicine. *Lancet* **343**, 1199-206.
- Arnelle, D. R., and Stamler, J. S. (1995): NO⁺, NO, and NO⁻ donation by S-nitrosothiols: implications for regulation of physiological functions by S-nitrosylation and acceleration of disulfide formation. *Arch Biochem Biophys* **318**, 279-85.
- Askew, S. C., Butler, A. R., Flitney, F. W., Kemp, G. D., and Megson, I. L. (1995): Chemical mechanisms underlying the vasodilator and platelet anti-aggregating properties of S-nitroso-N-acetyl-DL-penicillamine and S-nitrosoglutathione. *Bioorg Med Chem* **3**, 1-9.
- Aster, R. H., and Jandl, J. H. (1964): Platelet sequestration in man. I. Methods. *J Clin Invest* **43**, 843.
- Authi, K. S., Watson, S. P., and Kakkar, V. V. (1993): Mechanisms of Platelet Activation and Control, Plenum Press, New York.
- Azeredo, L., Pacheco, A. P., Lopes, I., Oliveira, R., and Vieira, M. J. (2003): Monitoring cell detachment by surfactants in a parallel plate flow chamber. *Water Sci Technol* **47**, 77-82.
- Azuma, H., Ishikawa, M., and Sekizaki, S. (1986): Endothelium-dependent inhibition of platelet aggregation. *Br J Pharmacol* **88**, 411-5.
- Bailey, N. T. (1995): *Statistical methods in biology*. University Press. Cambridge.
- Baker, G. R., Sullam, P. M., and Levin, J. (1997): A simple, fluorescent method to internally label platelets suitable for physiological measurements. *Am J Hematol* **56**, 17-25.

- Bannai, M., Mazda, T., and Sasakawa, S. (1985): The effects of pH and agitation on platelet preservation. *Transfusion* **25**, 57-9.
- Beloso, P. H., and Williams, D. L. (1997): Reversibility of S-nitrosothiol formation. *Chemical Communications* **1**, 89-90.
- Bennett, B. M., Kobus, S. M., Brien, J. F., Nakatsu, K., and Marks, G. S. (1986): Requirement for reduced, unliganded hemoprotein for the hemoglobin- and myoglobin-mediated biotransformation of glyceryl trinitrate. *J Pharmacol Exp Ther* **237**, 629-35.
- Berne, R. M., and Levy, M. N. (1993): Physiology, pp. 1071. In R. Farell (Ed.), Mosby - Year Book Inc., St. Louis.
- Beutler, E., and Williams, W. (1995): Williams Hematology, McGraw-Hill, Inc., Health Professions Division, New York.
- Bohl, K. S., and West, J. L. (2000): Nitric oxide-generating polymers reduce platelet adhesion and smooth muscle cell proliferation. *Biomaterials* **21**, 2273-2278.
- Brass, L. F. (1991): The biochemistry of platelet activation, pp. 1177-1193. In R. Hoffman (Ed.): *Hematology: Basic Principles and Practice*, Churchill Livingstone Inc., New York.
- Brinkman, E., Poot, A., Beugeling, T., van der Does, L., and Bantjes, A. (1989): Surface modification of copolyether-urethane catheters with poly(ethylene oxide). *Int J Artif Organs* **12**, 390-4.
- Brune, B., and Lapetina, E. G. (1989): Activation of a cytosolic ADP-ribosyltransferase by nitric oxide- generating agents. *J Biol Chem* **264**, 8455-8.
- Brune, B., von Knethen, A., and Sandau, K. B. (1998): Nitric oxide and its role in apoptosis. *Eur J Pharmacol* **351**, 261-72.
- Buechler, W. A., Ivanova, K., Wolfram, G., Drummer, C., Heim, J. M., and Gerzer, R. (1994): Soluble guanylyl cyclase and platelet function. *Ann N Y Acad Sci* **714**, 151-7.
- Bui, L. N., and Thompson, M. (1993): Surface modification of the biomedical polymer poly(ethylene terephthalate). *Analyst* **118**, 463-474.
- Butler, A. R., Flitney, F. W., and Williams, D. L. (1995): NO, nitrosonium ions, nitroxide ions, nitrosothiols and iron-nitrosyls in biology: a chemist's perspective. *Trends Pharmacol Sci* **16**, 18-22.
- Butler, A. R., and Williams, D. L. H. (1993): The physiological role of nitric oxide. *Chemical Society Reviews*, 233-241.

- Byler, D. M., Gosser, D. K., and Susi, H. (1983): Spectroscopic estimation of the extent of S-nitrosothiol formation by nitrite action on sulfhydryl groups. *Journal of Agricultural and Food Chemistry* **31**, 523-527.
- Campbell, D. L., Stamler, J. S., and Strauss, H. C. (1996): Redox modulation of L-type calcium channels in ferret ventricular myocytes. Dual mechanism regulation by nitric oxide and S-nitrosothiols. *J Gen Physiol* **108**, 277-93.
- Catani, M. V., Bernassola, F., Rossi, A., and Melino, G. (1998): Inhibition of clotting factor XIII activity by nitric oxide. *Biochem Biophys Res Commun* **249**, 275-8.
- Chhajlani, V., Axelsson, K. L., Ahlner, J., and Wikberg, J. E. (1989): Purification of soluble guanylate cyclase enzyme from human platelets. *Biochem Int* **19**, 1039-44.
- Chotard-Ghodsniya, R., Drochon, A., and Grebe, R. (2002): A new flow chamber for the study of shear stress and transmural pressure upon cells adhering to a porous biomaterial. *J Biomech Eng* **124**, 258-61.
- Christopherson, K. S., and Bredt, D. S. (1997): Nitric oxide in excitable tissues: physiological roles and disease. *J Clin Invest* **100**, 2424-9.
- Cook, J. A., Kim, S. Y., Teague, D., Krishna, M. C., Pacelli, R., Mitchell, J. B., Vodovotz, Y., Nims, R. W., Christodoulou, D., Miles, A. M., Grisham, M. B., and Wink, D. A. (1996): Convenient colorimetric and fluorometric assays for S-nitrosothiols. *Analytical Biochemistry* **238**, 150-158.
- Cunningham, D. A., and Siegel, B. A. (1982): Radiolabeled platelets, pp. 143-164. In L. M. Freeman, and H. S. Weissman (Eds): *Nuclear Medicine Annual 1982*, Raven Press, New York.
- Dadsetan, M., Mirzadeh, H., Sharifi-Sanjani, N., and Salehian, P. (2001): In vitro studies of platelet adhesion on laser-treated polyethylene terephthalate surface. *J Biomed Mater Res* **54**, 540-6.
- Datz, F. L. (1986): Radiolabeled leukocytes and platelets. *Invest Radiol* **21**, 191-200.
- de Brito Alves, S., de Queiroz, A. A., and Higa, O. Z. (2003): Digital image processing for biocompatibility studies of clinical implant materials. *Artif Organs* **27**, 444-6.
- delaTorre, A., Schroeder, R. A., Bartlett, S. T., and Kuo, P. C. (1998): Differential effects of nitric oxide-mediated S-nitrosylation on p50 and c-jun DNA binding. *Surgery* **124**, 137-41; discussion 141-2.
- DeMaster, E. G., Quast, B. J., Redfern, B., and Nagasawa, N. T. (1995): Reaction of nitric oxide with the free sulfhydryl group of human serum albumin yields a sulfenic acid and nitrous oxide. *Biochemistry* **34**, 11494-11499.

- Desai, A. G., and Thakur, M. L. (1986): Radiolabeled blood cells: techniques and applications. *Crit Rev Clin Lab Sci* **24**, 95-122.
- Desai, N. P., and Hubbell, J. A. (1991): Biological responses to polyethylene oxide modified polyethylene terephthalate surfaces. *Journal of Biomedical Materials Research* **25**, 829-843.
- Dicks, A. P., and Williams, D. L. (1996): Generation of nitric oxide from S-nitrosothiols using protein-bound Cu²⁺ sources. *Chemistry and Biology* **3**, 655-659.
- Dimmeler, S., and Brune, B. (1992): Characterization of a nitric-oxide-catalysed ADP-ribosylation of glyceraldehyde-3-phosphate dehydrogenase. *Eur J Biochem* **210**, 305-10.
- Dimmeler, S., Lottspeich, F., and Brune, B. (1992): Nitric oxide causes ADP-ribosylation and inhibition of glyceraldehyde-3-phosphate dehydrogenase. *J Biol Chem* **267**, 16771-4.
- Duan, X. (2001): Exploiting endogenous nitric oxide to improve the haemocompatibility of biomaterials. Doctor of Philosophy thesis, Oklahoma State University, Stillwater, 181 p.
- Duan, X., and Lewis, R. S. (2002): Improved haemocompatibility of cysteine-modified polymers via endogenous nitric oxide. *Biomaterials* **23**, 1197-203.
- Durrani, A. A., Hayward, J. A., and Chapman, D. (1986): Biomembranes as models for polymer surfaces. II. The syntheses of reactive species for covalent coupling of phosphorylcholine to polymer surfaces. *Biomaterials* **7**, 121-5.
- Fang, K., Johns, R., Macdonald, T., Kinter, M., and Gaston, B. (2000): S-nitrosoglutathione breakdown prevents airway smooth muscle relaxation in the guinea pig. *Am J Physiol Lung Cell Mol Physiol* **279**, L716-21.
- Fang, K., Ragsdale, N. V., Carey, R. M., MacDonald, T., and Gaston, B. (1998): Reductive assays for S-nitrosothiols: implications for measurements in biological systems. *Biochem Biophys Res Commun* **252**, 535-40.
- Field, L., Grimaldi, J. A., Jr., Hanley, W. S., Holladay, M. W., Ravichandran, R., Schaad, L. J., and Tate, C. E. (1977): Biologically oriented organic sulfur chemistry. 15. Organic disulfides and related substances. 41. Inhibition of the fungal pathogen *Histoplasma capsulatum* by some organic disulfides. *J Med Chem* **20**, 996-1001.
- Flatow, F. A., Jr., and Freireich, E. J. (1966): The increased effectiveness of platelet concentrates prepared in acidified plasma. *Blood* **27**, 449-59.
- Foerster, J., Harteneck, C., Malkewitz, J., Schultz, G., and Koesling, D. (1996): A functional heme-binding site of soluble guanylyl cyclase requires intact N-termini of alpha 1 and beta 1 subunits. *Eur J Biochem* **240**, 380-6.

- Fournier, R. L. (1999): *Basic Transport Phenomena in Biomedical Engineering*. Taylor & Francis. Philadelphia.
- Frank, I. E., and Todeschini, R. (1994): *The data analysis handbook*. Elsevier. Amsterdam.
- Freedman, J. E., Frei, B., Welch, G. N., and Loscalzo, J. (1995): Glutathione peroxidase potentiates the inhibition of platelet function by S-nitrosothiols. *J Clin Invest* **96**, 394-400.
- Freedman, J. E., Loscalzo, J., Barnard, M. R., Alpert, C., Keaney, J. F., and Michelson, A. D. (1997): Nitric oxide released from activated platelets inhibits platelet recruitment. *J Clin Invest* **100**, 350-6.
- Furchgott, R. F., and Zawadzki, J. V. (1980): The obligatory role of endothelial cells in the relaxation of arterial smooth muscle by acetylcholine. *Nature* **288**, 373-6.
- Garbers, D. L. (1992): Guanylyl cyclase receptors and their endocrine, paracrine, and autocrine ligands. *Cell* **71**, 1-4.
- Gaston, B., Reilly, J., Drazen, J. M., Fackler, J., Ramdev, P., Arnette, D., Mullins, M. E., Sugarbaker, D. J., Chee, C., Singel, D. J., and et al. (1993): Endogenous nitrogen oxides and bronchodilator S-nitrosothiols in human airways. *Proc Natl Acad Sci USA* **90**, 10957-61.
- Gergel, D., and Cederbaum, A. I. (1997): Interaction of nitric oxide with 2-thio-5-nitrobenzoic acid: implications for the determination of free sulfhydryl groups by Ellman's reagent. *Arch Biochem Biophys* **347**, 282-8.
- Giovannoni, G., Land, J. M., Keir, G., Thompson, E. J., and Heales, S. J. (1997): Adaptation of the nitrate reductase and Griess reaction methods for the measurement of serum nitrate plus nitrite levels. *Ann Clin Biochem* **34**, 193-8.
- Girardeaux, C., Zammateo, N., Art, M., Gillon, B., Pireaux, J. J., and Caudano, R. (1996): Amination of poly (ethylene-terephthalate) polymer surface for biochemical applications. *Plasmas and Polymers* **1**, 327-346.
- Glusa, E. (1991): Hirudin and platelets. *Semin Thromb Hemost* **17**, 122-5.
- Golander, C.-G., and Kiss, E. (1988): Protein adsorption on functionalized and ESCA-characterized polymer films studied by ellipsometry. *Journal of Colloid and Interface Science* **121**, 240-253.
- Gordge, M. P., Hothersall, J. S., Neild, G. H., and Dutra, A. A. (1996): Role of a copper (I)-dependent enzyme in the anti-platelet action of S-nitrosoglutathione. *Br J Pharmacol* **119**, 533-8.

- Gordge, M. P., Hothersall, J. S., and Noronha-Dutra, A. A. (1998): Evidence for a cyclic GMP-independent mechanism in the anti-platelet action of S-nitrosoglutathione. *Br J Pharmacol* **124**, 141-8.
- Gordge, M. P., Meyer, D. J., Hothersall, J., Neild, G. H., Payne, N. N., and Noronha-Dutra, A. (1995): Copper chelation-induced reduction of the biological activity of S-nitrosothiols. *Br J Pharmacol* **114**, 1083-9.
- Gow, A. J., Buerk, D. G., and Ischiropoulos, H. (1997): A novel reaction mechanism for the formation of S-nitrosothiol in vivo. *J Biol Chem* **272**, 2841-5.
- Gow, A. J., and Stamler, J. S. (1998): Reactions between nitric oxide and haemoglobin under physiological conditions. *Nature* **391**, 169-73.
- Gupta, K. K. (1969): Cholesterol, platelets adhesiveness and fibrinolytic activity in ischaemic heart disease. *J Assoc Physicians India* **17**, 323-31.
- Haddad, I. Y., Crow, J. P., Hu, P., Ye, Y., Beckman, J., and Matalon, S. (1994): Concurrent generation of nitric oxide and superoxide damages surfactant protein A. *Am J Physiol* **267**, L242-9.
- Hanley, D. C., and Harris, J. M. (2001): Quantitative dosing of surfaces with fluorescent molecules: characterization of fractional monolayer coverages by counting single molecules. *Anal Chem* **73**, 5030-7.
- Harrison, D. G. (1997): Cellular and molecular mechanisms of endothelial cell dysfunction. *J Clin Invest* **100**, 2153-7.
- Hausladen, A., Privalle, C. T., Keng, T., DeAngelo, J., and Stamler, J. S. (1996): Nitrosative stress: activation of the transcription factor OxyR. *Cell* **86**, 719-29.
- Hawkins, R. I. (1972): Smoking, platelets and thrombosis. *Nature* **236**, 450-2.
- Haynes, D. H. (1993): Effects of cyclic nucleotides and protein kinases on platelet calcium homeostasis and mobilization. *Platelets* **4**, 231-242.
- Herring, M., Baughman, S., Glover, J., Kesler, K., Jesseph, J., Campbell, J., Dilley, R., Evan, A., and Gardner, A. (1984): Endothelial seeding of Dacron and polytetrafluoroethylene grafts: the cellular events of healing. *Surgery* **96**, 745-55.
- Heyman, P. W., Cho, C. S., McRea, J. C., Olsen, D. B., and Kim, S. W. (1985): Heparinized polyurethanes: in vitro and in vivo studies. *J Biomed Mater Res* **19**, 419-36.
- Hogg, N. (2000): Biological chemistry and clinical potential of S-nitrosothiols. *Free Radical Biology & Medicine* **28**, 1478-1486.

- Hogg, N., Singh, R. J., Konorev, E., Joseph, J., and Kalyanaraman, B. (1997): S-Nitrosoglutathione as a substrate for gamma-glutamyl transpeptidase. *Biochem J* **323**, 477-81.
- Holmsen, H. (1994): Significance of testing platelet functions in vitro. *Eur J Clin Invest* **24 Suppl 1**, 3-8.
- Hou, Y., Guo, Z., Li, J., and Wang, P. G. (1996): Seleno compounds and glutathione peroxidase catalyzed decomposition of S-nitrosothiols. *Biochem Biophys Res Commun* **228**, 88-93.
- Ignarro, L. J., Buga, G. M., Wood, K. S., Byrns, R. E., and Chaudhuri, G. (1987a): Endothelium-derived relaxing factor produced and released from artery and vein is nitric oxide. *Proc Natl Acad Sci U S A* **84**, 9265-9.
- Ignarro, L. J., Byrns, R. E., Buga, G. M., and Wood, K. S. (1987b): Endothelium-derived relaxing factor from pulmonary artery and vein possesses pharmacologic and chemical properties identical to those of nitric oxide radical. *Circ Res* **61**, 866-79.
- Ignarro, L. J., Lipton, H., Edwards, J. C., Baricos, W. H., Hyman, A. L., Kadowitz, P. J., and Gruetter, C. A. (1981): Mechanism of vascular smooth muscle relaxation by organic nitrates, nitrites, nitroprusside and nitric oxide: evidence for the involvement of S-nitrosothiols as active intermediates. *J Pharmacol Exp Ther* **218**, 739-49.
- Jackson, K. (2002): Personal Communication, Molecular Biology Resource Facility, University of Oklahoma Health Sciences Center, Norman.
- Jensen, D. E., Belka, G. K., and Du Bois, G. C. (1998): S-Nitrosoglutathione is a substrate for rat alcohol dehydrogenase class III isoenzyme. *Biochem J* **331**, 659-68.
- Jia, L., Bonaventura, C., Bonaventura, J., and Stamler, J. S. (1996): S-nitrosohaemoglobin: a dynamic activity of blood involved in vascular control. *Nature* **380**, 221-6.
- Jobin, F. (1970): Blood platelets and cardiovascular disorders. *Union Med Can* **99**, 1055-61.
- Jocelyn, P. C. (1987): Spectrophotometric assay of thiols. *Methods Enzymol* **143**, 44-67.
- Jourd'heuil, D., Mai, C. T., Laroux, F. S., Wink, D. A., and Grisham, M. B. (1998): The reaction of S-nitrosoglutathione with superoxide. *Biochem Biophys Res Commun* **244**, 525-30.
- Keaney, J. F., Jr., Simon, D. I., Stamler, J. S., Jaraki, O., Scharfstein, J., Vita, J. A., and Loscalzo, J. (1993): NO forms an adduct with serum albumin that has endothelium-derived relaxing factor-like properties. *J Clin Invest* **91**, 1582-9.

- Keen, J. H., Habig, W. H., and Jakoby, W. B. (1976): Mechanism for the several activities of the glutathione S-transferases. *J Biol Chem* **251**, 6183-8.
- Kelm, M., and Schrader, J. (1990): Control of coronary vascular tone by nitric oxide. *Circ Res* **66**, 1561-75.
- Kim, Y. J., Kang, I. K., Huh, M. W., and Yoon, S. C. (2000): Surface characterization and in vitro blood compatibility of poly(ethylene terephthalate) immobilized with insulin and/or heparin using plasma glow discharge. *Biomaterials* **21**, 121-30.
- Kitamoto, Y., Tomita, M., Kiyama, S., Inoue, T., Yabushita, Y., Sato, T., and Ryoda, H. (1991): Antithrombotic mechanisms of urokinase immobilized polyurethane. *Thromb Haemost* **65**, 73-6.
- Kluge, I., Gutteck-Amsler, U., Zollinger, M., and Do, K. Q. (1997): S-nitrosoglutathione in rat cerebellum: identification and quantification by liquid chromatography-mass spectrometry. *J Neurochem* **69**, 2599-607.
- Knowles, R. G., and Moncada, S. (1994): Nitric oxide synthases in mammals. *Biochem J* **298**, 249-58.
- Kottke-Marchant, K., Anderson, J. M., Umemura, Y., and Marchant, R. E. (1989): Effect of albumin coating on the in vitro blood compatibility of Dacron arterial prostheses. *Biomaterials* **10**, 147-55.
- Kowaluk, E. A., and Fung, H. L. (1990): Spontaneous liberation of nitric oxide cannot account for in vitro vascular relaxation by S-nitrosothiols. *J Pharmacol Exp Ther* **255**, 1256-64.
- Kroll, M. H., and Schafer, A. I. (1989): Biochemical mechanisms of platelet activation. *Blood* **74**, 1181-95.
- Lander, H. M. (1997): An essential role for free radicals and derived species in signal transduction. *Faseb J* **11**, 118-24.
- Lander, H. M., Jacovina, A. T., Davis, R. J., and Tauras, J. M. (1996): Differential activation of mitogen-activated protein kinases by nitric oxide-related species. *J Biol Chem* **271**, 19705-9.
- Liu, X., Miller, M. J., Joshi, M. S., Thomas, D. D., and Lancaster, J. R., Jr. (1998): Accelerated reaction of nitric oxide with O₂ within the hydrophobic interior of biological membranes. *Proc Natl Acad Sci U S A* **95**, 2175-9.
- Malinski, T., and Taha, Z. (1992): Nitric oxide release from a single cell measured in situ by a porphyrinic-based microsensor. *Nature* **358**, 676-8.

- Marley, R., Feelisch, M., Holt, S., and Moore, K. (2000): A chemiluminescence-based assay for S-nitrosoalbumin and other plasma S-nitrosothiols. *Free Radic Res* **32**, 1-9.
- Mathias, C. J., and Welch, M. J. (1984): Radiolabeling of platelets. *Semin Nucl Med* **14**, 118-27.
- Mayer, B., and Hemmens, B. (1997): Biosynthesis and action of nitric oxide in mammalian cells. *Trends Biochem Sci* **22**, 477-81.
- Mayer, B., Pfeiffer, S., Schrammel, A., Koesling, D., Schmidt, K., and Brunner, F. (1998): A new pathway of nitric oxide/cyclic GMP signaling involving S-nitrosoglutathione. *J Biol Chem* **273**, 3264-70.
- McAninly, J., Williams, D. L., Askew, S. C., Butler, A. R., and Russell, C. (1993): Metal ion catalysis in nitrosothiol (RSNO) decomposition. *J Chem Soc Chem Commun* **14**, 1758-1759.
- McBride, J. A. (1968): Platelet adhesiveness: the effect of centrifugation on the measurement of adhesiveness in platelet-rich plasma. *J Clin Pathol* **21**, 397-401.
- Menshikov, M., Ivanova, K., Schaefer, M., Drummer, C., and Gerzer, R. (1993): Influence of the cGMP analog 8-PCPT-cGMP on agonist-induced increases in cytosolic ionized Ca²⁺ and on aggregation of human platelets. *Eur J Pharmacol* **245**, 281-4.
- Meyer, D. J., Kramer, H., Özer, N., Coles, B., and Ketterer, B. (1994): Kinetics and equilibria of S-nitrosothiol-thiol exchange between glutathione, cysteine, penicillamines and serum albumin. *FEBS* **345**, 177-180.
- Meyers, K. M., Seachord, C. L., Holmsen, H., Smith, J. B., and Prieur, D. J. (1979): A dominant role of thromboxane formation in secondary aggregation of platelets. *Nature* **282**, 331-3.
- Michel, T., and Feron, O. (1997): Nitric oxide synthases: which, where, how, and why? *J Clin Invest* **100**, 2146-52.
- Mirza, U. A., Chait, B. T., and Lander, H. M. (1995): Monitoring reactions of nitric oxide with peptides and proteins by electrospray ionization-mass spectrometry. *J Biol Chem* **270**, 17185-8.
- Model, M. A., and Healy, K. E. (2000): Quantification of the surface density of a fluorescent label with the optical microscope. *J Biomed Mater Res* **50**, 90-6.
- Moncada, S., Palmer, R. M., and Higgs, E. A. (1991): Nitric oxide: physiology, pathophysiology, and pharmacology. *Pharmacol Rev* **43**, 109-42.

- Monsan, P., Puzo, G., and Mazarguil, H. (1975): Mechanisms of glutaraldehyde-protein bound formation. *Biochimie* **57**, 1281-1292.
- Mordvintsev, P. I., Rudneva, V. G., Vanin, A. F., Shimkevich, L. L., and Khodorov, B. I. (1986): [Inhibition of platelet aggregation by dinitrosyl iron complexes with low molecular weight ligands]. *Biokhimiia* **51**, 1851-7.
- Moro, M. A., Russel, R. J., Celtek, S., Lizasoain, I., Su, Y., Darley-Usmar, V. M., Radomski, M. W., and Moncada, S. (1996): cGMP mediates the vascular and platelet actions of nitric oxide: confirmation using an inhibitor of the soluble guanylyl cyclase. *Proc Natl Acad Sci U S A* **93**, 1480-5.
- Myers, P. R., Minor, R. L., Jr., Guerra, R., Jr., Bates, J. N., and Harrison, D. G. (1990): Vasorelaxant properties of the endothelium-derived relaxing factor more closely resemble S-nitrosocysteine than nitric oxide. *Nature* **345**, 161-3.
- Nathan, C. (1997): Inducible nitric oxide synthase: what difference does it make? *J Clin Invest* **100**, 2417-23.
- Nguyen, B. L., Saitoh, M., and Ware, J. A. (1991): Interaction of nitric oxide and cGMP with signal transduction in activated platelets. *Am J Physiol* **261**, H1043-52.
- Nojiri, C., Okano, T., Jacobs, H. A., Park, K. D., Mohammad, S. F., Olsen, D. B., and Kim, S. W. (1990): Blood compatibility of PEO grafted polyurethane and HEMA/styrene block copolymer surfaces. *J Biomed Mater Res* **24**, 1151-71.
- Oae, S., Kim, Y. H., Fukushima, D., and Shinhama, K. (1978): New synthesis of thionitrites and their chemical reactivities. *J Chem Soc Perkin Trans 1*, 913-917.
- Palmer, R. M., Ferrige, A. G., and Moncada, S. (1987): Nitric oxide release accounts for the biological activity of endothelium-derived relaxing factor. *Nature* **327**, 524-6.
- Pawloski, J. R., Swaminathan, R. V., and Stamler, J. S. (1998): Cell-free and erythrocytic S-nitrosohemoglobin inhibits human platelet aggregation. *Circulation* **97**, 263-7.
- Persichini, T., Colasanti, M., Lauro, G. M., and Ascenzi, P. (1998): Cysteine nitrosylation inactivates the HIV-1 protease. *Biochem Biophys Res Commun* **250**, 575-6.
- Perutelli, P., and Mori, P. G. (1992): The human platelet membrane glycoprotein IIb/IIIa complex: a multi functional adhesion receptor. *Haematologica* **77**, 162-8.
- Phaneuf, M. D., Berceci, S. A., Bide, M. J., Quist, W. C., and LoGerfo, F. W. (1997): Covalent linkage of recombinant hirudin to poly(ethylene terephthalate) (Dacron): creation of a novel antithrombin surface. *Biomaterials* **18**, 755-65.
- Plackett, R. L., and Burman, J. P. (1946): The design of optimum multifactorial experiments. *Biometrika* **33**, 305-3332.

- Pou, S. J., Anderson, D. E., Surichamorn, W., Keaton, L. L., and Tod, M. L. (1994): Biological studies of a nitroso compound that releases nitric oxide upon illumination. *Mol Pharmacol* **46**, 709-15.
- Pryor, W. A., Church, D. F., Govindan, C. K., and Crank, G. (1982): Oxidation of thiols by nitric oxide and nitrogen dioxide: synthetic utility and toxicological implications. *Journal of Organic Chemistry* **47**, 156-159.
- Pryor, W. A., and Lightsey, J. W. (1981): Mechanisms of nitrogen dioxide reactions: initiation of lipid peroxidation and the production of nitrous acid. *Science* **214**, 435-437.
- Puri, R. N., and Colman, R. W. (1997): ADP-induced platelet activation. *Crit Rev Biochem Mol Biol* **32**, 437-502.
- Radomski, M. W., and Moncada, S. (1993): The biological and pharmacological role of nitric oxide in platelet function. *Adv Exp Med Biol* **344**, 251-64.
- Radomski, M. W., Palmer, R. M., and Moncada, S. (1987a): Comparative pharmacology of endothelium-derived relaxing factor, nitric oxide and prostacyclin in platelets. *Br J Pharmacol* **92**, 181-7.
- Radomski, M. W., Palmer, R. M., and Moncada, S. (1987b): The role of nitric oxide and cGMP in platelet adhesion to vascular endothelium. *Biochem Biophys Res Commun* **148**, 1482-9.
- Radomski, M. W., Rees, D. D., Dutra, A., and Moncada, S. (1992): S-nitroso-glutathione inhibits platelet activation in vitro and in vivo. *Br J Pharmacol* **107**, 745-9.
- Ramamurthi, A., and Lewis, R. S. (1997): Measurement and modeling of nitric oxide release rates for nitric oxide donors. *Chem Res Toxicol* **10**, 408-13.
- Ramamurthi, A., and Lewis, R. S. (1998): Design of a novel apparatus to study nitric oxide (NO) inhibition of platelet adhesion. *Ann Biomed Eng* **26**, 1036-43.
- Ramamurthi, A., and Lewis, R. S. (2000): Influence of agonist, shear rate, and perfusion time on nitric oxide inhibition of platelet deposition. *Ann Biomed Eng* **28**, 174-81.
- Richards, F. M., and Knowles, J. R. (1968): Glutaraldehyde as a protein cross-linking reagent. *Journal of Molecular Biology* **37**, 231-233.
- Riddell, D. R., Graham, A., and Owen, J. S. (1997): Apolipoprotein E inhibits platelet aggregation through the L-arginine:nitric oxide pathway. Implications for vascular disease. *J Biol Chem* **272**, 89-95.
- Riddles, P. W., Blakeley, R. L., and Zerner, B. (1979): Ellman's reagent: 5,5'-dithiobis(2-nitrobenzoic acid) - a reexamination. *Analytical Biochemistry* **94**, 75-81.

- Ruel, J., Lemay, J., Dumas, G., Doillon, C., and Charara, J. (1995): Development of a parallel plate flow chamber for studying cell behavior under pulsatile flow. *Asaio J* **41**, 876-83.
- Sage, S. O., Sargeant, P., Heemskerk, J. W., and Mahaut-Smith, M. P. (1993): Calcium influx mechanisms and signal organisation in human platelets. *Adv Exp Med Biol* **344**, 69-82.
- Sakariassen, K. S., Muggli, R., and Baumgartner, H. R. (1989): Measurements of platelet interaction with components of the vessel wall in flowing blood. *Methods Enzymol* **169**, 37-70.
- Samouilov, A., and Zweier, J. L. (1998): Development of chemiluminescence-based methods for specific quantitation of nitrosylated thiols. *Analytical Biochemistry* **258**, 322-330.
- Sase, K., and Michel, T. (1997): Expression and regulation of endothelial nitric oxide synthase. *Trends in Cardiovascular Research* **7**, 28-37.
- Savi, P., and Herbert, J. M. (1996): ADP receptors on platelets and ADP-selective antiaggregating agents. *Med Res Rev* **16**, 159-79.
- Scharfstein, J. S., Keaney, J. F., Jr., Slivka, A., Welch, G. N., Vita, J. A., Stamler, J. S., and Loscalzo, J. (1994): In vivo transfer of nitric oxide between a plasma protein-bound reservoir and low molecular weight thiols. *J Clin Invest* **94**, 1432-9.
- Schmidt, H. H., Hofmann, H., Schindler, U., Shutenko, Z. S., Cunningham, D. D., and Feelisch, M. (1996): No .NO from NO synthase. *Proc Natl Acad Sci U S A* **93**, 14492-7.
- Schmidt, H. H., and Walter, U. (1994): NO at work. *Cell* **78**, 919-25.
- Schrör, K., Tschöpe, D., and Rösen, P. (1994): Megakaryocytes and platelets in cardiovascular diseases. Proceedings of a workshop held at the 27th meeting of the European Society of Clinical Investigation, Heidelberg, Germany, 15 April 1993. *Eur J Clin Invest* **24 Suppl 1**, 1-52.
- Scorza, G., Pietraforte, D., and Minetti, M. (1997): Role of ascorbate and protein thiols in the release of nitric oxide from S-nitroso-albumin and S-nitroso-glutathione in human plasma. *Free Radical Biology & Medicine* **22**, 633-642.
- Sexton, D. J., Muruganandam, A., McKenney, D. J., and Mutus, B. (1994): Visible light photochemical release of nitric oxide from S- nitrosoglutathione: potential photochemotherapeutic applications. *Photochem Photobiol* **59**, 463-7.
- Siess, W. (1989): Molecular mechanisms of platelet activation. *Physiol Rev* **69**, 58-178.

- Simon, D. I., Mullins, M. E., Jia, L., Gaston, B., Singel, D. J., and Stamler, J. S. (1996): Polynitrosylated proteins: characterization, bioactivity, and functional consequences. *Proc Natl Acad Sci U S A* **93**, 4736-41.
- Singh, R. J., Hogg, N., Joseph, J., and Kalyanaraman, B. (1996): Mechanism of nitric oxide release from S-nitrosothiols. *J Biol Chem* **271**, 18596-603.
- Stamler, J. S., Jaraki, O., Osborne, J., Simon, D. I., Keaney, J., Vita, J., Singel, D., Valeri, C. R., and Loscalzo, J. (1992a): Nitric oxide circulates in mammalian plasma primarily as an S-nitroso adduct of serum albumin. *Proc Natl Acad Sci U S A* **89**, 7674-7.
- Stamler, J. S., Jia, L., Eu, J. P., McMahon, T. J., Demchenko, I. T., Bonaventura, J., Gernert, K., and Piantadosi, C. A. (1997): Blood flow regulation by S-nitrosohemoglobin in the physiological oxygen gradient. *Science* **276**, 2034-7.
- Stamler, J. S., Simon, D. I., Osborne, J. A., Mullins, M. E., Jaraki, O., Michel, T., Singel, D. J., and Loscalzo, J. (1992b): S-nitrosylation of proteins with nitric oxide: synthesis and characterization of biologically active compounds. *Proc Natl Acad Sci U S A* **89**, 444-8.
- Stamler, J. S., Singel, D. J., and Loscalzo, J. (1992c): Biochemistry of nitric oxide and its redox-activated forms. *Science* **258**, 1898-902.
- Stubauer, G., Giuffre, A., and Sarti, P. (1999): Mechanism of S-nitrosothiol formation and degradation mediated by copper ions. *J Biol Chem* **274**, 28128-28133.
- Swartz, D. R. (1996): Covalent labeling of proteins with fluorescent compounds for imaging applications. *Scanning Microsc Suppl* **10**, 273-84.
- Thakur, M. L., Welch, M. J., Joist, J. H., and Coleman, R. E. (1976): Indium-111 labeled platelets: studies on preparation and evaluation of in vitro and in vivo functions. *Thromb Res* **9**, 345-57.
- Trujillo, M., Alvarez, M. N., Peluffo, G., Freeman, B. A., and Radi, R. (1998): Xanthine oxidase-mediated decomposition of S-nitrosothiols. *J Biol Chem* **273**, 7828-34.
- Tullett, J. M., and Rees, D. D. (1999): Use of NO donors in biological systems. *Mol Biotechnol* **11**, 93-100.
- Turitto, V. T. (1982): Blood viscosity, mass transport, and thrombogenesis. *Prog Hemost Thromb* **6**, 139-77.
- Tyllianakis, P. E., Kakabakos, S. E., Evangelatos, G. P., and Ithakissios, D. S. (1994): Direct colorimetric determination of solid-supported functional groups and ligands using bicinchoninic acid. *Anal Biochem* **219**, 335-40.

- van Kooten, T. G., Schakenraad, J. M., Van der Mei, H. C., and Busscher, H. J. (1992): Development and use of a parallel-plate flow chamber for studying cellular adhesion to solid surfaces. *J Biomed Mater Res* **26**, 725-38.
- Vane, J. (1994): Towards a better aspirin. *Nature* **367**, 215-6.
- Vanin, A. F., Malenkova, I. V., and Serezhenkov, V. A. (1997): Iron catalyzes both decomposition and synthesis of S-nitrosothiols: optical and electron paramagnetic resonance studies. *Nitric Oxide* **1**, 191-203.
- Walsh, P. N., Mills, D. C., and White, J. G. (1977): Metabolism and function of human platelets washed by albumin density gradient separation. *Br J Haematol* **36**, 287-96.
- Weber, C., Reiss, S., and Langer, K. (2000): Preparation of surface modified protein nanoparticles by introduction of sulfhydryl groups. *Int J Pharm* **211**, 67-78.
- Williams, D. L. (1996): S-nitrosothiols and role of metal ions in decomposition to nitric oxide. *Methods Enzymol* **268**, 299-308.
- Wink, D. A., Darbyshire, J. F., Nims, R. W., Saavedra, J. E., and Ford, P. C. (1993): Reactions of the bioregulatory agent nitric oxide in oxygenated aqueous media: determination of the kinetics for oxidation and nitrosation by intermediates generated in the NO/O₂ reaction. *Chem Res Toxicol* **6**, 23-7.
- Wink, D. A., Kasprzak, K. S., Maragos, C. M., Elespuru, R. K., Misra, M., Dunams, T. M., Cebula, T. A., Koch, W. H., Andrews, A. W., Allen, J. S. (1991): DNA deaminating ability and genotoxicity of nitric oxide and its progenitors. *Science* **254**, 1001-3.
- Winterbourn, C. C. (1990): Oxidative reactions of hemoglobin. *Methods Enzymol* **186**, 265-72.
- Woods, B. P., Dennehy, A., and Clarke, N. (1976): Some observations on the preparation of platelet-rich plasma. *Thromb Haemost* **36**, 302-10.

Oklahoma State University
Institutional Review Board

Protocol Expires: 12/16/2003

Date: Tuesday, December 17, 2002

IRB Application No EG98004

Proposal Title: NOVEL POLYMERS DESIGNED TO MINIMIZE PLATELET

Principal
Investigator(s):

Randy Lewis
423 EN
Stillwater, OK 74078

Reviewed and
Processed as: Expedited

Approval Status Recommended by Reviewer(s): Approved

Dear PI :

Your IRB application referenced above has been approved for one calendar year. Please make note of the expiration date indicated above. It is the judgment of the reviewers that the rights and welfare of individuals who may be asked to participate in this study will be respected, and that the research will be conducted in a manner consistent with the IRB requirements as outlined in section 45 CFR 46.

As Principal Investigator, it is your responsibility to do the following:

1. Conduct this study exactly as it has been approved. Any modifications to the research protocol must be submitted with the appropriate signatures for IRB approval.
2. Submit a request for continuation if the study extends beyond the approval period of one calendar year. This continuation must receive IRB review and approval before the research can continue.
3. Report any adverse events to the IRB Chair promptly. Adverse events are those which are unanticipated and impact the subjects during the course of this research; and
4. Notify the IRB office in writing when your research project is complete.

Please note that approved projects are subject to monitoring by the IRB. If you have questions about the IRB procedures or need any assistance from the Board, please contact Sharon Bacher, the Executive Secretary to the IRB, in 415 Whitehurst (phone: 405-744-5700, sbacher@okstate.edu).

Sincerely,



Carol Olson, Chair
Institutional Review Board

VITA ²

Heather D N Fahlenkamp

Candidate for the Degree of

Doctor of Philosophy

Thesis: THE CHARACTERIZATION, OPTIMIZATION, AND UTILIZATION OF
IMMOBILIZED THIOL GROUPS ON A POLYMERIC SURFACE

Major Field: Chemical Engineering

Biographical:

Personal Data: Born in Enid, Oklahoma, on June 11, 1974, the daughter of John and Helena Gappa.

Education: Graduated from Chisholm High School, Enid, Oklahoma in May 1992; received a Bachelor of Science degree in Chemical Engineering from Oklahoma State University, Stillwater, Oklahoma in May 1997. Completed the requirements for the Master of Science degree with a major in Bioengineering at the University of Utah, Salt Lake City, Utah in May, 2000. Completed the requirements for the Doctor of Philosophy degree with a major in Chemical Engineering at Oklahoma State University in December 2003.

Experience: Undergraduate research assistant; Oklahoma State University, Department of Chemical Engineering, 1995 to 1996. Summer process engineer intern; Diamond Shamrock, Dumas, Texas, Summer 1996. Graduate research assistant; University of Utah, Department of Bioengineering, 1997 to 1999. Collaborative research assistant; Oklahoma State University, Department of Veterinary Clinical Sciences, 2001 to 2002. Graduate research assistant; Oklahoma State University, Department of Chemical Engineering, 2000 to present.

Professional Memberships: Phi Kappa Phi National Honor Society, Tau Beta Pi National Engineering Honor Society, American Institute of Chemical Engineers, Biomedical Engineering Society, Society of Women Engineers.